IDENTIFICATION OF FIBULIN-1 AS A HUMAN BONE MARROW STROMAL (HS-5) DERIVED FACTOR THAT INDUCES PROSTATE CANCER CELL DEATH

by

Kornkamon Nopmongkol

A dissertation submitted to the Faculty of the
University of Delaware in partial fulfillment of the requirements
for the degree of Doctor of Philosophy in Biological Sciences

Spring 2015

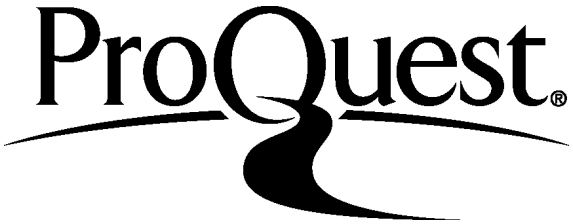

IDENTIFICATION OF FIBULIN-1

AS A HUMAN BONE MARROW STROMAL (HS-5) DERIVED FACTOR

THAT INDUCES PROSTATE CANCER CELL DEATH

by

Kornkamon Nopmongkol

Approved: _____

Robin W. Morgan, Ph.D.
Chair of the Department of Biological Sciences

Approved: _____

George H. Watson, Ph.D.
Dean of the College of Arts and Sciences

Approved: _____

James G. Richards, Ph.D.
Vice Provost for Graduate and Professional Education

I certify that I have read this dissertation and that in my opinion it meets the academic and professional standard required by the University as a dissertation for the degree of Doctor of Philosophy.

Signed: _____

Robert A. Sikes, Ph.D.
Professor in charge of dissertation

I certify that I have read this dissertation and that in my opinion it meets the academic and professional standard required by the University as a dissertation for the degree of Doctor of Philosophy.

Signed: _____

Kenneth L. van Golen, Ph.D.
Member of dissertation committee

I certify that I have read this dissertation and that in my opinion it meets the academic and professional standard required by the University as a dissertation for the degree of Doctor of Philosophy.

Signed: _____

Catherine B. Kirn-Safran, Ph.D.
Member of dissertation committee

I certify that I have read this dissertation and that in my opinion it meets the academic and professional standard required by the University as a dissertation for the degree of Doctor of Philosophy.

Signed: _____

Robert W. Mason, Ph.D.
Member of dissertation committee

I certify that I have read this dissertation and that in my opinion it meets the academic and professional standard required by the University as a dissertation for the degree of Doctor of Philosophy.

Signed: _____

Anja Nohe, Ph.D.
Member of dissertation committee

ACKNOWLEDGMENTS

As an international student, completing a Ph.D. degree here is one of my most memorable journeys. I have had so many people who helped me along the way, both in academic and non-academic perspectives, and I would not be able to do this without them. However, one special person that immensely helped me through this journey is Dr. Robert Sikes, my advisor. He kindly accepted me to work in his lab since 2010, and started training me to be an independent researcher. Due to my future career, he also showed me what a good advisor should be, and how to manage my own lab in the future. For 5 years, I learned, observed and improved a lot due to his training. I appreciate the way he taught each student with different approaches, and this would be an excellent example for me when I have my own lab. Moreover, as my "Papa", he also taught me to become a better and independent woman. I am greatly appreciative for everything he has done to help every student, including me, in our lab. He is patient, accessibility, generous and intellectuality make me feel honored to work with him during this long journey. I could not be more thankful.

I would like to thank my committee members who helped, guided, and discussed my project with me for 5 years. I would like to thank Dr. Kenneth van Golen who also accepted me for my second rotation as well as serving as the chair for my qualifying exam. Moreover, his questions and experimental insight were always helpful for my project. I would like to thank Dr. Catherine Kirn-Safran who urged me to look at my project in broad and interdisciplinary views. I would like to thank Dr. Anja Nohe for providing me with constructive criticisms and support. Moreover, I

would like to thank Dr. Robert Mason for his insight biochemical suggestions. I owe a debt of gratitude to all of my committee members for helping to shape me into the scientist I am today. I am very appreciative.

During my time here, I had a chance to collaborate with Dr. Kelvin Lee and Dr. Leila Choe from Delaware Biotechnology Institute (DBI). I would like to thank them for their help with generating and analyzing MS/MS data. Moreover, I would like to thank all faculty and staff in the Department of Biological Sciences for providing me with a pleasant and welcoming atmosphere. I appreciated all the help I got through my journey. In addition, I would like to thank all members in Sikes' lab (my lab family): Dr. Fayth Miles, Dr. Adam Aguiar, Dr. Keith Jansson, Dr. Jomnarong Lertsuwan, Dr. Erica Dashner, Dr. Madhura Joglekar, Dr. Senem Kurtoglu, and Ms. Rachel Hanson M.S. for all their help, support, guidance and friendship. I also would like to thank our undergraduate students: Irene Rhobi Marwa, Jacob Rubin, Meghan Kirk, Joseph Morris and Michael Gerges for the training experience I got from helping them and for maintaining the laboratory in a good shape.

I would not be able to complete this journey without the greatest support from my friends and family here and in Thailand. I would like to thank mom and dad for letting me quit medical school and follow my path as a scientist without hesitation. They keep on supporting me in all steps and aspects of my life. Last but certainly not least; I would like to thank my fiancé, friend, lab mate and the greatest supporter, Dr. Jomnarong Lertsuwan. Thank you for being with me for almost 12 years. I appreciate his love, support, understanding and guidance both in academic and non-academic

aspects. Without his unconditional support, I would not be able to accomplish all the goals I wished for and have accomplished to date.

TABLE OF CONTENTS

LIST OF TABLES

LIST OF FIGURES

LIST OF ABBREVIATIONS

ADAMTS	a disintegrin-like and metalloprotease with thrombospondin motifs proteases
ADT	Androgen deprivation therapy
ANOVA	Analysis of Variance
Anxa2	Annexin II
AT-domain	Anaphylotoxin-like domain
BMM	Bone marrow macrophage
BMP	Bone morphogenetic protein
BMS	Bone marrow stromal
BPH-1	Benign prostatic hyperplasia-1
BSA	Bovine serum albumin
CAM	Cell adhesion molecule
Cas	CRISPR associated nuclease
cbEGF	Calcium binding epidermal growth factor
CCL	Chemokine (C-C motif) ligand
CRISPR	Clustered regularly interspaced short palindromic repeats
CRPC	Castrate resistant prostate cancer
CM	Conditioned media
CT scan	Computerized tomography scan
DN-TβRII	Dominant-negative mutant of TGF-β receptor type II
DMEM	Dulbecco's Modification of Eagle's Medium
DPCs	Disseminating prostate cancer cells
DRE	Digital Rectal Exam
DTT	Dithiothreitol
ECL	Enhanced chemiluminescence
ECM	Extracellular matrix/matrices
EGF	Epidermal growth factor
EMT	Epithelial to mesenchymal transition
ET1	Endothelin-1
FBS	Fetal bovine serum
FC domain	Fibulin type domain
GAS6	Growth arrest specific-6
HDF	Human diploid fibroblast
HEK	Human embryonic kidney
HRP	Horseradish peroxidase
HSC	Hematopoietic stem cell

HS-5 DF	HS-5 derived factor
IFN	Interferon
IGF	Insulin-like growth factor
IL	Interleukin
iMC	Immature myeloid cell
IP	Immunoprecipitation
LTBP2	Latent binding protein 2
LTC	Long-term culture
mDC	Myeloid dendritic cell
MDSC	Myeloid-derived suppressor cell
MEM	Minimum Essential Medium Eagle
MET	Mesenchymal to epithelial transition
M-MLV	Maloney murine leukemia virus
MMP	Matrix metalloproteinase
MS/MS	Tandem mass spectrometry
NED	Neuroendocrine differentiation
NSE	Neuron-specific enolase
OPG	Osteopotegerin
PBS	Phosphate buffer saline
PCa	Prostate cancer
pDC	Plasmacytoid dendritic cell
PSA	Prostate specific antigen
PTHrP	Parathyroid hormone related protein
qRT-PCR	Quantitative reverse transcription polymerase chain reaction
Qscn6	Sulfyhydryl oxidase Q6
RANK	Receptor activator of the nuclear factor kappa-B
RANKL	Receptor activator of the nuclear factor kappa-B ligand
RIPA	Radioimmunoassay precipitation
SDF-1	Stromal cell-derived factor-1
SDS-PAGE	Sodium Dodecyl Sulfate Polyacrylamide Gel Electrophoresis
SEM	Standard error of the mean
SF	Serum free
shRNA	Short hairpin RNA
SHBG	Sex hormone-binding globulin
SOC	Super Optimal broth with Catabolite repression
TAE	Tris-acetate EDTA
TAK-1	TGF-β activates kinase 1
TALEN	Transcription activator-like effector nuclease
TAM	Tumor-associated macrophage
TBS	Tris buffer saline
TGF-β1	Transforming growth factor beta 1
TGFBR2	Transforming growth factor beta receptor 2
TIMP-1	Tissue inhibitor of metalloproteinase-1

TNF	Tumor necrosis factor
Treg	Regulatory T cell
uPA	Urokinase-type plasminogen activator

ABSTRACT

Prostate cancer (PCa) is one of the most important health problems affecting men in the USA. It is estimated that one in seven men will be diagnosed with PCa in their lifetime. In this year alone, 220,800 new cases and 86,380 deaths were estimated. This makes PCa the most common cancer diagnosed and the second leading cause of cancer related death in men. Although early detection and treatment of localized PCa can increase 5-year survival rates to almost 100%, the survival rate drops dramatically, to around 30%, in patients with advanced metastatic PCa. Most PCa patients develop bone metastases causing bone pain, bone fracture and spinal cord compression, which ultimately reduces their quality of life and leads to the lethal phenotype of PCa. Hormonal therapy, in the form of androgen deprivation therapy (ADT), is given as the first line therapy for metastatic PCa; however, this can only suppress disease progression temporarily. Within 1.5-3 years after treatment began, many patients become resistant to the treatment and develop a more aggressive, castrate-resistant form of prostate cancer (CRPC). The development of CRPC bone lesions is associated with rapid disease progression and further reduction of patient survival. In this scenario, the average survival drops to less than 12 months. Bone metastasis remains the major cause of death in PCa patients; however, the rationale behind metastatic site preference or the mechanism(s) driving PCa colonization in bone is still unknown. In contrast to a well-known ‘seed and soil’ theory by Paget, which states that non-random metastasis is the result of favorable interactions between the cancer and the target tissue, results from our lab and others have suggested possible negative

interactions between PCa cells and bone microenvironment. Specifically, previous data from our lab showed that bone marrow stromal (BMS) cells derived from marrow sinusoidal area called HS-5 cells secreted a soluble factor(s), which induced PCa cell apoptosis. While a fraction of the PCa cells underwent apoptosis, the surviving cells developed a neuroendocrine differentiated phenotype, which was shown to correlate with more aggressive behavior of PCa. Taken together, these results were contrary to Paget's theory and suggested that the initial interaction between the paracrine factor(s) from the bone marrow environment and PCa could be negative. Furthermore, overcoming this condition might be a driving force for PCa cell survival and subsequent development into the more aggressive form. Therefore, identification of the apoptotic inducing factor(s) produced by bone stromal cells would be an essential step towards understand this initial interaction between PCa cells and the bone microenvironment.

Consistent with previous research, my data also demonstrated that HS-5 conditioned media (HS-5 CM) contained paracrine factor(s) that induce apoptosis in three cell lines from LNCaP human PCa progression model, namely LNCaP, C4-2 and C4-2B. In this study, the biochemical characteristics of an HS-5 derived factor (HS-5 DF) that induced PCa cell death were investigated. Firstly, proteolytic enzyme sensitivity was tested using typsin. The results showed the apoptotic-inducing activity of HS-5 dropped significantly after the treatment with trypsin suggesting that HS-5 DF is a protein that contains at least one trypsin recognition site. Furthermore, as HS-5 CM was pretreated with varied high temperatures, the results showed that apoptotic-inducing activity of HS-5 CM was inversely related to the pretreatment temperature of the CM thereby indicating a heat sensitivity of HS-5 DF. These results also

demonstrated protein properties of HS-5 DF. HS-5 DF activity remained steady when exposed to different pHs including pH 4, 7, and 10. These data indicated that the activity of HS-5 DF is stable across pH 4-10. In addition, the tentative size for HS-5 DF was studied by using size selected centrifugal filters. The data showed that the death-inducing activity of HS-5 CM remained in the fractions containing proteins that are greater than 30 kDa, but smaller than 100kDa, suggesting that the size of HS-5 DF is between 30 kDa and 100 kDa. To test for the requirement of disulfide bonding of HS-5 DF, a strong reducing agent, dithiothreitol (DTT) was used. Results from the more aggressive C4-2 and C4-2B lines showed lower death inducing activity of HS-5 CM pretreated with DTT as compared to the groups treated with HS-5 CM alone. This strongly implies a requirement for disulfide bonding for HS-5 DF to function properly. When size selection experiments were performed after DTT treatment, the results showed an increase activity in the smaller size fractions in both 30 kDa and 100 kDa cutoff filters. This indicated oligomerization and/or multi-proteins interactions of HS-5 DF. Another experiment was carried out to determine a suitable procedure to concentrate HS-5 CM for future experiments. It was shown that speed vacuum concentration could be used as a procedure to concentrate HS-5 CM without losing its activity.

High levels of transforming growth factor beta 1 (TGF-β1) have been correlated in the serum of PCa patients with bone metastases. This led to our interest in the effects of TGF-β1 on HS-5 DF. Previous experiments from our group showed that CM collected from HS-5 cells pretreated with TGF-β1 (HS-5/TGF-β1 CM) had significantly lower death-inducing activity than the vehicle control pretreated group. Consistent with these data, my results also showed an inhibitory effect of TGF-β1 pre-

treatment on HS-5 DF. Therefore, HS-5/TGF-β1 CM samples, which had significantly lower PCa death induction, were used as negative controls for proteomic approaches. Using high resolution one-dimensional Sodium Dodecyl Sulfate Polyacrylamide Gel Electrophoresis (SDS-PAGE), several protein band alterations in HS-5 CM after TGF-β1 treatment were observed. The bands that showed differential expression between HS-5 CM and HS-5/TGF-β1 CM were pulled followed by in-gel tryptic digestion and tandem mass spectrometry (MS/MS) to acquire the lists of upregulated and downregulated candidates. Among the down regulated HS-5 DF candidates, fibulin-1 showed a stronge potential to be an HS-5 DF due to its characteristics and its specificity. Accordingly, fibulin-1 was picked for further investigation.

My data showed a dramatically higher fibulin-1 expression in HS-5 cells compared to a weakly expression in PCa cells indicating a potential cancer suppressive role of fibulin-1 on PCa cells. Furthermore, the level of fibulin-1 dropped significantly in both whole cell lysates and HS-5/TGF-β1 CM after HS-5 cells were treated with TGF-β1. These results confirmed the MS/MS data and showed strong associations between fibulin-1 level in HS-5 CM and its PCa death inducing activity. Since opposing effects of a tumor promoting fibulin-1C and a tumor suppressive fibulin-1D were noted in many studies, the expressions of the two isoforms were determined in HS-5 cells. It was shown that both filbulin-1C and 1D isoforms were found in HS-5 cells. Interestingly, HS-5 cells expressed higher level of a tumor suppressive fibulin-1D than a tumor promoting fibulin-1C. Upon TGF-β1 treatment, both fibulin-1C and 1D were down regulated indicating a suppression of FBLN1 gene expression by TGF-β1. To further test for a probability of fibulin-1 as an HS-5 DF inducing PCa cells death, CMs from cell lines expressing different level of fibulin-1

including HS-5, HS-27a and HEK293 were used. The results showed that the higher expression of fibulin-1 in HS-5 CM correlated with greater PCa cell death inducing activity from CM as compared to cell lines with lower fibulin-1 expression. Once again, these data showed that fibulin-1 level in CM was associated with PCa death induction of the CMs. To further determine the direct involvement of fibuln-1 in HS-5 CM and its PCa death induction, fibulin-1 was partially removed from HS-5 CM by immunoprecipitation (IP). The results showed that HS-5 CM that underwent IP with a fibulin-1 specific antibody showed significantly lower fibulin-1 level in CM compared to HS-5 CM underwent only the preclearing step (with protein A agarose) or the one underwent IP with IgG isotype antibody control. This result strongly suggested that fibulin-1 in HS-5 CM contributed to PCa cell death induction. As all data indicated strong associations between fibulin-1 and PCa cell death inducing activity from HS-5 CM, the fibulin-1 gene was knocked down in HS-5 cells to test directly for its PCa death induction. The results showed that fiblulin-1 was successfully knocked down in HS-5 (HS-5^{CRISPR_fib1}) cells by using clustered regularly interspaced short palindromic repeats (CRISPR)/ CRISPR associated nuclease (Cas) system leading to drastically lower level of fibulin-1 in HS-5^{CRISPR_fib1} CM. When the CM from HS-5^{CRISPR_fib1} cells was introduced to PCa cells, PCa cell death was reduced significantly compared to the CM from HS-5 cells transfected with the control plasmid (HS-5^{CRISPR_GFP}). This also confirmed the association of fibulin-1 expression in HS-5 cells and HS-5 CM with PCa death induction of HS-5 CM. Accordingly, this study suggested a novel role of fibulin-1 as a BMS HS-5 DF that could potentially function as an initial defense mechanism of the bone microenvironment to prevent disseminating prostate cancer cells (DPCs) bone colonization.

Chapter 1

INTRODUCTION

The prostate gland is a walnut-sized organ in male reproductive system located below urinary bladder and in front of rectum. Surrounding the urethra, it is responsible for secreting approximately 25% of ejaculatory secretions. As a male accessory sex organ, the prostate secretes a solution rich in sugar, zinc and proteolytic enzymes. The functions of prostatic secretion are to nourish, protect and support the movement of spermatozoa as well as to liquefy semen by PSA [1]. Interestingly, the prostate is one of the most common sites to develop malignancy in United States men having with the highest incidence of all solid tumors since 1975 and the highest number of expected new cases for 2015 [2]. Like other types of cancer, prostate cancer (PCa) becomes more aggressive with increasing grade and metastasis to other organs. Prevalent metastatic sites for PCa include bone (90%), lung (46%), liver (25%), pleura (21%) and adrenal glands (13%) [3]. The mechanisms behind the preferential metastasis to and bone colonization of PCa remain elusive. Moreover, effective diagnostic methods and treatments that are highly effective and specific for PCa bone metastasis are still in need. This leads to our interest in studying the interactions between PCa and cells of the bone microenvironment in order to unravel the mechanism(s) behind PCa bone metastasis, which could potentially contribute to the better diagnostics and treatments in the near future.

1.1 Prostate Cancer Statistics and Treatment Options

PCa is a major health problem worldwide. PCa is the second leading most frequently diagnosed cancer in men. Interestingly, more than 60% of cases were reported in economically developed countries, namely Northern and Western Europe, North America and Oceania [4]. In 2012 alone, over 1 million new cases of PCa were diagnosed making it the second most diagnosed cancer in men and fourth most diagnosed cancer globally. With this high incidence, PCa had more than 300,000 estimated deaths in 2012, which made PCa the fifth most common cause of cancer related deaths in men worldwide [4, 5]. For United States, PCa has been the most commonly diagnosed cancer in men since 1975. In 2015, the estimated cases for PCa were higher than 230,000 cases. Despite the highest incidence, PCa is only the second leading cause of cancer death in American men with the estimated number of deaths being about 27,000 cases in 2015 [2, 6].

The results from Digital Rectal Exam (DRE), transrectal ultrasound, prostate specific antigen (PSA), biopsy and bone scan are used to diagnose and determine the stage and grade (progression) of PCa. For the early stages, confined and regional PCa, standard therapies include active surveillance, radiotherapy and prostatectomy [7-9]. Most patients diagnosed with local PCa have a 5-year survival rate approaching 100%; however, the survival rate drops significantly to around 30% in patients with metastatic PCa. For these advance stages, androgen deprivation therapy (ADT), by chemical or surgical castration, is frequently given to the patients with or without combination with chemotherapy [10-13]. Unfortunately, ADT only leads to a decrease in PSA level and a temporary tumor regression. Within 1.5-3 years after ADT, many patients develop a more aggressive castrate resistant prostate cancer (CRPC), which will no longer respond to ADT [14, 15]. When CRPC takes place, the survival time

further decreases to approximately 9-18 months. Even more limited are successful response to chemotherapy at this stage. Some treatments showed a successful of survival to more than 30 months in clinical trails [16-18]. Standard therapy for CRPC is docetaxel-based chemotherapy with or without the combination of other drugs, which could be given during the treatment course or after docetaxel. Many of these drugs, such as prednisone, carbazitaxel, abiraterone acetate and enzalutamide, together with docetaxel showed the promising results in improving pateint survival rates in clinical trials [17]. However, due to the complications and side effects of chemotherapy, the effective treatments as well as a more efficient way for early detection and prediction of CRPC are still in needed.

1.2 Prostate Cancer Bone Metastasis

Among all metastatic sites for PCa, 70%-90% of PCa patients develop bone metastases [13, 19, 20]. The development of CRPC bone lesions is associated with rapid disease progression and a drastic reduction in patient survival where the average survival drops to 9-12 months [14, 21]. It also was shown in an autopsy study that 80% of patients who died of PCa had bone metastases [3]. Of patients with bone metastases, most of them would have osteosclerotic lesions, which are mixed lesions of osteolytic and osteoblastic lesions. Osteosclerotic lesions lead to the deposition of irregular bone structure that is susceptible to bone fracture [13, 22, 23]. Many PCa patients with bone metastasis experience skeletal; related events including bone pain, bone fracture and the risk for spinal cord compression, which ultimately reduces their quality of life [14, 24]. As the major cause of death in PCa patients, the rationale behind preference for bone or the mechanisms driving PCa bone colonization are still unknown. To date, the famous ‘seed and soil’ hypothesis by Paget [25] is being used

to explain the possible mechanisms for bone metastasis in many types of cancer, including PCa. In this model, the growing tumor (seed) depends upon or favors the bone environment (soil) to grow outside its primary location [26-28]. However, a growing body of research is showing that this model might not be entirely true for PCa [29-33].

PCa metastasis involves a multiple step process including local migration, invasion, intravasation, circulation, extravasation and colonization into the new metastatic environment [34]. The beginning step of metastasis is associated with the detachment of cancer cells from the primary location and migration to nearby blood or lymphatic vessels. Research has shown that metastatic PCa cells have decreased cell adhesion and underwent epithelial to mesenchymal transition (EMT) to increase their migratory ability. E-cadherin, a cell adhesion molecule (CAM) expressed highly in epithelial cells, was downregulated in metastatic PCa cells. In contrast, a mesenchymal cadherin, N-cadherin was upregulated in these cells. This cadherin switch also was correlated with high grade disease and invasiveness of PCa cell lines [35-38]. Moreover, β-catenin, which functions together with E-cadherin in maintaining cell-to-cell adhesion between epithelial cells, also was downregulated in high grade PCa [39]. Yet, another study showed that these proteins were re-expressed in metastatic PCa cells in bone [40] indicating a possible mesenchymal to epithelial transition (MET) in bone during PCa bone colonization. In addition to this cadherin switch, normal prostate epithelial α6 integrins were downregulated in biopsy samples corresponding to an increase of PCa migration and invasion [41, 42].

In addition to migration on extracellular matrices (ECM), PCa invasion through ECM also is needed for PCa metastasis. For PCa cells to be able to invade

through ECM, proteolytic enzymes secreted by PCa cells are required to degrade ECM proteins. It has been shown that matrix metalloproteinases (MMPs), especially MMP-2 and MMP-9, were higher in serum of metastatic PCa patients than those with non-metastatic PCa [43]. This suggested correlations between these MMPs and PCa metastasis. Moreover, the ratio between MMP-2/-9 to tissue inhibitor of metalloproteinase-1 (TIMP-1) was increased in PCa tissues compared to normal tissue. This increased ratio also correlated with high Gleason score and poor prognosis of the patients [44-46]. In addition to MMPs, urokinase-type plasminogen activator (uPA) serine protease was shown to be associated with ECM degradation. Upregulation of uPA and its receptor was found in high tumor grade samples as well as PCa cell lines with high metastatic activity [47-49]. uPA could also activate MMP-2/-9, which further drives PCa invasion by leading to degradation of basement membrane proteins [47]. Last but not least, prostate-specific antigen (PSA), which is known as a diagnostic marker for PCa, could also play a role in PCa invasion. As a kallikrein-like serine protease [50], PSA was shown to be able to degrade fibronectin, the main component in ECM. Therefore, this brought the possibility that PSA could be another factor facilitating PCa invasion through ECM [51].

After migration, invasion and intravasation into blood/lymphatic circulation, PCa cells must survive through the circulation and then extravasate to the new metastatic environment. As the rationale behind PCa preference to bone is not known, chemotaxis could be one of the possible mechanisms that attracts the disseminating prostate cancer cells (DPCs) to bone. Current studies showed that DPCs express similar surface molecules, respond to the same signals, and accordingly compete for the same niche as hematopoietic stem cells (HSCs) [13, 19, 52-55]. One of the most

well studied regulators is CXCL12, or stromal cell-derived factor-1 (SDF-1), which is expressed strongly by bone marrow mesenchymal cells [19, 56]. Bone marrow derived CXCL12 is produced primarily by bone endothelial cells and osteoblasts in the endosteal region of bone marrow [57]. This ligand is known to interact with the chemokine receptors, CXCR4 and CXCR7, on HSCs and cancer cells. Several studies have shown that metastatic PCa cells also express both CXCR4 and CXCR7, and upregulation of these receptors correlated with poor prognosis [52, 53, 58-61]. Accordingly, CXCL12-CXCR4 (or CXCR7) potentially could serve as a strong chemotaxis system attracting DPCs to bone. Supporting this hypothesis, it has been shown that PCa cells had preferential adherence to human bone marrow endothelial (HBME-1) cells than endothelial cells from other sources [62, 63]. Subsequently, a model called "dock and lock" model was proposed to explain this interaction between PCa cells and bone endothelial cells [64, 65]. In this model, bone epithelial cells expressed adhesion molecule called P-selectin, which can interact with sialyl-Lewis^x carbohydrate on the surface of PCa cells. It was hypothesized that this interaction together with integrin binding could facilitate the attachment between PCa cells and bone endothelial cells [64, 66-69] during extravasation. Finally, aggressive prostate cancer cells showed a preference to interact with and invade through bone marrow endothelial cells over other bone marrow derived cell types [70]

PCa cells and osteoclasts expressed similar types of integrins that could potentially facilitate PCa spreading in bone [71]. It has been shown that these integrins mediated PCa cell migration on bone ECM proteins including osteopontin, tronectin, laminin and collagen I [71-76]. Another research showed that bone metastatic PCa highly expressed cadherin-11, osteoblast cadherin, which might play a role in PCa

bone colonization as well [77]. In addition, growing evidence supported the interactions between osteoblast and PCa cells in endosteal niche. Activation of CXCR4 on PCa cells resulted in the upregulation of αVβ3 integrin and CD164, which potentially supported the tight binding of PCa cells to osteoblasts [53, 59, 78]. The binding between osteoblasts and PCa cells could support cancer cell dormancy in a process similar to HSCs quiescence [53]. One molecule that has been proposed to play an important role in this reversible cell cycle arrest of both PCa cells and HSCs is annexin II (Anxa2). Both PCa cells and HSCs express Anxa2R receptor that can interact with Anxa2 expressed on osteoblasts [79, 80]. The binding of Anxa2 to Anxa2R on PCa induces the expression of Axl, a receptor for growth arrest specific-6 (GAS6). GAS6 also is expressed in osteoblast [81]. Consequently, this additional binding via GAS6/Axl has been shown to induce growth arrest and drug resistance of PCa cells possibly leading to a chemo-resistant tumor dormancy stage [53, 81].

1.3 Bone Microenvironment and Prostate Cancer Colonization

1.3.1 Osteoclasts/Osteoblasts and PCa Bone Colonization

Once in the bone, bidirectional interactions between PCa cells and bone cells are important for PCa bone colonization and tumor growth. Two of the most important bone cells affecting PCa colonization are bone forming osteoblasts and bone resorbing osteoclasts. Osteoblast growth and differentiation is regulated by many growth factors and signaling molecules including bone morphogenetic proteins (BMPs), insulin-like growth factors (IGFs), transforming growth factor-β (TGF-β) and Wnt. During bone formation, osteoblasts secrete many of these factors that will be embedded in the bone matrix. Later, such factors can be released from the bone matrix by the activity of

osteoclasts. On the other hand, the differentiation of osteoclasts are regulated by the presence of receptor activator of the nuclear factor kappa-B ligand (RANKL) on developing osteoblasts and osteopotegerin (OPG) secreted by mature osteoblasts that can interact with receptor activator of the nuclear factor kappa-B (RANK) on pre-osteoclasts [34, 82-84]. PCa cells stimulate osteoclast and osteoblast activity simultaneously. The released growth factors from the bone matrix create the 'vicious cycle' that promotes the tumor growth in the new environment [85]. Such a cycle leads to mixed lesions (osteosclerotic) that are partially osteolytic (bone degrading) and osteoblastic (bone forming). This type of lesions is a unique characteristic of PCa bone metastasis [53, 81].

Bone resorption could contribute many growth factors to facilitate PCa cell growth and survival in the new environment. Accordingly, metastatic PCa cells secrete cytokines and factors activating osteoclast maturation and activity. One of the factors produced by PCa cells is soluble RANKL [86-89]. In typical bone remodeling process, RANKL is expressed by osteoblasts and interacts directly with RANK on pre-osteoclasts. This binding activates TGF-β activated kinase 1 (TAK1) and tumor necrosis factor receptor-associated factor binding adaptor protein 2 (TAB2). TAK1 then activates nuclear factor kappa-B (NF-κB) and AP-147 resulting in the transcription of genes needed for osteoclast maturation [84]. Similarly, The binding of RANKL to RANK mediates osteoclast induced bone resorption leading to osteolytic lesions or regions of active bone remodeling in PCa bone metastasis [13, 90]. It has been shown that therapy targeting on RANK-RANKL interaction, such as RANKL antibody, reduces skeleton related events (SREs) and bone pain, prolongs the bone metastasis-free period and delays the time to develop bone metastasis in PCa patients

[91, 92]. Even though one study showed that a recombinant RANKL antagonist, RANK-Fc reduced osteolytic lesions and PCa growth in vivo [87], most studies showed that inhibiting RANK-RANKL disrupts the vicious cycle rather than affecting tumor proliferation itself [87]. In addition to factors secreted from PCa cells, factors released from bone resorption by osteoclasts also played an important role in PCa bone colonization. One of the factors is TGF-β. The dual role of TGF-β on tumor progression, which change from tumor suppression in normal epithelial cells and early tumor to tumor supportive in the more advance stage, were noted [32, 93, 94]. TGF-β was activated by the cleavage of TGF-β precursor by osteoclast-derived protease as well as PCa cell-derived PSA and uPA [95, 96]. It was shown in xenograft model that BMP-7, an antagonist for TGF-β signaling, inhibited osteolytic metastases in a bone specific manner [97]. This suggested the potential role of TGF-β in PCa bone colonization via osteolytic support.

While osteolytic activity can be found in PCa metastases, osteoblastic (bone forming lesions) or osteosclerotic (mixed lesions with the total bone gain) activity is a hallmark for PCa bone metastasis. PCa cells were shown to produce parathyroid hormone-related protein (PTHrP), which could enhance osteoclast differentiation in vitro and in vivo [98]. PTHrP induces osteoclast differentiation by upregulating RANKL in osteoblasts and downregulating OPG, a decoy ligand inhibiting osteoclast differentiation [98]. On the other hand, the direct effects of PTHrP on osteoblasts were noted in many studies. It has been shown that PTHrP induces osteoblast differentiation leading to the increase of osteoblast population and activity [53, 98, 99] as well as protecting osteoblasts and PCa cells from apoptosis [53, 99, 100]. Indeed, PTHrP administration to mice increases bone colonization of prostate cancer cells in vivo

[101-103]. These data suggested the roles of PTHrP in supporting both osteolytic and osteoblastic bone metastases. However, it has been shown that PTHrP could be cleaved by PSA leading to a decrease in bone resorption but increase in osteoblast activity. These studies indicated that during PCa progression, the rising level of PSA could regulate the switch of PTHrP functions from osteolytic to an osteoblastic process in PCa bone colonization [104, 105].

However, PTHrP is not the only factor affecting osteoblasts during PCa bone colonization. Canonical Wnt signaling via Frizzled-Dishevelled-β-catenin axis was shown to stimulate osteoblast differentiation and bone formation [106]. In PCa bone metastasis, Wnt secreted by PCa cells also stimulated osteoblast differentiation and cancer cell proliferation leading to osteoblastic lesions in PCa colonization [107]. Wnt signaling could be regulated by the expression of the Wnt antagonist, DKK1, which was shown to be expressed in early stages of PCa, but the expression was decreased in bone metastatic PCa [108]. It has been shown that inhibition of DKK1 led to osteoblastic lesions from PC3; while, overexpression of DKK1 in C4-2B led to osteolytic lesions instead of osteosclerotic phenotypes [109]. This suggested the inhibition of osteoblastic activity by DKK1 during PCa bone colonization. The regulation of Wnt signaling mediating osteoblastic activity via DKK1 were also affected by another protein called Endothelin-1 (ET-1). ET-1 induced osteoblast proliferation, while inhibiting osteoclast formation and motility [110]. The proposed mechanism for osteoblastic induction by ET-1 was through the crosstalk of Wnt signaling leading to the suppression of DKK1 [111]. In PCa, it has been shown that exogenous ET-1 increased PCa cell proliferation, and the plasma level of ET-1 was associated with osteoblastic metastases in PCa patients [110, 112-116]. ET-1 receptor

antagonist also showed promising results through inhibition of osteoblastic activity in many PCa bone metastases [117].

In addition, PCa cells also secrete some cytokines, which contribute to osteoblastic activity during PCa bone colonization. One of the factors is bone morphogenic protein (BMP). BMPs were showed to initiate osteoblast differentiation in vitro and in vivo [118, 119] as well as stimulate cancer cell migration [120]. Osteoblast-derived BMP-2 was shown to stimulate PCa cell migration; while, BMP-6 and 7 expression was significantly higher in osteoblastic bone lesions than the normal bone of PCa patients [120-124]. Introduction of BMP-6 antibody to mice with PCa cells led to the reduction of osteoblast number and increased tumor growth [125]. Similar effects could be observed as Noggin, a BMP antagonist, led to osteolytic induction instead of osteoblastic activity in PCa bone metastases [126]. These results suggested a role for BMPs in osteoblastic induction during PCa bone colonization. Another protein family affecting PCa bone metastasis is insulin-like growth factors (IGFs). In the normal bone remodeling process, IGFs could be released from bone matrix during bone resorption and promoted the activity of osteoblast in bone deposition [83, 127]. For PCa, IGF-I was upregulated in PCa bone metastases, and the level of IGF-I has been shown to correlate with PCa progression [128-133]. Even though overexpression of IGF-I in C4-2 and PC3 cells showed no significant effect on osteoblastic activity in vivo, an inhibitor of the IGF-I receptor led to the inhibition of PCa growth in vitro [34, 134]. Therefore, more research is needed to investigate the role of IGF-I in PCa bone colonization.

1.3.2 Blood Cells and PCa Bone Colonization

Since bone marrow is where hematopoiesis takes place, the effects of blood cells on PCa bone colonization have been investigated in many studies. In bone marrow, naïve immature myeloid cells (iMCs) could differentiate into mature macrophages, granulocytes and neutrophils. However, upon the interaction of bone microenvironment and tumor cells, iMCs differentiation was blocked leading to the production of myeloid-derived suppressor cells (MDSCs), which had immune suppressive capabilities and could promote tumor growth [52, 135-137]. MDSCs could promote tumor growth by secreting angiogenic factors as well as undergo differentiation into osteoclasts thereby leading to increased bone resorption [138-140]. MDSCs also produced TGF-β, which could promote parathyroid hormone related protein (PTHrP) expression in tumor cells thereby accelerating the vicious cycle during bone colonization by cancer cells. It has been shown that mice lacking myeloid-derived TGF-β showed a significant reduction in bone metastasis [141]. These data suggested the potential role of MDSCs in cancer progression; therefore, therapies targeted on preventing MDSC expansion and supporting MDSC differentiation are under investigated. In addition to MDSCs, tumor-associated macrophages (TAMs) have been shown to correlate with poor prognosis of PCa [142]. TAMs contributed to immune suppression by secreting anti-inflammatory cytokines as well as proteolytic enzymes, which support angiogenesis and the release of growth factors from bone matrix [143, 144]. For PCa, it was shown that PCa expressed chemoattractant protein called CCL2 or monocyte chemoattractive protein I, which could recruit TAMs and osteoclast precursors to metastatic sites. Moreover, bone marrow macrophages (BMMs) were shown to express capthesin K, another matrix

degrading enzyme that could promote the vicious cycle and tumor progression in PCa bone metastasis [145, 146].

In addition to MDSCs and macrophages, other immune cells including dendritic cells and T-cells also affect PCa bone colonization. Antigen presenting dendritic cells can be divided into two groups: myeloid dendritic cells (mDCs) and plasmacytoid dendritic cells (pDCs). The presence of pDCs was shown to correlate with many types of cancer including PCa [147]. pDCs were shown to secrete large amount of cytokines including interleukin (IL)-15, chemokine (C-C motif) ligand (CCL)5 and CCL2, which attracted and stimulated osteoclast activity [145, 148]. Even though it was not shown in PCa, depletion of pDCs led to a decrease in bone metastasis for breast cancer in vivo [149]. These studies suggested the role of pDCs in providing a pre-metastatic niche for the tumor. T cells also were shown to have dual roles in PCa bone colonization. Even though T cell-derived IL-17 and tumor necrosis factor (TNF)-α could function in an autocrine manner by simulating RANKL expression and promoting osteoclast differentiation, they also were known to produce interferon (IFN)-γ that could inhibit osteoclastogenesis [150, 151]. Accordingly, T cells showed both promoting and preventing potentials for tumor bone colonization. In PCa, regulatory T cells (Treg) were recruited to bone by CXCR4/CXCL12 signaling. Treg cells inhibited osteoclast differentiation in vitro, and the mice with PCa showed increased bone mineral density after the introduction of Tregs in vivo. These studies suggested that Tregs could play a role in osteoblastic PCa metastases [152]. In addition, mature megakaryocytes, the source of plasma platelets, were shown to affect PCa bone colonization as well. Expansion of megakaryocytes in bone marrow was shown to significantly reduce PCa bone metastasis in an animal model [153]. In direct

co-culture experiments, megakaryocytes significantly reduced PCa growth and induced PCa cell apoptosis [154]. With various effects of blood cells on PCa bone colonization, treatments targeting these cells are under investigated [155-157].

1.3.3 Bone Stromal Cells and PCa Bone Colonization

To study bone stromal : PCa cell interactions, a bone marrow stromal (BMS) cell line model developed by Roecklein and Torok-Storb [158] was used. These cells were generated from a bone aspirate from a 30 year-old healthy male donor. Adherent cells from the marrow samples were grown in long-term culture (LTC) media. Then LTCs were immortalized by retroviral LXSN-16 E6/E7 transduction. The clones were selected under G418 selection to derive HS-(1-27) BMS clones [158]. Two particular cell lines called HS-5 and HS-27a were used broadly due to their abilities to secrete wide range of cytokines and represented different groups of BMS cells from the hemaopoietic niche. It has been shown that conditioned media (CM) from HS-5 cells contained cytokines that support the proliferation of committed hematopoietic progenitor cells (CD^{38+}) [158-160]. This led to the hypothesis that HS-5 cells reside in the sinusoid area overlapping with committed hematopoietic progenitor cells; therefore, they could be located in one of the first microenvironments that PCa cells encountered after extravasation from nearby vessels during PCa bone metastasis. On the other hand, HS-27a was shown to support only cobblestone area formation for hematopoietic stem cells (CD^{38low}). This suggested the location of HS-27a habitat located more toward the endosteal area in bone [160].

Once co-culture with metastatic PCa, PC3 cells, HS-27a expressed increasing levels of some extracellular matrices (versican and tenascin) and chemokines (CCL5, CXCL5 and CXCL16) [161]. On the other hand, HS-5 showed the upregulation of

soluble N-cadherin and CXCR7 when co-cultured with PC3 cell. Interestingly, PC3 showed upregulation of several MET related genes including α6 integrin, E-cadherin and N-cadherin when co-culture with HS-5 cells along with these changes the growth rate of PC3 in co-culture with HS-5 decreases [162]. Moreover, both co-culture models and CM from metastatic PCa, C4-2 cells and bone adaptive, C4-2B were showed to suppress endoglin, an auxiliary co-receptor for TGF-β signaling, in HS-5, HS-27a and primary bone stromal cells. Similarly, CM from PC3, DU145 and C4-2B led to lower TGF-β secretion and decreased cell proliferation in HS-5 and HS-27a [30]. These suggested that PCa cells produce cytokines that could suppress or alter TGF- β signaling in BMS cells. When BMS cells derived from an osteosarcoma specimen were co-cultured with androgen sensitive PCa, LNCaP cells, LNCaP underwent genetic, morphological and behavioral changes to a more aggressive phenotypes [163]. These data indicate the interactions between BMS cells and PCa cells induced both genetic and phenotypic changes in response to each other.

Despite the famous 'seed and soil' theory from Paget where the metastatic sites would provide a favorable environment supporting tumor growth and colonization [25], other explanations were suggested for PCa bone metastasis. It has been shown that circulating DPCs are genetically heterogeneous, while cells in tumor masses at metastatic sites show genetic homogeneity [164, 165]. This suggested that heterogeneous circulating DPCs might be selected to survive under pressure from the new bone environment pressure in Darwinian manner to develop genetically homogeneous metastases [53, 165, 166]. This hypothesis corresponded to the recent data from Sikes' lab and others showing the negative interactions between PCa cells and the bone microenvironment [29-33, 167]. Specifically, data from Sikes' lab has

shown that HS-5 cells secreted paracrine factor(s) inducing LNCaP, C4-2 and C42B cell death via apoptosis. Correspond to the Darwinian selection hypothesis mentioned; the surviving cells undergo neuroendocrine differentiation (NED), which has been shown to correlate with an aggressive phenotype of PCa [31-33]. As one of the factors from HS-5 CM responsible for PCa NED induction was identified to be IL-6 [31], the factor(s) contributing to PCa cell death are still unidentified. Even though several attempts have been made to investigate the reciprocal interactions between PCa cells and BMS, these interactions still remain elusive. Accordingly, identifying this HS-5 derived factor(s) (HS-5 DF) that induce PCa apoptosis would be an essential step forward in understanding the initial mechanism of PCa bone colonization and/or providing a novel therapy to prevent bone colonization or slow the growth of bone metastases.

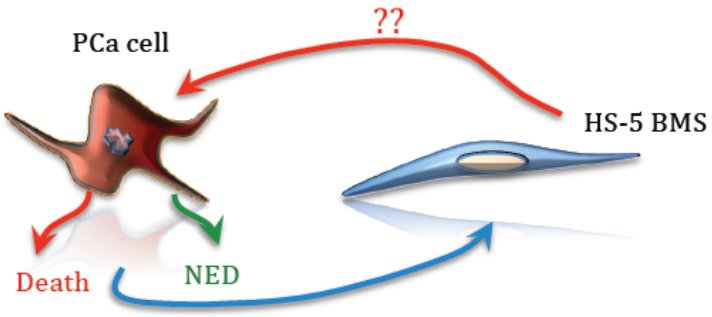

Figure 1: The model shows reciprocal interactions between PCa cells and HS-5 BMS cells showing PCa apoptotic inducing effect by unidentified paracrine factor(s) secreted by HS-5 BMS cells. The surviving cells would undergo NED to a more aggressive phenotype (courtesy Dr. Robert A. Sikes)

1.4 Fibulin Protein Family

Fibulins are a family of secreted glycoproteins characterized by the presence of two structural modules: repeated epidermal growth factor (EGF)-like modules and a unique C-terminal fibulin-type module [168-170]. They are known to have various structural roles in ECM and embryonic development. However, some research has shown that they also can modulate many biological processes, such as cell growth, adhesion, migration and tumorigenesis [168, 169, 171]. Fibulin structures consist of 3 domains: domain I, II and III. Domain I is called the N-terminal domain and contains the signal peptides, which are variable among the family members. In some fibulin members, this domain also contains an anaphylotoxin-like (AT) module that has structural similarity to proteins in the complement system involved in inflammation and immune responses. Domain II represents the central portion of fibulins. It contains a varied number of EGF- like modules, where some of them are modified to have a specific calcium binding site called the calcium binding EGF-like (cbEGF) domain. Lastly, domain III consists of C-terminal modules, which are different structurally between the family members and various isoforms; therefore, this area is called fibulin-type (FC) domain [168, 171, 172].

To date, 7 fibulin family members have been discovered, which are expressed from different genes. Fibulin-1 was the first fibulin discovered in 1989 by affinity chromatography to investigate proteins interacting with the β subunit of the fibronectin receptor [173]. After that, fibulin-2 and fibulin-3 were discovered by comparative sequence analysis of a cDNA library of mouse fibroblast and senescent human diploid fibroblasts (HDF), respectively [174, 175]. Fibulin-4 also was cloned from sequence homology gene searches for new fibulin members; however, fibulin-5 was isolated from vascular smooth muscle cells in the study for genes that regulate the

transition of cells from a quiescent to proliferative state [176-178]. Fibulin-6 was identified in *Caenorhabditis elegans* as a gene that was important for cell-cell and cell-matrix interactions [179]. Lastly, fibulin-7 was identified as a gene associated with odontoblast differentiation and dentin formation [180]. Fibulin members could be divided into 2 main groups. The first group includes fibulin-1 and fibulin-2, both of which contain 3 AT modules in the N-terminal domain contributing to the total size of 100 kDa and 200 kDa, respectively. The second group, however, consists of fibulin proteins without AT modules including fibulin-3,-4,-5,-6 and -7. Except for fibulin-6, other members in this group are in the range of 50-60 kDa and mostly do not contain any recognizable module s/protein motifs in domain I. In contrast, fibulin-6 is comprised of 44 tandem immunoglobulin and 6 thrombospondin type-1 modules in domain I bringing the size of fibulin-6 to as large as 600 kDa [169].

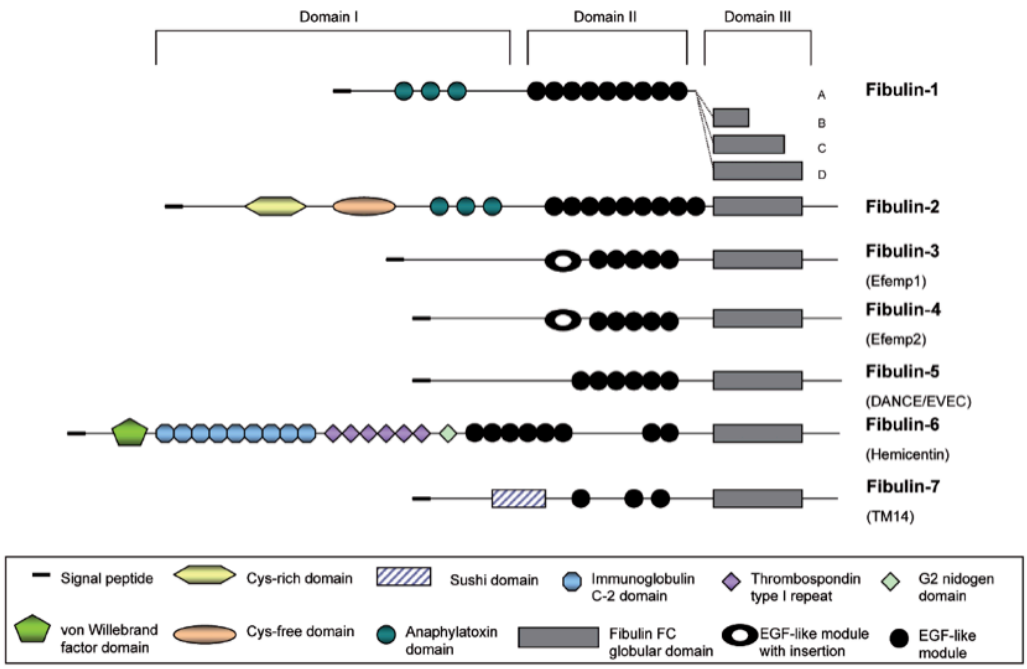

Figure 2: Domain structures of the fibulin protein family. All fibulins consist of 3 main domains: domain I, II and III. Domain I contains signal peptides for all members with special modules in fibulin-1,-2,-6 and -7. Domain II is the middle portion with tandem repeats of EGF-like modules, and domain III contains the divergent fibulin FC module, which identifies the specific type of fibulin. (used with permission [180])

With their abilities to interact with many ECM proteins, the expression of fibulin family members was found in many connective tissues. Fibulin-1 and fibulin-2 have overlapping expression in many organs [181-184]. Both of them were expressed highly in areas in which polarized epithelial cells undergo EMT during development, such as, endocardial cushion tissues, perichondrial structures and neural crest. Both of them continue to be expressed in basement membranes and cartilage [184, 185]. While fibulin-1 is found in the walls of in great vessels, brain, kidney, lung and liver [184], fibulin-2 is expressed mainly in the heart, placenta and ovary [171]. During embryonic organogenesis, fibulin-1 was shown to play an important role and highly expressed during digit and limb formation [186]; in contrast, similar effects were seen during heart development for fiblin-2 [185]. Fibulin-3 was found in mesenchyme that later developed into bone and cartilage [187]. It was shown to be important in the development of bone and cartilage in the cranial area, ribs, vertebrae, appendicular skeleton as well as the regulation of skeletal shape in the body [187, 188]. Fibulin-4 was shown to be expressed highly in the heart and vessel walls, moderately in skeletal muscle, but weakly expressed in other connective tissues, such as brain, lung, pancreas and kidney [176, 189]. Compared to fibulin-1, -2 and -3, fibulin-4 was not shown to have significant roles during developmental process; however, it was shown that the level of fibulin-4 correlated with the prognosis of osteoarthritis [189]. Fibulin-5 was shown to be expressed primarily in regions undergoing EMT during development as well as in elastic tissues, such as the dorsal aorta, vascular smooth muscle of great vessels, heart, ovary, kidney, testes and pancreas [170, 171, 177, 178]. Fibulin-5 was shown to have a crucial role in the assembly of elastic fibers functioning as an intermolecular bridge between microfibrils [170, 190]. In addition, fibulin-5 could

interact with TGF-β latent binding protein 2 (LTBP-2), a protein that also affected elastic fiber assembly [191]. Fibulin-6 is expressed in retinal epithelial/endothelial cells and skin fibroblasts [192, 193]. The physiological functions of fibulin-6 have not been elucidated completely. Nevertheless, recent studies showed that it might be associated with cardiac fibroblast migration during heart failure and age-related macular degeneration [193, 194]. The last family member, fibulin-7 was found expressed in teeth, placenta, cartilage and hair follicles. It was shown that fibulin-7 functioned in tooth development with high expression in pre-odontoblasts and odontoblasts [180]. Regardless to the structural roles that fibulin family members play in connective tissues and development, the effects of fibulins, especially fibulin-1 in other diseases, including cancer has been noted in several recent studies, which will be the focus of the next part of this introduction.

1.5 Fibulin-1: Structures and Physiological Functions

In humans, the fibulin-1 gene (FBLN1) is located on the long arm of chromosome 22 at position 22q13.31 [170, 172, 195]. As the first family member identified, the fibulin 1 structure has been well studied. This 90-100kDa protein is comprised of three domains including the amino-(N-)terminal domain, the central domain and the carboxy-(C-)terminal domain with a structure similar to other types of fibulin. The N-terminal domain consists of three anaphylatoxin-like (AT) modules. Each ~40 amino acid long module contains four to six cysteines that are responsible for three disulfide bridges stabilizing its α-helix structure. The central domain consists of nine 40 amino acid long EGF-like modules, also stabilized by three disulfide bonds each. Most EGF-like modules contain consensus cbEGF-like modules. Lastly, the C-terminal domain is composed of a ~120-140 amino acid long fibulin type specific

module which specifies the subtypes of fibulin-1. To date, four different isoforms of fibulin-1 have been identified due to alternative splicing and are designated fibulin-1A, -1B, -1C and 1D. The four isoforms are different from each other in their domain III ranging from lacking of domain III in isoform 1A, containing short 35 residues in isoform 1B, or consisting of longer 117 and 137 residues for 1C and 1D, respectively [172]. While fibulin-1A and 1B were barely detected in human placenta, fibulin-1C and 1D are expressed in most tissues and cell cultures [171, 172, 195].

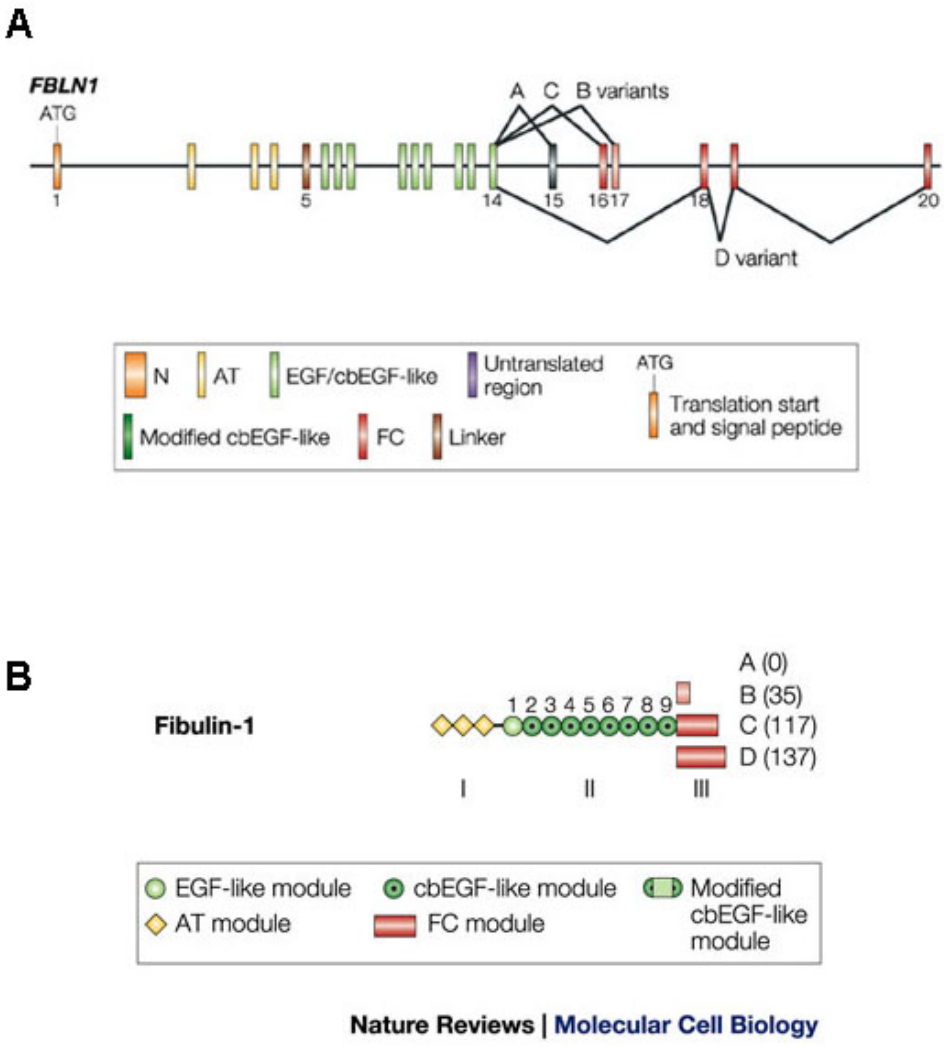

Figure 3: A) mRNA structure for fibulin-1 mRNA showing exon and intron components for each fibulin-1 isoform due to alternative splicing. Fibulin-1 isoforms are different after exon 14. After exon 14, fibulin-1A, 1B and 1C consist of exon 15, 16 and 17 respectively; while, fibulin-1D is comprised of 3 exons: exon 18, 19 and 20. B) Modular structures of fibulin-1 isoforms with different length of FC domain corresponding to the different exons picked from alternative splicing. (used with permission [172])

Fibulin-1 has been shown to interact with many ECM proteins including laminin, aggrecan, versican, nidogen, elastin and tropoelastin. Therefore, its possible role in ECM assembly and stability have been noted [171]. Fibulin-1 co-localized with fibulin-2 in elastic fiber, especially in aorta and neuronal structures [171, 172]. With the interaction with tropoelastin, fibulin-1 was shown to play a role in elastin nucleus assembly during elastic fiber assembly [196]. Fibulin-1 also was shown to interact with fibronectin and associated with fibronectin-based fibrils produced by fibroblasts and other cell types [182, 197]. It also was localized to basement membranes in many tissues and interacted with basement membrane components specifically fibronectin and nidogen [198, 199]. This suggested its potential to affect other cellular processes via these molecules, such as cell migration and cell proliferation [171, 200]. Moreover, fibulin-1 was shown to interact with the large chondroitin sulfate proteoglycans aggrecan and versican in cartilage to link these ECM proteins thereby providing stability and providing a mechanism to strengthen cartilage [201]. The interaction between fibulin-1 and a disintegrin-like and metalloprotease with thrombospondin motifs proteases (ADAMTS) was noted. It was shown to enhance ADAMTS activity to cleave aggrecan suggesting its role in tissue remodeling regulation [202]. Moreover, fibulin-1 was shown to interact with sex hormone-binding globulin (SHBG) indicating its ability to regulate steroid hormone activity by sequestering SHBG in the ECM [203]. Other than as one of the ECM components, a soluble form of fibulin-1 was detected at a relatively high concentration in human and mouse serum (10-50 μg/ml) [195, 204, 205]. This suggested other possible functions of circulating fibulin-1 in the body. In addition to its structural roles, it was shown to be one of the binding partners for fibrinogen and was incorporated into fibrin clot. It

also could function as a bridge between cells and fibrinogen assisting in platelet adhesion during the blood clotting process [206, 207].

Fibuln-1 expression was predominant in areas where cells underwent EMT during embryonic development including endocardial cushion, hair follicles, tooth and neural crest [184]. The importance of fibulin-1 during developmental processes was highlighted in many animal studies. In the first experiment, mouse models lacking of fibulin-1 were created by homologous recombination in embryonic stem cells. These animals underwent hemorrhage in their cranial mesenchyme, skin and skeletal muscles. These models also showed endothelial abnormalites as well as defective renal glomeruli, which failed to develop properly. Most mice died within 24-48 hrs after birth indicating severe phenotypes associated with a lack of fibulin-1 [208]. Another study using mice lacking of fibulin-1 derived from gene trap insertion techniques reported similar effects of lethal hemorrhage and early death. In addition, these mice showed the abnormalities in their arteries, pharyngeal glands, nerves and cephalic skeleton [209]. In fibulin-1 knockout *C. elegans,* the organisms showed smaller size features and defective gonads [210]. These results suggested a central role for fibulin-1 in embryonic development in mice and *C. elegans*. In addition, rescue experiments for fibulin-1 knockout *C. elegans* revealed isoform specific functions of fibulin-1C and 1D to be responsible for different parts of organ development [210]. Furthermore, some researches pointed out that the level of fibulin-1 affected eye development and is involved in eye disorders. Both fibulin-1 and fibulin-4 were associated with retinopathies [211]; and, the elevated levels of fibulin-1 and fibulin-3 were found in murine models of retinopathy, especially the ones with rod photoreceptor degeneration [212]. These experiments suggested that not only the

expression of fibulin-1 is needed for proper development, but also the level of fibulin-1 needs to be tightly regulated for normal developmental processes to occur. In humans, chromosomal translocation of FBLN1 was involved in synpolydactyly (malformation of the hands), a dominant inherited disease causing metacarpal and metatarsal synostoses (bone fusion) [213]. A chromosomal translocation at intron 19 (last intron) for FBLN1 gene was hypothesized to involve in abnormal cell migration and apoptosis during digit formation leading to digit malformation [171]. In addition, a defect in fibulin-1D caused by mutation of exon 19 in the FBLN1 gene was associated with autosomal dominant giant platelet syndromes causing deafness, renal disease and eye abnormalities [214].

1.6 Fibulin-1 and Cancer

Dual roles of fibulin-1 in cancer have been suggested by many research groups. Overexpression of fibulin-1D and purified fibulin-1 proteins, which contain equal amount of fibulin-1C and -1D isoforms, have been shown to inhibit cell motility, adhesion and invasion in many types of cancer including epidermal carcinoma, breast cancer, melanoma, fibrosarcoma, ovarian cancer and renal carcinoma [215-218]. Elevated expression of fibulin-1D suppressed anchorage-independent growth and induced apoptosis of human fibrosarcoma-derived cells in vitro, while delaying tumor formation in vivo [216, 219]. In addition, fibulin-1D has been shown to inhibit papillomavirus-E6-protein-mediated transformation, potentially through direct protein-protein interaction [220]. Moreover, downregulation of FBLN1 has been shown in many types of cancer supporting its tumor suppressive potential. FBLN1 was shown to be downregulated through promoter methylation in gastric cancer, renal carcinoma and hepatocellular carcinoma [218, 221, 222]. Another group

also showed a significant decrease in fibulin-1C and -1D mRNA in PCa cells and prostate cancerous tissue compared to benign tissue [223]. It has been suggested that downregulation of fibulin-1 correlates with renal carcinoma progression; while, overexpression of fibulin-1 causes a significant decrease in renal cancer cell growth, enhanced cell apoptosis and decreased cell motility and angiogenesis in vitro and in vivo [218].

While the tumor suppressive role of fibulin-1, especially fibulin-1D, has been demonstrated clearly in previous studies, others have revealed differential effects associated with the splice-variants fibulin-1C and -1D. Ectopic expression of fibulin-1C and -1D showed contrasting effects on cellular activity [168]. Moreover, the opposing effects of fibulin-1C to fibulin-1D have been shown in breast cancer and ovarian cancer [224-227]. Increased expression of fibulin-1C:1D mRNA ratio has been observed in ovarian carcinomas compared to normal ovaries [224]. Even though the ratio between the two splice variants has not been quantified in breast cancer, elevated levels of fibulin-1 have been observed in breast cancer [225, 226]. This suggests an oncogenic role of fibulin-1C contrasting to the tumor suppressive role of fibulin-1D. The suggested mechanism behind fibulin-1C preference in breast cancer and ovarian cancer was thought to be regulated by estrogen. In this context, estradiol treatment significantly decreased the half-life of fibulin-1D mRNA in breast cancer while preferentially inducing expression of fibulin-1C in ovarian and breast cancer [224, 228]. Therefore, the balance between splice-variant-specific activities of fibulin-1 could be an important factor contributing to its oncogenic or tumor suppressive role in cancer progression including PCa.

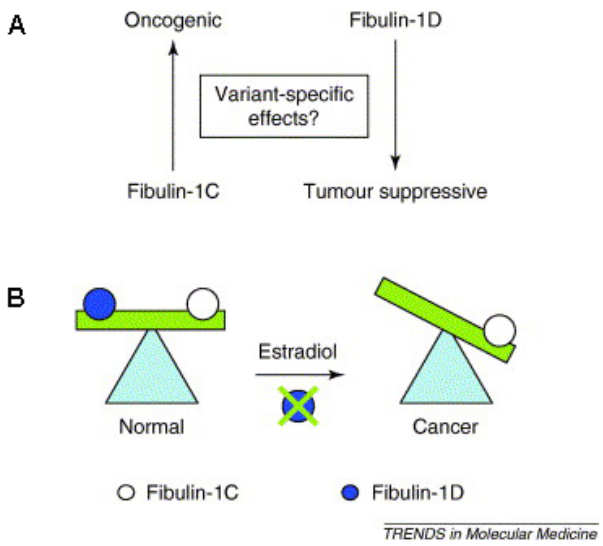

Figure 4: A) proposed splice variant specific activities of fibulin-1C and fibulin-1D in tumorigenesis B) The proposed model for fibulin-1 isoforms and their roles in ovarian caner. The balance between the two isoforms was needed to keep the cells normal. However, upon the exposure of estradiol, the expression of fibulin-1D was reduced significantly leading to the imbalance between the two isoforms and the predominance of fibulin-1C, which had tumor supportive/enhancing effects. (used with permission [168])

Chapter 2

MATERIALS AND METHODS

2.1 Cell Lines and Cultures

LNCaP, C4-2 and C4-2B isogenic human PCa cell lines were maintained in T-medium (Gibco, 02-0056DJ) supplemented with 5% (v/v) fetal bovine serum (FBS) (Atlas Biologicals, F-0050-A). Benign prostatic hyperplasia-1 (BPH-1) cells were also maintained in T-medium with 5% FBS. Human bone marrow stromal cell lines, HS-5 and HS-27a, were maintained in Dulbecco's Modification of Eagle's Medium (DMEM) (Corning cellgro, 10-013-CV) supplemented with 10% (v/v) FBS. The human embryonic kidney cell line, HEK293 was maintained in Minimum Essential Medium Eagle (MEM) (Corning cellgro, 10-010-CV) with 10% FBS (v/v). Unless specifically stated, all cells were maintained at 37°C in a humidified atmosphere of 95% air and 5% CO_2. Media was changed three times a week.

2.2 Conditioned Media (CM) Collection and Usage

CMs were collected from 100% confluent plates of each cell line. The cell lines were maintained in the suitable media supplemented with FBS as mentioned, and were fed fresh media 24 hours before CM collection. Then, cells were rinsed twice with PBS solution, and the media were replaced by serum free media (SF); SF-DMEM (Corning cellgro, 17-205-CV) for HS-5 and HS-27a and SF-MEM (Corning cellgro, 17-305-CV) for HEK293. CM was harvested every 48 hours for 4 days, and CMs from the same collection period were used in comparison to each other. Before use,

CMs were filtered through 0.22 μm filter (EMD Millipore, SE1M179M6) to remove any floating cells or debris. Unless specifically stated, all CM treatments on PCa cells were done with 1:1 (v/v) of CM: 5% FBS supplemented T-media for 48 hours.

2.3 Biochemical Characterization of HS-5 DF

2.3.1 Trypsin Digestion

Total protein content in HS-5 CM was assayed by using Pierce 660 nm protein assay kit (Thermo scientific, 22660). Then, trypsin (Sigma, T-497) was added to CM at 1: 2 (w/w) of trypsin: total protein content. The solution was incubated at 37°C for 20 hours. After that, trypsin was inactivated by the addition of trypsin inhibitor (Sigma Aldrich, T6522) 1:2 (w/w) of trypsin inhibitor: trypsin followed by the incubation at 37°C for 15 minutes according to the manufacturer's protocol. The activity of HS-5 CM was compared to the control CM from the original pull.

2.3.2 Heat Sensitivity Test

Same batch of HS-5 CM was divided into 3 groups. The first group was exposed to 37°C, which is a default temperature for HS-5 CM treatment. The second group was exposed to 70°C, and the last group was exposed to 100°C. All heat exposure lasted for 15 minutes; then the CMs were cooled down to room temperature and returned to 37°C before introducing to PCa cells.

2.3.3 pH Stability Test

HS-5 CM was divided into 3 groups: pH 4, pH 7 (default pH for HS-5 CM) and pH 10. CMs were adjusted to a designated pH by 1N HCL and 1N NaOH and left

at 4°C for 48 hours. The pHs then were adjusted back to pH 7 and warmed up to 37°C before introducing to PCa cells.

2.3.4 Size Selection

HS-5 CM was filtered through Amicon Ultra-15 centrifugal filters for 30 kDa (Millipore, UFC9030024) and 100 kDa (Millipore, UFC910024) cutoff. After adding 15 ml of HS-5 CM into the devices, the tubes were centrifuged at 550 x g. The devices were centrifuged for 40 minutes and 15 minutes for 30 kDa and 100 kDa filters respectively. After that, retentate fractions containing proteins that are bigger than the filter size were re-adjusted back to the original volume with SF-DMEM.

2.3.5 Disulfide Bond Reduction with Dithiothreitol (DTT)

DTT (Sigma Aldrich, D-0632) was added to HS-5 CM to achieve 10 mM concentration. The CM was then left at 25°C for 48 hours. According to the manufacture (Sigma Aldrich), the half-life of DTT at 20°C is 10 hours. Therefore, the treated CM was left at 4°C for at least a week to ensure that all DTT had been degraded before introducing the CM to PCa cells.

2.3.6 Protein Concentration for HS-5 CM

The same batch of HS-5 CM was divided into control HS-5 CM and HS-5 CM that would be used for protein concentration. Two hundred microliters of HS-5 CM was aliquoted to each 1.5 mL centrifuge tubes. The samples were concentrated using a speed vacuum concentrator (Savant) at 4°C for 10 minutes to achieve ¼ of the original volume (50 µL). For functionality test, the concentrated samples were re-adjusted back to the original volume by SF DMEM. PCa cell death induction was compared between HS-5 CM before and after the concentration process.

2.4 Apoptosis Assay

All PCa cells were plated at $1x10^5$ cells/well in tissue culture grade 24-well plates (Greiner Bio-One, 662160). Twenty-four after plating, half of the media was replaced by the proper HS-5 CM/treatments to achieve 1:1 ratio of T-media with 5% FBS:treatment (2.5% final FBS). The cells were left in CM for 24 hours before harvesting using 50 mM EDTA (Gibco, 15575-038). Apoptosis assay was performed on collected cell pellets by using Cell Death Detection ELISAplus kit (Roche, 11774425001), which measured DNA fragmentation.

2.5 Live/Dead Assay

All PCa cells were plated at $1x10^5$ cells/well in tissue culture grade 6-well plates (Corning, 3516). After letting the cells attach for 24 hours, half of the media was replaced by the CM treatments to achieve 1:1 ratio of T-media with 5% FBS:treatment. The cells were treated for 48 hours. After 48 hours, the cells were simultaneously treated with calcein AM and ethidium homodimer using Live/dead viability /cytotoxicity kit for mammalian cells (Invitrogen, L3224) to stain live and dead cells respectively. After 30 minutes of incubation, the pictures from at least 5 different fields in each treatment were visualized and captured under fluorescent microscope (Nikon, TE 2000E). The quantification was done by using Photoshop (Adobe Photoshop CS6) to measure pixel density for green (living cells) and red (dead cells) to obtain average dead/live ratio in each treatment. Previously, Sikes' lab demonstrated a direct correlation between pixel density and cell number (data not shown)

2.6 Transforming Growth Factor-Beta 1 (TGF-B1) Treatment on HS-5 Cells

Fifty percent confluent HS-5 cells were treated with TGF-β1 (R&D systems, 240-B-010) to achieve the final concentration of 10 ng/mL in DMEM containing 10% FBS. The treatment was refreshed everyday by half-changes of the media with TGF-β1 for 4 days. After that, the cells were rinsed twice with PBS followed by additional washes using SF-DMEM for three times (5 minutes each). Media was then replaced by SF-DMEM to start CM collection cycles as described above.

2.7 Sodium Dodecyl Sulfate Polyacrylamide Gel Electrophoresis (SDS-PAGE) and Silver Staining

SDS-PAGE was performed on 5%-11% gradient polyacrylamide gel with 3.3% bis-acrylamide. 2.5 μg of proteins from CM was used for the gels under reducing conditions. The first gel was run at 275 V for 12 hours at 4°C followed by silver staining using Pierce Silver Staining kit (Thermo scientific, 24612) according to manufacturer's protocol (Figure 17). Another gel run under the same conditions (Appendix A) was stained with SYPRO Ruby stain using SYPRO Ruby protein staining kit (Biorad, 170-3125) according to the manufacturer's protocol before being used for MS/MS.

2.8 Tandem Mass Spectrometry (MS/MS)

MS/MS was performed by the cooperation with Dr. Kelvin Lee and Dr. Leila Choe at Delaware Biotechnology Institute (DBI) according to this protocol. The gel bands showing differential expression with TGF-β1 treatment were excised for analysis. Trypsin (Promega, V5111) digestion was performed at 37°C as previously described [229] including reduction/alkylation with DTT (BioRad, 161-0611) and iodoacetamide (Sigma Aldrich, I1149), respectively. Subsequently, the samples were

desalted and concentrated using Ziptips (Millipore) and applied to a target plate with alpha-Cyano-4-hydroxycinnamic acid matrix (Sigma Aldrich, C8982). Data were collected on a 4800 MALDI TOFTOF Analyzer (ABSciex) in positive ion, reflector mode over a mass range of 900-4000 m/z, with internal calibration. Selected peaks were analyzed further by MS/MS at 1kV with default calibration. The combined MS and MS/MS data were submitted to Mascot v2.2 (Matrix Science) and searched against NCBI database, with trypsin specificity, 75ppm mass tolerance, 0.3 Da MS/MS tolerance, and the following variable modifications: carbamidomethylation (C) and oxidation (M). The protein identification was made based on a database match of 95% confidence or greater, including four MS/MS matches >99% confidence.

2.9 Western Blot Analysis

Cell pellets were collected from 100% confluent cells grown on 100 mm tissue culture dishes (Greiner Bio-One, 664-160) by either scraping in 1 mL of T-media (Figure 18A, 21A, 23A, and Appendix C) or treating with 50 mM EDTA (Figure 19A) after rinsing once with PBS for 30 seconds. Cell pellets were lysed for 45 minutes in modified Radioimmunoassay precipitation (RIPA) buffer containing 50 mM Tris–HCl pH 7.4, 1% Triton X-100, 0.25% deoxycholate, 150 mM NaCl supplemented with Roche complete Minitabs (Roche, 04693124001) and Halt Phosphatase inhibitor cocktail (Thermo scientific, 78420) at the supplier's recommended concentration. Cell pellet samples were incubated for 45 minutes on ice to get protein extracts. After that the samples were centrifuged at 5000 rpm at room temperature for 5 minutes. The supernatants were collected as protein samples. Protein concentration for cell pellet samples was obtained by using BCA protein assay kit (Pierce, 23225), and protein concentration for CMs was obtained by using Pierce 660 nm protein assay kit (Thermo

scientific, 22660) according to manufacture's protocols. Fifteen microgram of proteins were subjected to SDS-PAGE using 4–12% Bis–Tris polyacrylamide gels (Life Technologies, BG04125BOX) in Bolt™ MES SDS running buffer (Life Technologies, B0002) at 165 V for 40 minutes at room temperature and transferred at 55 V to BA85 nitrocellulose membrane (GE, 10401196) using Bolt™ transfer buffer (Life Technologies, BT00061) at 4°C overnight. Membranes were blocked for 1.5 hours at room temperature in blocking buffer containing 4% w/v bovine serum albumin (BSA) in 0.1% v/v Tween 20 in tris buffer saline (TBST). All blots were incubated in primary antibody and secondary antibody diluted in blocking solution at 4°C overnight and at room temperature for 75 minutes, respectively. The blots were washed 3 x 5 minutes in between blocking and incubations with TBST. Primary antibodies used in this study included mouse anti fibulin-1 monoclonal antibody (Abcam, ab54652) at 1:2000 dilution and rabbit anti actin monoclonal antibody (Sigma Aldrich, A2066) at 1:5000 dilution. Secondary antibodies included anti-mouse IgG conjugated with horseradish peroxidase (HRP) (Cell Signaling Technology, 7076) at 1:5000 dilution and goat anti-rabbit IgG conjugated with horseradish peroxidase (Cell Signaling Technology, 7074) at 1:5000 dilution. Proteins were visualized by autoradiography using enhanced chemiluminescence (ECL), an HRP chemiluminescent substrate (Millipore, WBKLS0500) and exposed to Kodak Min R 2000 film (Kodak, 181 1884).

2.10 Quantitative Reverse Transcription Polymerase Chain Reaction (qRT-PCR)

Total cellular RNA from cell lysates was isolated using the RNeasy mini kit (Qiagen, 74104) according to the manufacturer's instructions. Following extraction, RNA samples were treated with RNAse-free DNase I (Roche, 04716728001) to

eliminate contaminating DNA according to manufacturer's protocol. RNA quality and quantity were analyzed spectrophotometrically using a NanoDrop ND-1000 spectrophotometer with software version 3.1.2 (Thermo Scientific) and electrophoretically (Appendix B). For electrophoresis, 5 μg of total RNA was separated in 0.8% w/v agarose in 0.5X Tris-acetate EDTA (TAE) buffer with 0.5 μg/mL ethidium bromide at 100 V for 45 minutes at room temperature. After the quality check, 5 μg total RNA was reverse transcribed in a final volume of 20 μL using Maloney murine leukemia virus (M-MLV) reverse transcriptase (Life Technologies, 28025- 013) in 50 mM Tris-HCl, 75 mM KCl, 3 mM $MgCl_2$ buffer provided by supplier and according to supplier's protocol. qRT-PCR was performed on an Applied Biosystems 7300 Real Time PCR system. Each well contained 20 ng of cDNA, 12.5 μL of Applied biosystems: power SYBR Green PCR Master Mix (Life technologies, 4367659), 1 μL each of 10 μM forward and reverse primers and ddH_2O to the final volume of 25 μL. The primers used in this experiment included fibulin-1 common forward primer (5' CCG CTG CCT GGC CTT CGA 3'), fibulin-1C reverse primer (5' CCT CCT CAT TGC CGC CG 3'), fibulin-1D reverse primer (5' CCG CAG GTT CCC TTC CG 3'), GAPDH forward primer (5' CAG GCC GGA TGT GTT CGC 3') and GAPDH reverse primer (5' CGT TCT CAG CCT TGA CGG TG 3'). After an initial denaturation at 95°C for 1 minute, the following cycles were used throughout this experiment: 40 cycles of 95°C for 15 seconds and 61°C for 1 minute. Relative expression levels of fibulin-1C and fibulin-1D were calculated from $2^{-\Delta Ct}$ value of each fibulin-1 isoform to house keeping gene (GAPDH) (Figure 20A). Relative gene expressions of fibulin-1C and fibulin-1D upon TGF-β1 treatment were

calculated from $2^{-\Delta\Delta Ct}$ value of each fibulin-1 isoform to house keeping gene and to the control groups (Figure 20B).

2.11 Immunoprecipitation (IP)

1.4 mL of HS-5 CM was pre-cleared with 50 µL PBS-washed protein A agarose beads (Cell signaling, 9863) on rotating shaker at 4°C for 2 hours. The beads were then removed from the CM by centrifuging at 600 rpm for 1 minute as suggested by the manufacturer's protocol. After pre-clearing, rabbit anti fibulin-1 monoclonal antibody (Abcam, ab175204) was added to the sample subjected to IP for fibulin-1, and rabbit (DA1E) monoclonal antibody IgG isotype control (sepharose ® bead conjugate) (Cell signaling, 3423S) was added to the sample subjected to IP by isotype control antibody at 1:70 (w/w) ratio to the samples. The antibodies were incubated with samples on a rotating shaker at 4°C overnight. Then, 50 µL of PBS-washed protein A agarose beads was added to samples again to precipitate the protein-antibody out. The beads were incubated with the samples at 4°C for 4 hours before being centrifuged at 600 rpm for 1 minute to collect the IP samples. IP samples were washed with 1 mL of cold PBS for three times before being mixed and boiled in Bolt® LDS Sample Buffer (Life technologies, B0007) at 100°C for 5 minutes. The boiled IP samples were then centrifuged to obtain protein sample in the supernatants, which then were used in western blot analysis or live/dead assays. After IP, the CMs were filtered through 0.22 µm filters (EMD Millipore, SE1M179M6) before being used to treat the cells and as the samples for western blot analysis.

2.12 Generating of Fibulin-1 Knockdown HS-5 Cells (HS-5^{CRISPR_fib1}) with CRISPR-Cas9 System

The protocol in this section was performed according to Ran, et al. (2013) [230]. To generate fibulin-1 knockdown HS-5 cells, pSpCas9(BB)-2A-GFP plasmids for CRISPR-Cas9 system carrying a GFP marker were used (Addgene, PX485). gRNA targeted on fibulin-1 gene was designed by using an online CRISPR designing tool (http://tools.genomeengineering.org) [230]. The target for gRNAs in this experiment was on exon 11 of fibulin-1 gene (gRNA_fib1) using the following sequences: 5' CAC CGC TGG TAG GAG CCG TAG ACG T 3' (top strand) and 5' AAA CAC GTC TAC GGC TCC TAC CAG C 3' (bottom strand). gRNAs were phosphorylated and annealed in the reaction containing 1 µL of T4 polynucleotide kinase (New England Biolabs, M0201S), 1 µL T4 ligation buffer 10X (New England Biolabs, B0202S), 6 µL of ddH_2O and 1 µL each of 100 µM gRNA_fib1 top strand and 100 µM gRNA_fib1 bottom strand. The phosphorylation and annealing process was incubated at 37°C for 30 minutes, 95°C for 5 minutes and ramp down to 25°C at 5°C/minute.

The phosphorylated and annealed oligos were diluted at 1:200 dilution with room temperature ddH_2O. Then the oligos were cloned into pSpCas9(BB)-2A-GFP plasmid with the reaction containing 100 ng of pSpCas9(BB)-2A-GFP, 2 µL of diluted oligos, Fermentas Tango buffer (Fermentas/Thermo Scientific, BY5), 1 µL of 10 mM DTT (Fermentas/Thermo Scientific, R0862), 1 µL of 10 mM Adenosine 5' triphosphate (ATP) (New England BioLabs, P0756S), 1 µL of FastDigest BbsI (Fermentas/ Thermo Scientific, FD1014), 0.5 µL of T7 DNA ligase with 2X rapid ligation buffer (Enzymatics, L602L) and ddH_2O to the final volume of 20 µL. The reaction would be incubated at the following condition: 6 cycles of 37°C for 5 minutes

and 21°C for 5 minutes. After that, these ligated plasmids were treated with PlasmidSafe exonuclease to digest any linearized plasmids that might have been left in the reaction. This step consisted of 11 µL of ligation reaction, 1.5 µL of PlasmidSafe buffer 10X (came with the enzyme), 1 µL of PlasmidSafe exonuclease (Epicentre, E3101K), 1.5 µL of 10 mM ATP (New England BioLabs, P0756S). The PlasmidSafe reaction was incubated at 37°C for 30 minutes followed by 70°C for 30 minutes to inactivate the exonuclease.

Circularized vector was transformed into *E. coli* DH5α. Two nanograms of plasmid vector was added to 50 µL of competent ice-chilled *E. coli* DH5α. Heat shock was performed at 42°C for 90 seconds, then 200 µL of Super Optimal broth with Catabolite repression (SOC) medium was added to the transformed cells for *E. coli* recovery. The bacterial suspension was shaken horizontally in an orbital shaker for 1 hour at 37°C. After shaking, 100 µL of the bacterial suspension was spread on LB agar plate containing 100 µg/mL ampicillin. The plate was incubated agar up at 37°C overnight. Single isolated colonies were picked and transferred to 50 mL LB broth with 100 µg/mL ampicillin and were grown for 18 hours at 37°C. Subsequently, cell pellets were collected by centrifuging at 5000 rpm for 10 minutes. Plasmid was extracted using Plasmid Miniprep kit (Bio-Rad, 732-6100) according to manufacturer's protocol. Plasmid concentration was assessed with NanoDrop ND-1000 spectrophotometer with software version 3.1.2 (Thermo Scientific). The plasmids were sent out for sequence verification (Genewiz).

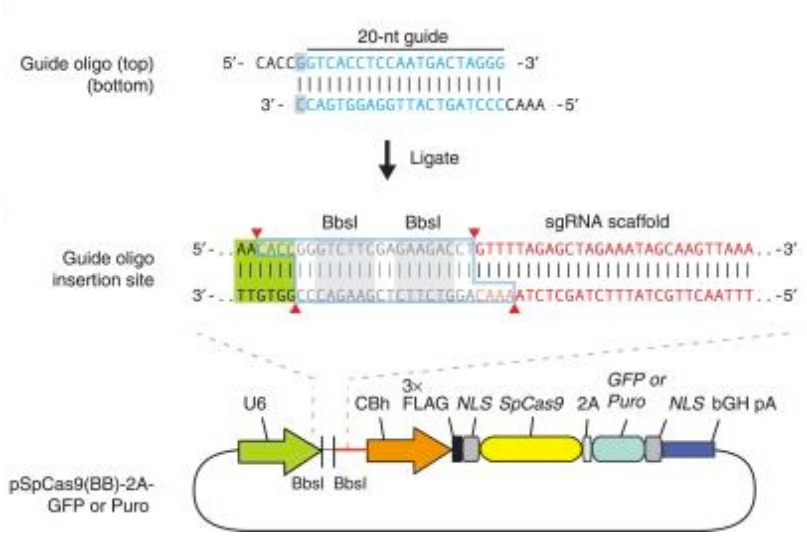

Figure 5: Model showing the example of annealed gRNAs that have been cloned into pSpCas9(BB)-2A-GFP between two BbsI sites. Diagram of pSpCas9(BB)-2A-GFP plasmid also is shown. (used with permission [230])

After sequence verification, the plasmid was transfected into 50% confluent HS-5 cells using X-tremeGene HP DNA transfection reagent (Roche, 06366244001) at 1:2 w/v ratio of plasmid:transfection reagent. Forty-eight hours after transfection, HS-5 cells were inspected under fluorescent microscope to verify GFP expression of pSpCas9(BB)-2A-GFP-gRNA_fib1 plasmid (HS-5^{CRISPR_fib1})and pSpCas9(BB)-2A-GFP control plasmid (HS-5^{CRISPR_GFP}). Then, GFP positive population was isolated from the transfected population by Fluorescence Activated Cell Sorting (FACS) on BD FACS Aria II cell sorter (BD Biosciences, Center for Translational Cancer Research, HFGCC). The selector gates were set by using untransfected cells as negative controls. After that, the GFP positive cells were diluted further to form individual clones in 96-well tissue culture grade plates (Costar, 3595) before clonal expansion in DMEM with 10% FBS to yield enough cells for subsequent experiments. The clones from GFP positive cells were screened by western blot analysis to determine the expression of fibulin-1 compared to the HS-5 clones transfected with control pSpCas9(BB)-2A-GFP plasmid (Appendix C). The clones, which showed significant reduction of fibulin-1 compared to control plasmid-transfected cells, were selected for future experiments based on fibulin-1 expression levels.

2.13 Statistical Analysis

The Analysis of Variance (ANOVA) with Tukey's test was utilized for statistical analysis, and P-values < 0.05 were considered statistically significant. P-value for each experiment is specified in each figure legend. Data were represented as mean ± Standard error of the mean (SEM) of three separated experimental replicates each having triplicate samples per experiment unless indicated otherwise. To control

for interassay variation, raw data were normalized to controls, and error was normalized accordingly before comparisons were made.

Chapter 3

RESULTS

As the mechanisms behind PCa bone colonization are still elusive, negative interactions between PCa cells and bone microenvironment have been reported in many studies [29-33]. The change from genetically heterogeneous DPCs to the homogeneous solid tumor at the metastatic sites were noted in several studies suggesting a Darwinian selection process could take place during cancer colonization in the new metastatic sites [53, 164-166]. Supporting this hypothesis, previous results from Sikes' lab have shown PCa apoptotic induction by paracrine factor(s) from HS-5 cells as well as NED in the surviving population, which is correlated to an aggressive phenotype of PCa when found [31-33] (Appendix D). These studies showed an induction of apoptosis due to effect of HS-5 CM application onto cells of the LNCaP progression model of PCa. The LNCaP progression model is an isogenic series of cell lines derived through manipulation of the hormonal status of animal hosts carrying these tumors that comprised the weakly metastatic and androgen-sensitive LNCaP cell line and progresses to the highly metastatic and castrate-resistant C4-2 and bone adaptive, castrate resisitant, C4-2B as shown in Figure 6 [231-234]. This model is the most clinically relevant in vitro/vivo model for PCa due to its imitation of clinical PCa biology and progression [233, 234]. In addition, another study from Sikes' lab showed that HS-5 CM but not HS-27a CM induced PCa death specifically without any effects on breast cancer cells, non-malignant prostate cells and fibroblast cells [33] (Appendix E). Therefore, an unidentified factor(s) from HS-5 CM that induced PCa cell death

showed potential as a novel therapeutic, which could suppress PCa growth and/or as a novel marker for early detection for men at risk for PCa bone metastasis. Accordingly, identifying the soluble HS-5 DF would be an essential step to understand better the mechanisms involved in PCa bone metastasis and allow for development of the therapeutic and diagnostic potential of the DF.

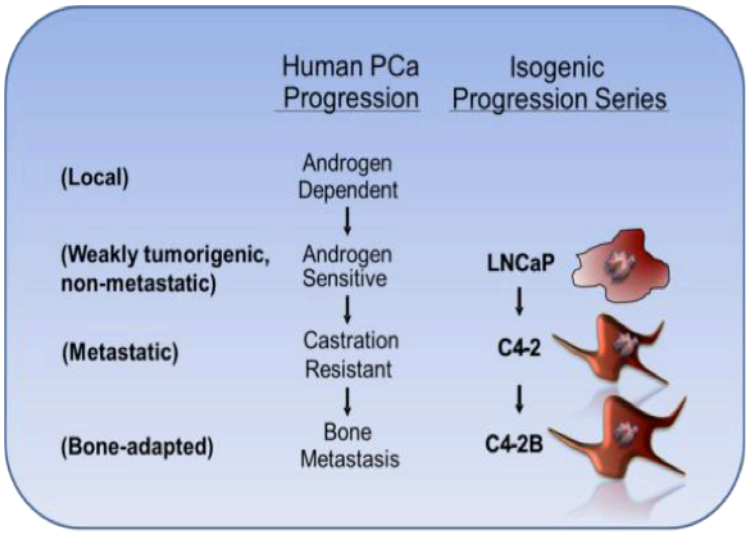

Figure 6: Diagram illustrating properties of the cells of the LNCaP progression model of human PCa: An isogenic in vitro/vivo model for PCa progression from an androgen sensitive and non-metastatic state, LNCaP cells, to a castrate resistant and metastatic intermediate, C4-2 cells, and finally to a bone adapted, castrate-resistant cell line, C4-2B (courtesy Dr. Robert A. Sikes).

3.1 Biochemical Characterization of HS-5 DF

Consistent with previous results, my data also showed that HS-5 CM induced PCa apoptosis and increased dead/live ratio of PCa cells treated with HS-5 CM in all 3 cell lines of the LNCaP progression model: LNCaP, C4-2 and C4-2B. Both previous studies and my data showed that PCa cell lines from the LNCaP progression model responded to HS-5 CM to a different degree. Most of the time, the level of PCa cell death induction by HS-5 CM was highest in the non-metastatic and androgen sensitive LNCaP cells followed by a metastatic and androgen independent C4-2 cells, and the least effects were seen in the bone adapted and androgen independent C4-2B cells. To investigate further the possible candidates for HS-5 DF, several biochemical characterizations were performed.

3.1.1 Trypsin Sensitivity

To test for the sensitivity of HS-5 DF for proteolytic enzyme, HS-5 CM was treated with trypsin before introducing to PCa cells. PCa apoptosis was determined after 24 hours of CM treatment. Data showed that LNCaP showed 4.32 fold higher in apoptotic index as compared to SF-DMEM control. However, after HS-5 CM was treated with trypsin (HS-5/trypsin CM), apoptotic induction from HS-5/trypsin CM reduced by 50.60% to 2.13 fold. Similar effects were seen in C4-2, which showed 51.83% reduction of apoptotic index from 3.17 to 1.53 fold compared to SF-DMEM after HS-5 CM was treated with trypsin. For the bone adapted C4-2B cells, the apoptotic index also was reduced by 57.51% from 3.12 fold in HS-5 CM to 1.33 fold in HS-5/trypsin CM compared to SF-DMEM. In conclusion, the induction of PCa apoptosis by HS-5 CM was reduced significantly, the average of 53%, after HS-5 CM was exposed to trypsin (Figure 7). This indicated that HS-5 DF that induces apoptosis

in PCa cells is sensitive to proteolytic cleavage by trypsin; hence, HS-5 DF could be a protein(s) that contained at least one trypsin recognition site.

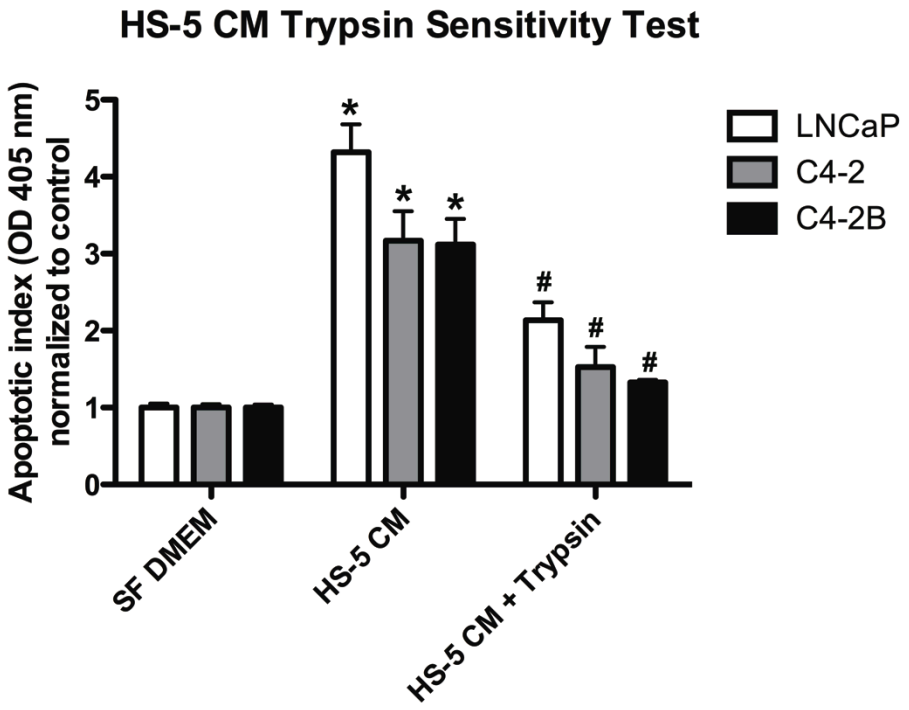

Figure 7: PCa cells, LNCaP, C4-2 and C4-2B, were treated with SF DMEM, HS-5 CM and HS-5 CM pre-exposed to trypsin (HS-5 CM + trypsin) for 24 hours prior to apoptosis assay. The activity of HS-5 DF dropped significantly after being exposed to trypsin showing trypsin sensitivity of the factor. The results came from 3 biological replicates of HS-5 CMs and PCa cells. Each biological replicate contained 3 internal replicates. Statistical analysis was done by ANOVA with Tukey's test. (* : P-value<0.0001 compared to SF DMEM, # : P-value<0.001 compared to HS-5 CM)

3.1.2 Heat Sensitivity

HS-5 CM was exposed to 70°C and 100°C before introducing to LNCaP, C4-2 and C4-2B to compare the induction of PCa apoptosis to HS-5 CM at 37°C. Consistent with previous data, the highest apoptotic index was seen in LNCaP cells treated with HS-5 CM at 37°C; however, apoptotic activity from HS-5 CM dropped significantly as the CM was pre-exposed to 70°C and 100°C. As compared to HS-5 CM at 37°C, apoptotic index of LNCaP cells was decreased significantly by 24.96% from 4.98 fold normalized to SF DMEM control to 3.74 fold in HS-5 pre-exposed to 70°C. The trend dramatically dropped by 71.06% to 1.44 fold in HS-5 CM pre-exposed to 100°C compared to HS-5 CM at 37°C. Similarly, HS-5 CM pre-exposed to 70°C and 100°C showed significantly lower apoptotic induction as compared to HS-5 CM at 37°C for C4-2. C4-2 apoptotic index was decreased from 4.18 fold in HS-5 CM at 37°C to 3.50 fold (16.28%) in HS-5 CM pre-exposed to 70°C and further reduced to 1.47 fold (83.72%) in HS-5 CM pre-exposed to 100°C. Accordingly, the results from both HS-5 CM sensitive cells showed that an apoptotic induction from HS-5 DF in HS-5 CM was decreasing as the temperatures were increasing. While not statistically different, the least responsive C4-2B also showed a reduction in the induction of apoptosis from HS-5 CM after pre-exposed to 100°C by 8.37% from 1.53 fold to 1.40 fold normalized to SF DMEM control. These data indicated that HS-5 DF is a heat sensitivity, and the effect of high temperature on HS-5 DF is irreversible.

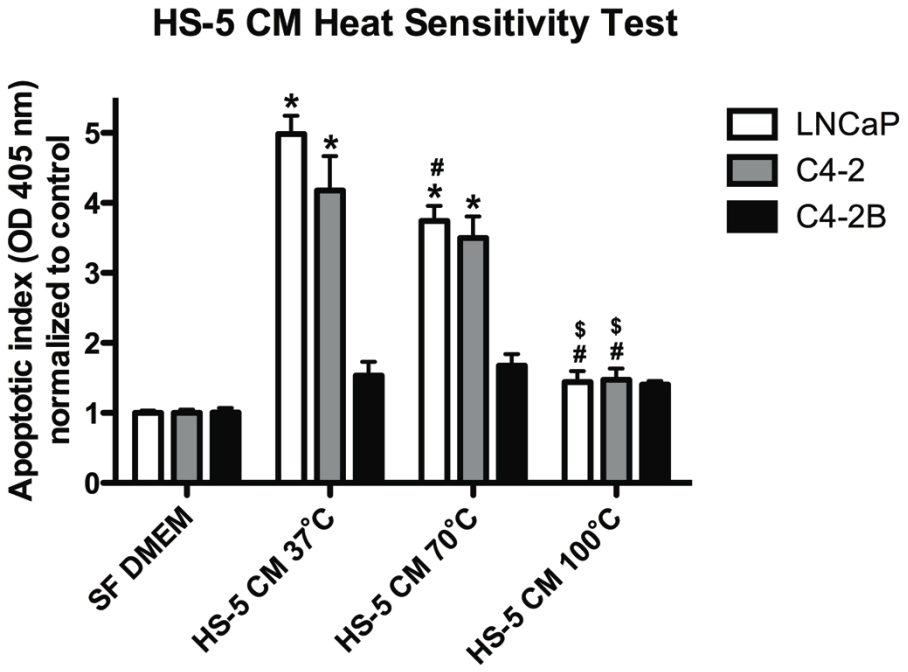

Figure 8: HS-5 CM showed a significant reduction in PCa apoptotic induction in LNCaP and C4-2 after exposing the CM to high temperatures. As the temperature was increasing, the apoptotic inducing activity of HS-5 DF in HS-5 CM was decreasing. Even though it is not statistically significant, a similar effects could be seen in C4-2B. The PCa cells were treated for 24 hours with SF DMEM control or HS-5 CM in each condition prior to performing an apoptosis assay. The results came from 2 biological replicates of HS-5 CMs and PCa cells. Each biological replicate contained 3 internal replicates. Statistical analysis was done by ANOVA with Tukey's test. (* : P-value<0.0001 compared to SF DMEM, # : P-value<0.001 compared to HS-5 CM at 37°C, $: P-value<0.05 compared to HS-5 CM at 70°C)

3.1.3 pH Stability

The HS-5 DF in HS-5 CM was tested for its stability after exposing to different pH, which is useful for future experiments to identify and purify HS-5 DF by proteomic methods, such as affinity or size exclusion column chromatography. HS-5 CM was pre-adjusted to pH 4 and 10 and held there for 48 hours before being adjusted back to pH 7. The induction of apoptosis from different pH groups on LNCaP, C4-2 and C4-2B was compared to HS-5 CM in the original pH (pH 7). Corresponding to previous data, highest activity of HS-5 CM was seen in LNCaP followed by C4-2, and the lowest activity was seen in a bone adapted C4-2B. After 24 hours of treatments, LNCaP, C4-2 and C4-2B showed statistically significant increase in average apoptotic index at 4.21, 4.09 and 1.67 fold, respectively, compared to SF DMEM control. No statistical difference was found between HS-5 CM pre-treated at pH 4, 7 or 10. These data indicated that the HS-5 DF was stable across pH 4-10 without losing its PCa death-inducing activity. In terms of protein structure, this suggested that pH treatment could not denature the DF or this denaturing effect is reversible in vitro.

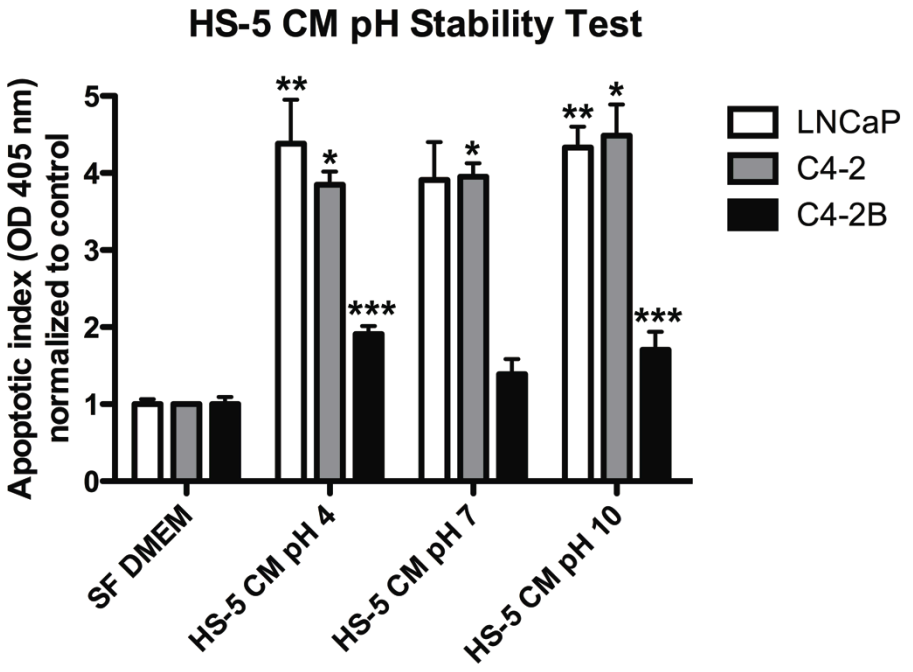

Figure 9: pH stability test for HS-5 DF was carried from HS-5 CM pre-treated to pH 4, 7 and 10 for 48 hours. LNCaP, C4-2 and C4-2B showed statistically significant increases in their apoptotic index after HS-5 CM treatments; however, no statistical difference was found when HS-5 CM was treated at different pHs. PCa apoptosis was assayed after 24 hours of treatment. Results came from 2 biological replicates of HS-5 CMs and PCa cells. Each biological replicate contained 3 internal replicates. Statistical analysis was done by ANOVA with Tukey's test. (* : P-value<0.0001, ** : P-value<0.01 and *** : P-value<0.05 compared to SF DMEM)

3.1.4 Size Selection Through a 30 kDa Cutoff Filter

To determine the tentative size of HS-5 DF in HS-5 CM, proteins in HS-5 CM were separated into 2 groups: fractions containing proteins, which are larger than 30 kDa (HS-5 CM >30 kDa) and smaller than 30 kDa (HS-5 CM <30 kDa). Size selected fractions were introduced to LNCaP, C4-2 and C4-2B to determine the fraction that contained the HS-5 DF. After 48 hours of treatments, dead/live ratio normalized to SF DMEM control in PCa cells populations treated with each fraction would be compared to HS-5 CM before size selection. The results showed a significant increase in dead/live ratio in all PCa cells after HS-5 CM treatment by 206.46 fold, 172.62 and 115.47 fold for LNCaP, C4-2 and C4-2B respectively. Interestingly, after size selection, PCa death induction was retained only in the fraction of HS-5 CM >30 kDa. Even though the results were not statistically different between PCa treated with HS-5 CM and HS-5 CM >30 kDa, a slight increase was seen in all PCa cell lines. In contrast, dead/live ratio for all PCa cell lines was significantly lower in HS-5 CM<30 kDa groups as compared to other HS-5 CM treatments. LNCaP, C4-2 and C4-2B treated with HS-5 CM <30 kDa showed only 13.50 fold, 19.66 fold and 63.78 fold, respectively, as compared to 280.26 fold, 192.12 fold and 174.24 fold as treated with HS-5 CM >30 kDa. These results indicated that the activity of HS-5 DF was retained in the fraction for proteins larger than 30 kDa; therefore, the tentative size for HS-5 DF should be bigger than 30 kDa.

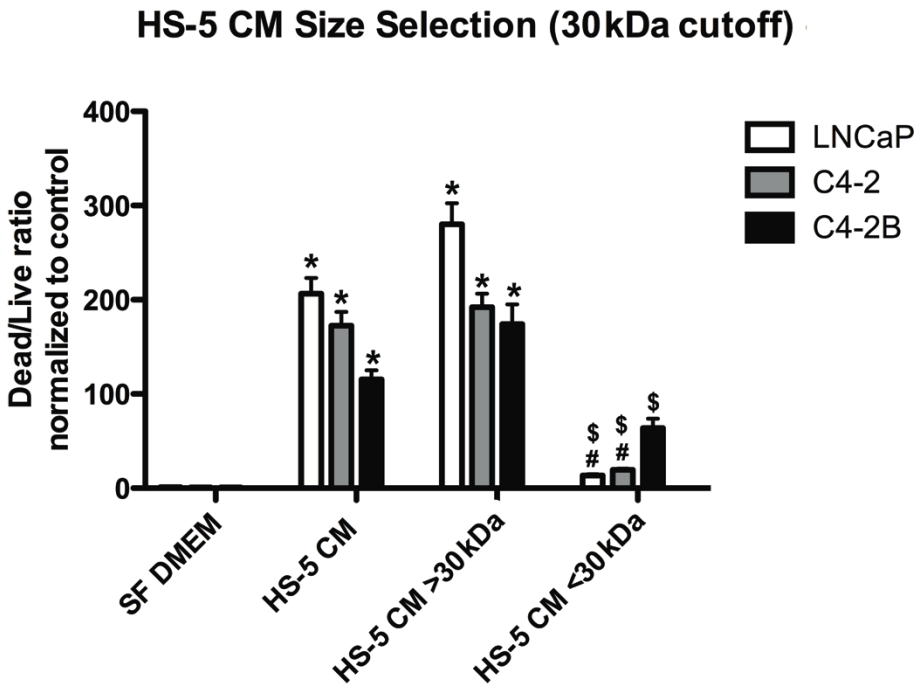

Figure 10: HS-5 CM was size-selected into HS-5 CM containing proteins that are bigger than 30 kDa (HS-5 CM >30 kDa) and HS-5 CM containing proteins that are smaller than 30 kDa (HS-5 CM <30 kDa). LNCaP, C4-2 and C4-2B treated with HS-5 CM showed significant increases in dead/live ratio. After size selection, PCa death inducing activity was retained only in HS-5 CM > 30 kDa. Live/dead assays were performed after 48 hours of treatment. Quantified data came from at least 5 fields for each treatment. Experiments were repeated in 3 biological replicates of HS-5 CM and PCa cells. Statistical analysis was done by ANOVA with Tukey's test. (* : P-value<0.0001 compared to SF DMEM, # : P-value<0.001 compared to HS-5 CM, $: P-value<0.05 compared to HS-5 CM >30 kDa)

3.1.5 Size Selection Through 100 kDa Cutoff Filter

Another size selection experiment was carried by using a 100 kDa cutoff filter to determine the tentative size range of HS-5 DF. Similar to previous experiments, HS-5 CM was divided into 2 groups: HS-5 CM with proteins that are larger than 100 kDa (HS-5 CM >100 kDa) and HS-5 CM with proteins that are smaller than 100 kDa (HS-5 CM <100 kDa). After 48 hours of treatments, PCa cells including LNCaP, C4-2 and C4-2B were subjected to live/dead assay to compare PCa death inducing activity in HS-5 CM >100 kDa, HS-5 CM <100 kDa and HS-5 CM before size selection normalized to SF DMEM control. Consistent with previous results, the data showed that LNCaP, C4-2 and C4-2B had significantly higher dead/live ratio at 56.38 fold, 23.15 fold and 31.39 fold with HS-5 CM treatment as compared to SF DMEM respectively. After size selection, even though low PCa death inducing activity could be seen in PCa cells treated with HS-5 CM >100 kDa, significantly higher effects were observed in PCa cells treated with HS-5 CM <100 kDa. The results showed 53.82 fold, 24.52 fold, 30.07 fold dead/live ratio in HS-5 CM <100 kDa consistent with HS-5 CM control groups; in contrast, only 22.88 fold, 13.09 fold, 19.59 fold were seen in HS-5 CM >100 kDa for LNCaP, C4-2 and C4-2B respectovely. Accordingly, the tentative size for HS-5 DF was shown to be smaller than 100 kDa, but greater than 30 kDa.

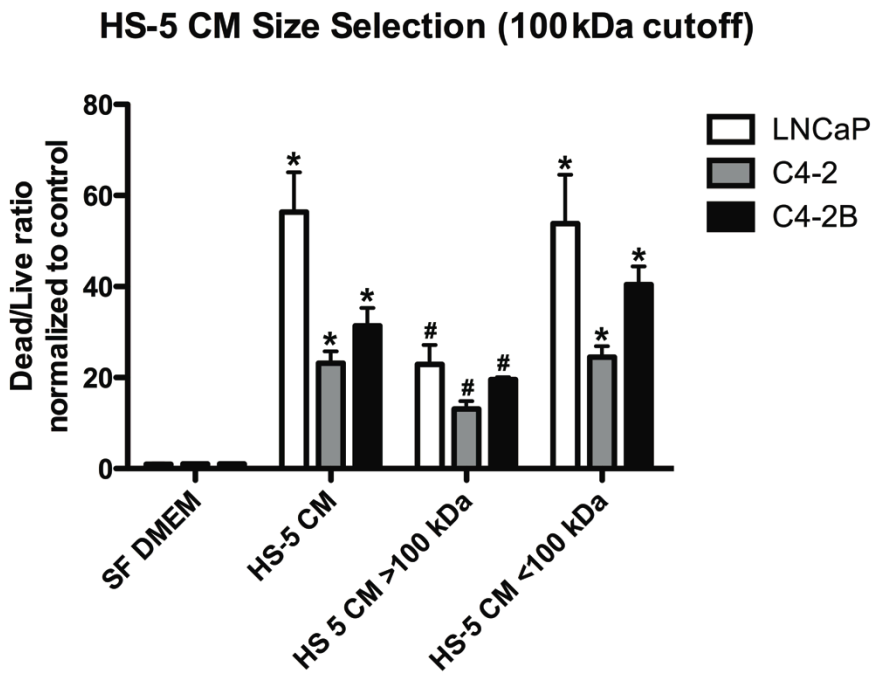

Figure 11: HS-5 CM was size-selected into HS-5 CM containing proteins that are bigger than 100 kDa (HS-5 CM >100 kDa) and HS-5 CM containing proteins that are smaller than 100 kDa (HS-5 CM <100 kDa). Live/dead assays were carried out on LNCaP, C4-2 and C4-2B after 48 hrs of treatments. All PCa cells showed significant increases in dead/live ratio after treatment with HS-5 CM and HS-5 CM <100 kDa. These higher dead/live ratios were statistically different from SF-DMEM and HS-5 CM >100 kDa. Quantified data came from at least 5 fields for each treatment. Experiments were repeated in 3 biological replicates of HS-5 CM and PCa cells. Statistical analysis was done by ANOVA with Tukey's test. (* : P-value<0.0001 compared to SF DMEM, # : P-value<0.05 compared to HS-5 CM and HS-5 CM <100 kDa)

3.1.6 Disulfide Bonds Reduction by DTT

Knowing that HS-5 DF is trypsin sensitive, indicating its protein property, the requirement of disulfide bonding in its structure was tested. In this experiment, HS-5 CM was exposed to a strong reducing agent, DTT. Then, PCa death induction was compared in LNCaP, C4-2 and C4-2B by Live/dead assay after 48 hours of treatments. Consistent to previous results, LNCaP showed to be most susceptible to HS-5 DF with 59.86 fold dead/live ratio higher than SF DMEM control as compared to C4-2 and C4-2B that have 40.99 and 41.97 fold dead/live ratio normalized to controls, respectively. DTT alone showed only a slight effect on PCa cell death. However, as proteins in HS-5 CM were reduced by DTT, a decrease in HS-5 DF activity was seen in C4-2 and C4-2B from 40.99 and 41.97 fold in HS-5 CM groups to 15.40 and 22.01 fold in HS-5 CM + DTT. This effect could not be seen in LNCaP. Interestingly, a slight increase of dead/live ratio in LNCaP was seen in HS-5 CM + DTT, but it was not statistically significant. Accordingly, the results from C4-2 and C4-2B suggested that disulfide bonding was important for HS-5 DF to induce PCa cell death in these two cell lines. The different trend in LNCaP indicated that HS-5 DF could be more than one protein or could interact with other proteins leading to functional difference in androgen sensitive versus androgen independent PCa cells, and/or the non-metastatic LNCaP cells could secrete some other factor(s) that protect HS-5 DF from reducing condition, which will be discussed later.

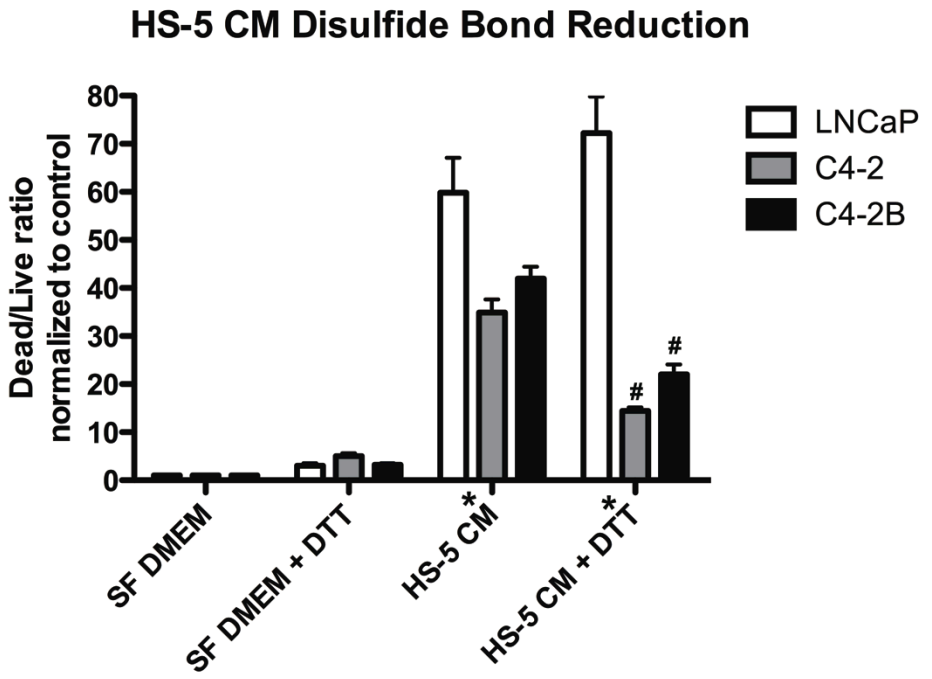

Figure 12: Proteins in HS-5 CM were reduced by DTT (HS-5 CM + DTT). After disulfide bonds were reduced, PCa death inducing activity in C4-2 and C4-2B decreased significantly in HS-5 CM + DTT as compared to HS-5 CM. Disulfide bonds reduction did not show significant effects on LNCaP death induction by HS-5 CM, and DTT itself did not affect PCa dead/live ratio significantly. Live/dead assays were performed on PCa cells after 48 hours of treatment. Quantified data came from at least 5 fields for each treatment. Experiments were repeated in 3 biological replicates of HS-5 CM and PCa cells. Statistical analysis was done by ANOVA with Tukey's test. (* : P-value<0.0001 compared to SF DMEM, # : P-value<0.001 compared to HS-5 CM)

3.1.7 Disulfide Bond Reduction by DTT Followed by Size Selection

To determine the effects of disulfide bond reduction on a tentative size range for HS-5 DF, the most responsive PCa cell line, LNCaP was chosen. These experiments were carried with the collaboration with Irene Marwa (undergraduate student in Dr. Sikes' lab). In these experiments, HS-5 CM treated with DTT (HS-5 CM + DTT) was used for size selection experiments to compare the activities of each fraction before and after DTT treatment. Similar to previous results, the death induction effect of HS-5 CM and HS-5 CM + DTT were not statistically different in LNCaP.

HS-5 DF retained in fraction containing proteins that are bigger than 30 kDa (HS-5 CM >30 kDa) at 32.40 fold of dead/live ratio compared to fraction containing proteins that are smaller than 30 kDa (HS-5 CM <30 kDa), which had only 7.49 fold of dead/live ratio normalized to SF DMEM control. Consistent to previous results, these data indicated that HS-5 DF was bigger than 30 kDa. After disulfide bond reduction, the shift in PCa death induction could be seen. The results showed a decrease in PCa death induction for HS-5 + DTT > 30 kDa by approximately 50% to 15.07 fold and an increase in HS-5 DF activity for the fraction containing smaller size proteins with DTT (HS-5 CM + DTT <30 kDa) to 15.82 fold (Figure 13). Accordingly, these results showed a potential role of disulfide bonding in HS-5 DF to be important in oligomerization or multi-proteins interactions.

In addition, similar results were seen when 100 kDa cutoff filter was used. Consistent with previous data, PCa death induction was primarily found in HS-5 CM fraction containing proteins, which are smaller than 100 kDa (HS-5 CM <100 kDa) with 46.48 fold of dead/live ratio normalized to SF DMEM control as compared to only 2.28 fold in HS-5 CM containing bigger proteins (HS-5 CM >100 kDa). After

DTT treatment, the shift in PCa death inducing activity to the smaller fraction could also be seen. In this experiment, PCa death induction was increased in HS-5 CM + DTT <100 kDa to 50.53 dead/live ratio normalized to control as compared to HS-5 CM + DTT >100 kDa, which had further decreased in dead/live ratio to 1.21 fold. These data confirmed the observation found in 30 kDa size selection experiment indicating the shift in PCa death induction to the smaller size fractions after disulfide bond reduction by DTT (Figure 14). These data suggested that HS-5 DF has some oligomerization and/or multi-proteins interactions via disulfide bond, and this factor might still function on LNCaP even after disulfide bond reduction.

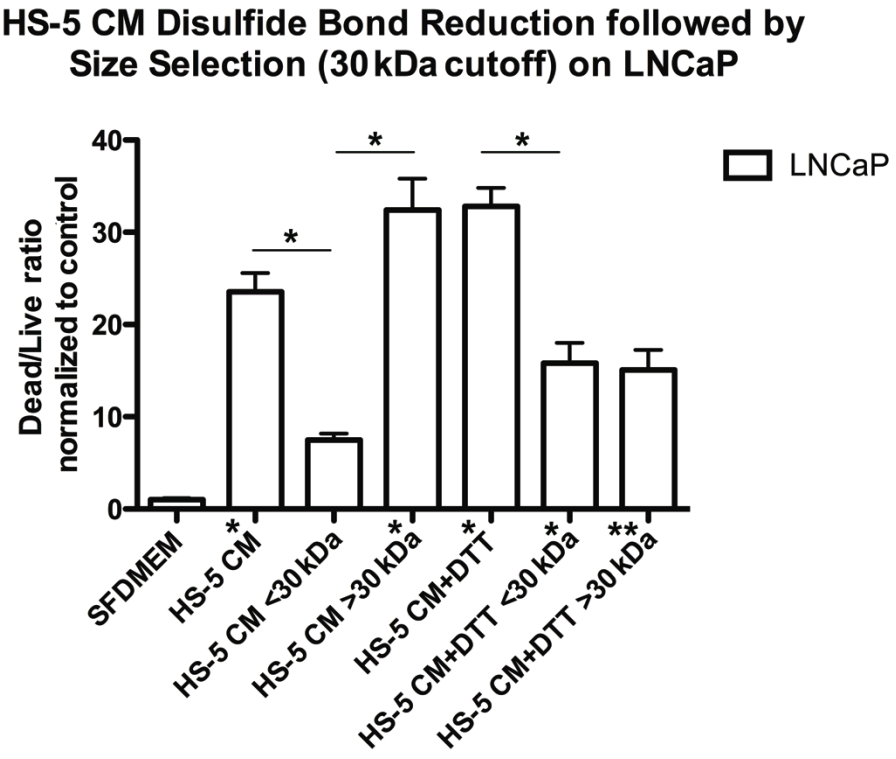

Figure 13: The effects of disulfide bond reduction by DTT on HS-5 DF size were tested on LNCaP cells. The results consistently showed that HS-5 DF is retained in HS-5 CM containing proteins that are bigger than 30 kDa (HS-5 CM >30 kDa). After disulfide bond reduction, PCa death induction was decreased in HS-5 CM + DTT >30 kDa; while, the opposite trend could be seen in LNCaP cells treated with HS-5 CM + DTT <30 kDa. The shift of HS-5 DF activity to the smaller size fraction suggested the possibilities of oilgomerization and/or multi-proteins interactions of HS-5 DF. Live/dead assays were performed on PCa cells after 48 hours of treatment. Quantified data came from at least 5 fields for each treatment. Experiments were repeated in 3 biological replicates of HS-5 CM and LNCaP. Statistical analysis was done by ANOVA with Tukey's test. (* : P-value<0.0001 compared to SF DMEM and between the groups as the bars indicated, ** : P-value<0.001 compared to SF DMEM) (courtesy Irene Marwa)

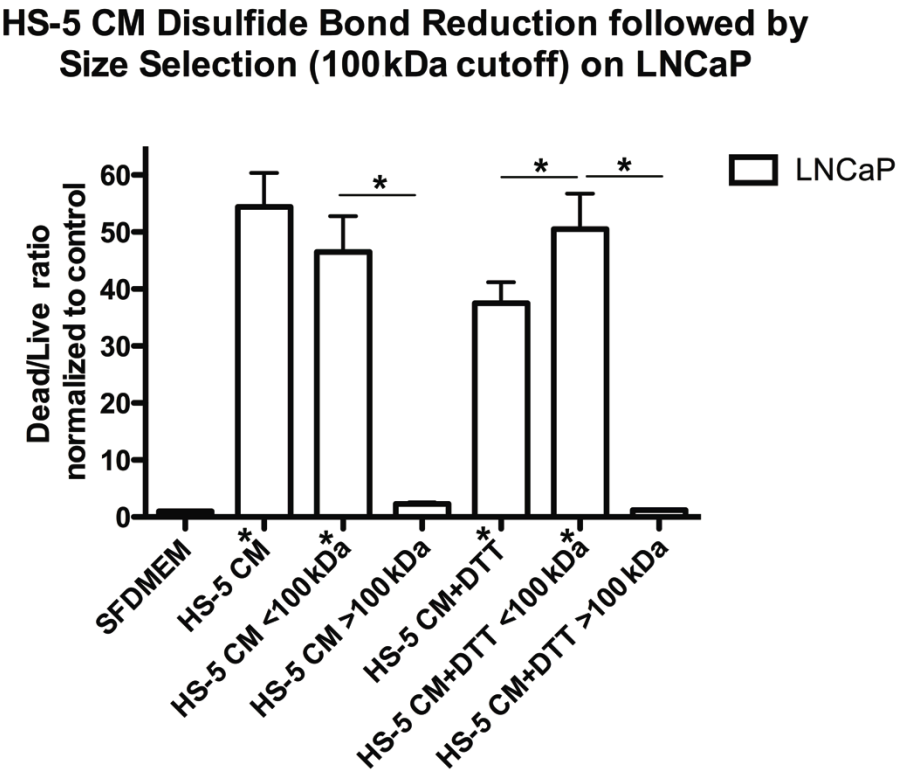

Figure 14: The effect of disulfide bond reduction on HS-5 DF size was confirmed again in 100 kDa size selection experiment on LNCaP cells. The results confirmed a significant higher activity of HS-5 DF in HS-5 CM containing proteins that are smaller than 100 kDa (HS-5 CM <100 kDa). After DTT treatment to reduce disulfide bonds in proteins residing in HS-5 CM, the shift in HS-5 DF's activity toward the fraction containing smaller size proteins could be observed (HS-5 CM + DTT <100 kDa). This also suggested oligomerization and/or multi-proteins interaction of HS-5 DF via disulfide bonding. Live/dead assays were performed on LNCaP cells after 48 hours of treatment. Quantified data came from at least 5 fields for each treatment. Experiments were repeated in 2 biological replicates of HS-5 CM and LNCaP. Statistic analysis was done by ANOVA with Tukey's test. (* : P-value<0.0001 compared to SF DMEM and between groups as the bars indicated) (courtesy Irene Marwa)

3.1.8 Ability to Retain PCa Death Induction after Concentration

To pursue the goal for identifying HS-5 DF in HS-5 CM, proteomic approaches would be used in the later steps. In addition, the enriched samples will be needed for the purification and for subsequent functionality tests. Therefore, the ability of HS-5 DF in HS-5 CM after protein concentration was tested to determine the most suitable methods to enrich the DF in HS-5 CM. In this experiment, proteins in HS-5 CM were concentrated by using speed vacuum concentrator before adjusting the volume back for functional test on PCa cells. Consistent with previous results, LNCaP showed the highest dead/live ratio when treated with HS-5 CM. Interestingly, after the concentration, not only did the HS-5 DF retained its activity, but the activity also was enhanced, almost doubling from 58.10 fold, 16.03 fold, 43.42 fold of dead/live ratio normalized to SF DMEM control in HS-5 CM to 96.49 fold, 32.24 fold, and 148.44 fold on LNCaP, C4-2 and C4-2B after HS-5 CM concentration respectively. This indicated that protein concentration by speed vacuum concentrator could be done without loosing PCa death inducing activity. Therefore, this method could be used to concentrate HS-5 CM samples for proteomic techniques in the future. Moreover, the enhanced activity of HS-5 DF after concentration suggested that HS-5 DF might co-exist with a mechanical force-labile inhibitor(s)/antagonist(s) that could not survive after the concentration process. Accordingly, interactions between HS-5 DF and other molecules were suggested again.

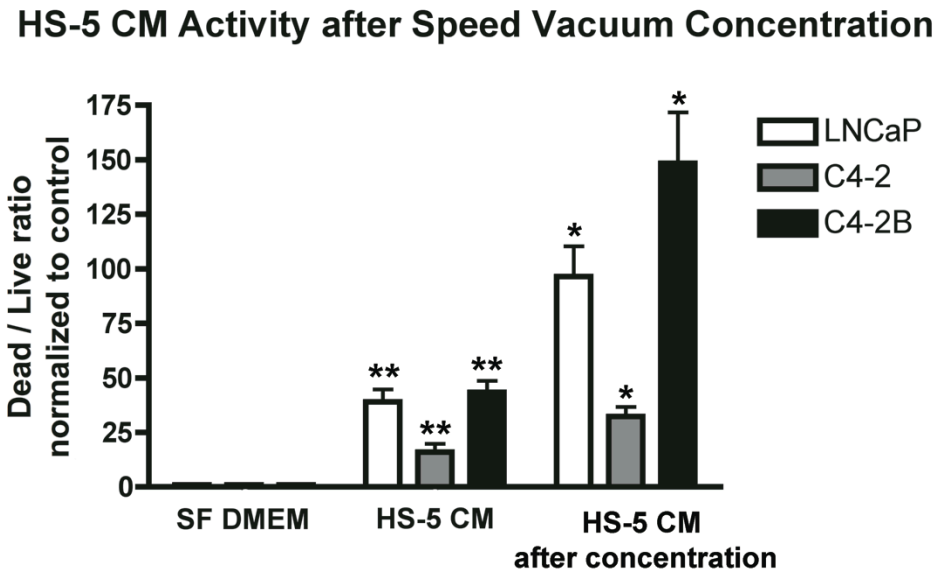

Figure 15: PCa death inducing activity of HS-5 DF after protein concentration using speed vacuum freeze drying concentration was shown. The results showed an enhanced activity of HS-5 DF after the concentration process. Therefore, this method could be used to concentrate the samples for HS-5 DF identification. Data imply a labile inhibitor or antagonist that is lost during concentration. Live/dead assays were performed on PCa cells after 48 hours of treatment. Quantified data came from at least 5 fields for each treatment. Experiments were repeated in 3 biological replicates of HS-5 CM and PCa cells. Statistical analysis was done by ANOVA with Tukey's test. (* : P-value<0.0001 and ** : P-value<0.01 compared to SF DMEM)

3.2 Preconditioning of HS-5 Cells with TGF-β1 Suppressed PCa Cell Death Induction and Led to Protein Pattern Alterations in HS-5 CM

Interestingly, high level of TGF-β1 has been reported in the serum of PCa patients with bone metastasis [235, 236] and correlates with getting bone metastasis. This led to our interest in the effects of TGF-β1 on HS-5 DF. Previous experiments from Sikes' lab showed the inhibitory effect of TGF-β1 on HS-5 DF [32, 33]. In these studies, HS-5 cells were pre-treated with TGF-β1 for 96 hours prior to CM collections in SF DMEM for 48 hours. The results showed that CM collected from HS-5 cells pre-treated with TGF-β1 (HS-5/TGF-β) had significantly lower death inducing activity than the vehicle pre-treated group. Consistent with these data, my results also showed that HS-5/TGF-β1 CM had significant lower PCa cell death induction on LNCaP and C4-2. In LNCaP cells, HS-5 DF activity was decreased by 53.46% (set A), 56.88% (set B) and 46.65% (set C) from HS-5/TGF-β1 CM as compared to HS-5 CM control. Similarly, the death inducing effects of HS-5/TGF-β1 CM were significantly lower in C4-2 treated with HS-5/TGF-β1 CM than those from control HS-5 CM by 66.29% (set A), 29.73% (set B) and 60.66% (set C). Accordingly, these data confirmed an inhibitory effect of TGF-β1 on HS-5 DF. These findings suggest a possible role of high circulating TGF-β1 in the colonization of bone by PCa that will be discussed later.

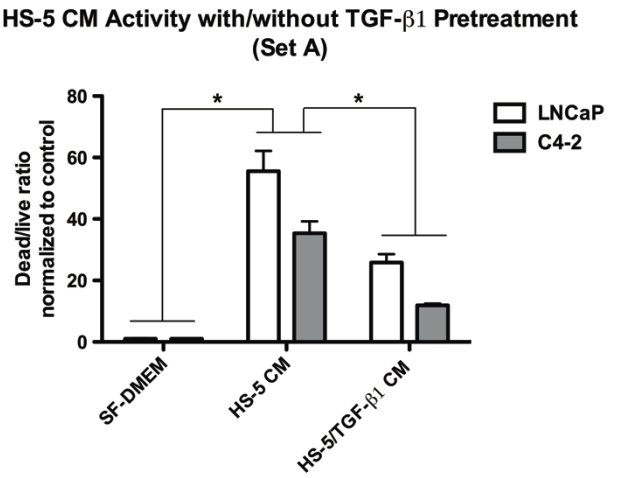
HS-5 CM Activity with/without TGF-β1 Pretreatment
(Set A)
Dead/live ratio
normalized to control
80
60
40
20
0
*
*
LNCaP
C4-2
SF-DMEM
HS-5 CM
HS-5/TGF-β1 CM

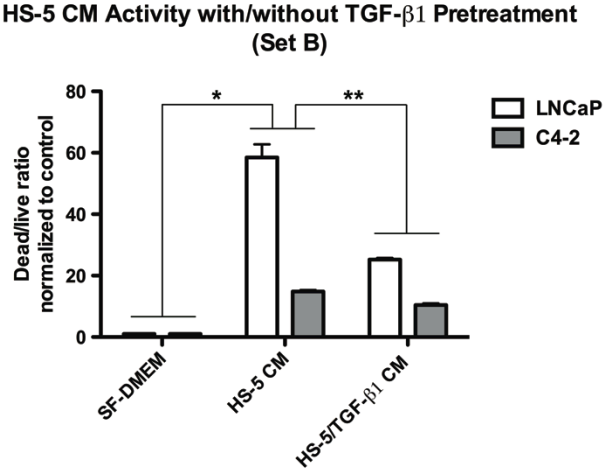
HS-5 CM Activity with/without TGF-β1 Pretreatment
(Set B)
Dead/live ratio
normalized to control
80
60
40
20
0
*
**
LNCaP
C4-2
SF-DMEM
HS-5 CM
HS-5/TGF-β1 CM

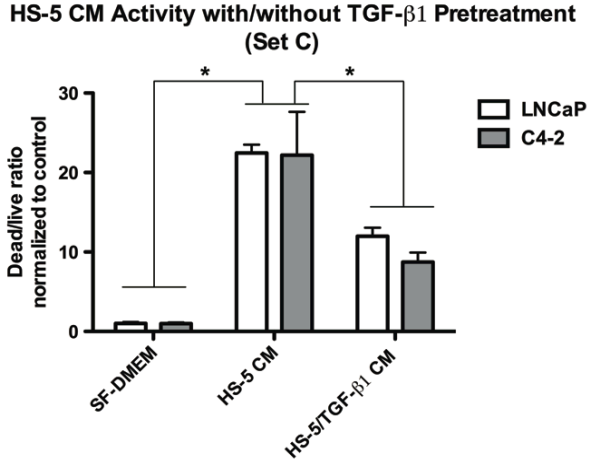
HS-5 CM Activity with/without TGF-β1 Pretreatment
(Set C)
Dead/live ratio
normalized to control
30
20
10
0
*
*
LNCaP
C4-2
SF-DMEM
HS-5 CM
HS-5/TGF-β1 CM

Figure 16: CM from HS-5 cells pretreated with TGF-β1 (HS-5/TGF-β1 CM) has decreased PCa cell death-inducing activity significantly as compared to control HS-5 CM. This indicated an inhibitory effect of TGF-β1 on HS-5 DF secretion and possibly biosynthesis. Similar results were observed for both LNCaP and C4-2. Live/dead assays were performed on PCa cells after 48 hours of treatment. Quantified data came from at least 5 fields for each treatment. Experiments were repeated in 3 biological replicates of HS-5 CM and PCa cells. Statistical analysis was done by ANOVA with Tukey's test (* : P-value<0.0001 and ** : P-value<0.05)

Taking advantage of these experiments, HS-5/TGF-β1 CM, which showed a significant decrease in PCa cell death inducing-activity, was used as negative samples for proteomic analysis. Firstly, protein patterns from control HS-5 CM and HS-5/TGF-β1 CM samples were compared by high resolution one-directional SDS-PAGE followed by silver staining (Figure 17). The results showed changes in the protein banding pattern after TGF-β1 treatment. Several protein bands that change noticeably are indicated in Figure 17. From previous data, HS-5 DF size range was indicated to be between 30 kDa and 100 kDa. Accordingly, 4 differentially expressed bands in this size range including 1 down-regulated band for 51.55 kDa and 3 up-regulated bands for 75.12 kDa, 49.82 kDa and 25.56 kDa were selected for further analysis by tandem mass spectrometry (MS/MS). The bands that showed differential expressions between the two groups were pulled, followed by in-gel tryptic digestion to use as samples for MS/MS. Finally, the peptide sequences were searched against the Mascot-NCBI database, and the proteins that met a 95% confidence match were provided in Table 1 and 2. The candidate proteins could be divided into upregulated candidates and downregulated candidates upon TGF-β1 treatment according to the signal from MS/MS.

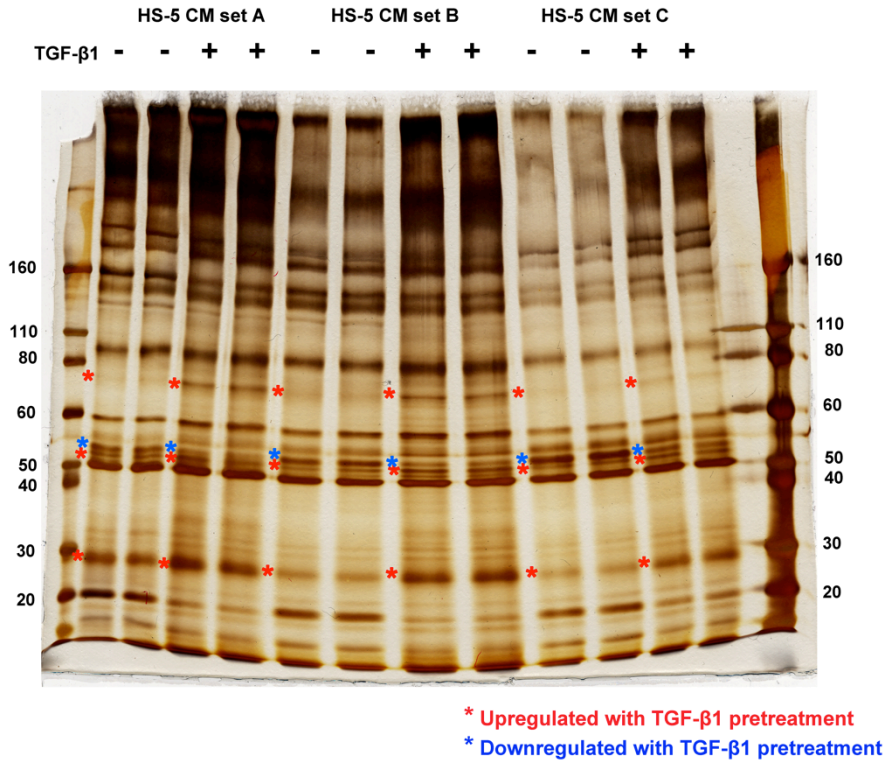

Figure 17: HS-5 CM and HS-5/TGF-β1 CM samples from Figure 16 were used for SDS-PAGE. 5%-11% gradient gel was used followed by silver staining. The bands labeled in red and blue showed proteins, which were upregulated and downregulated with TGF-β1 treatment, respectively. The indicated bands were used as samples for MS/MS analysis to identify possible HS-5 DF candidates.

Table 1: MS/MS was performed on protein bands showing differential expression upon TGF-β1 treatment to identify possible candidates for HS-5 DF. Protein identifications from peptide sequences obtained were searched against NCBI database via Mascot v 2.2. Those with >95% confidence are shown. The table below shows upregulated proteins in HS-5/TGF-β1 CM compared to HS-5 CM.

Protein name	**Gene ID**	**MW of the band that signal came from**
Tissue inhibitor of metalloproteinase-1 (TIMP-1)	4140011	25.56 kDa
Type I Collagen	30102	25.56 kDa
Moesin	4505257	75.12 kDa
ECM protein I	55958999	75.12 kDa

Table 2: MS/MS was performed from protein bands showing differential expression upon TGF-β1 treatment to identify possible candidates for HS-5 DF. Proteins were identified from peptide sequences searched against NCBI database via Mascot v 2.2. Those with >95% confidence are shown. Downregulated proteins in HS-5/TGF-β1 compared to HS-5 CM are shown in the table below.

Protein name	**Gene ID**	**MW of the band(s) that signal came from**
Matrix metalloproteinase-1 (MMP-1)	15341877	51.55 kDa /49.82 kDa
Matrix metalloproteinase-3 (MMP-3)	4505217	51.55 kDa /49.82 kDa
Pro-matrix metalloproteinase-1 (Prommp-1)	58176727	51.55 kDa /49.82 kDa
Fibulin-1	18490682	75.12 kDa

Among the protein candidates provided, fibulin-1 is the first HS-5 DF candidate that was selected for further investigations because of its role in cancer suppression for many types of cancers [224-227] and its regulation by TGF-β1. For example, it has been shown that another fibulin member, fibulin-5 could interact with latent TGF-β-binding protein 2 as part of an elastic assembly regulation [191]. Also, a recent study showed that TGF-β1 could inhibit FBLN1 gene expression and decrease soluble fibulin-1 in CM from airway smooth muscle cells (ASM) [237]. In addition, fibulin-1 was shown to be downregulated in PCa samples compared to the benign samples [223]. Accordingly, fibulin-1 seems to be the strongest candidate for HS-5 DF; therefore, it was selected for further experiments.

3.3 HS-5 Cells Expressed Significant Higher Level of Fibulin-1 than PCa Cells

The basal fibulin-1 protein level was compared between HS-5 BMS cells, BPH-1 cells, and PCa cells from LNCaP progression model including LNCaP, C4-2 and C4-2B. The results showed that HS-5 cells expressed dramatically higher levels of fibulin-1 protein than BPH-1 and PCa cells. This indicated the potential for tumor suppressive effects of fibulin-1 protein in PCa cells because their expression is low; indeed, the protein level was weakly detectible in PCa cells and BPH-1. Even though it was not statistically significant, fibulin-1 has higher expression in a bone adapted C4-2B than LNCaP and C4-2. This higher expression corresponds with the consistently observed lower response to HS-5 DF of C4-2B as compared to LNCaP and C4-2. Accordingly, these data indicate a possible adaption to fibulin-1 proteins by bone adapted PCa cells as well as the potential for fibulin-1 as the HS-5 DF in HS-5 CM.

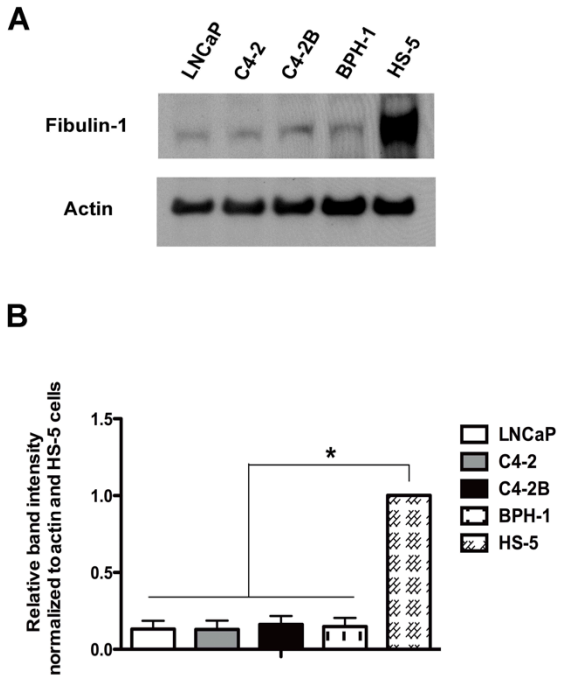

Figure 18: A) Fibulin-1 level from PCa cells including LNCaP, C4-2 and C4-2B, benign prostatic hyperplasia cells, BPH-1; and, the BMS cell line HS-5 cells were investigated by western blot analysis. HS-5 cells showed significant higher fibulin-1 level than PCa cells and BPH-1. B) Quantified data from western blot analysis for fibulin-1 showing statistically different expression levels between PCa, BPH-1 and HS-5 cells. Quantified data came from 3 separated blots from 3 biological replicates of each cell lines. Statistical analysis was done by ANOVA with Tukey's test. (* : P-value<0.0001)

3.4 TGF-β1 Treatment of HS-5 Cells Led to Lower Expression of Fibulin-1

As the candidate for HS-5 DF, the level of fibulin-1 in HS-5 cells upon TGF-β1 treatment was investigated in both the whole cell lysate and in the CM. After being treated with TGF-β1 for 96 hours, the same amount of proteins from HS-5 cell pellets from HS-5/TGF-β1 cells and control HS-5 cells were used for western blot analysis for fibulin-1. The results showed that fibulin-1 levels were significantly reduced in HS-5 cells pretreated with TGF-β1 as compared to control HS-5 cells (Figure 19A and B). To confirm the results from MS/MS analysis, the same amount of proteins from HS-5 CM and HS-5/TGF-β1 CM were used for western blot analysis for fibulin-1. Consistent with MS/MS results, HS-5/TGF-β1 CM contained lower fibulin-1 protein as compared to control HS-5 CM (Figure 19C and D). This indicated a suppressive effect of TGF-β1 on fibulin-1 in both HS-5 cells and HS-5 CM which corresponded to decreased PCa death inducing activity of HS- 5/TGF-β1 CM.

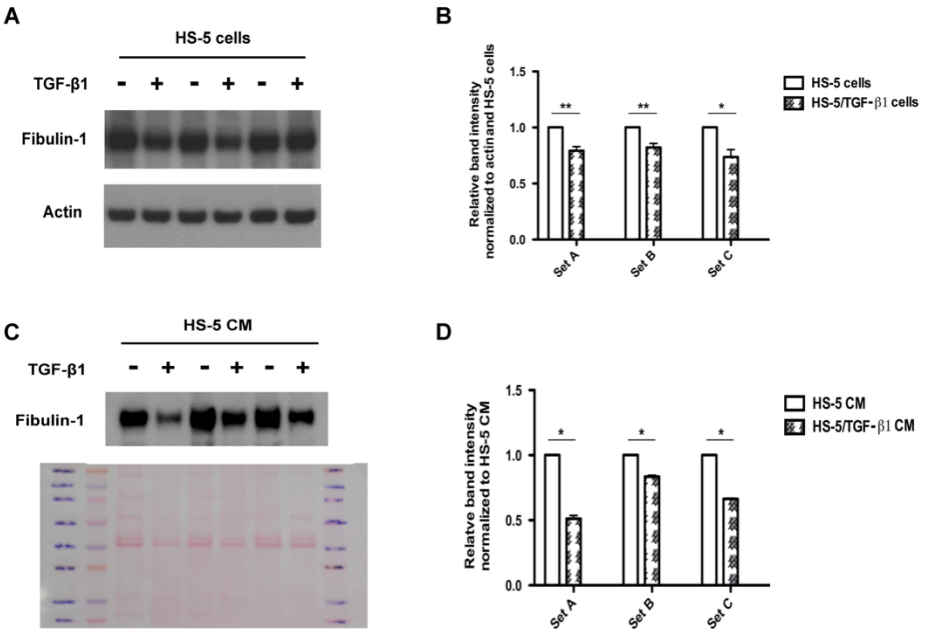

Figure 19: A) Western blot analysis showed that TGF-β1 treatment led to a downregulation of fibulin-1 in HS-5 cells. B) Quantified data from western blot in experiments for figure 19A showed statistically significant reduction of fibulin-1 in HS-5 cells after TGF-β1 treatment. C) CM collected from HS-5 cells pretreated with TGF-β1 showed significantly lower level of fibulin-1 as compared to control HS-5 CM. The amount of proteins in each lane was shown by a Ponceau S staining the blot. D) Quantified data from western blot in experiments for figure 19C showed that fibulin-1 in HS-5/TGF-β1 CMs was decreased significantly as compared to control HS-5 CM. Quantified data came from 3 separated blots from each experiment. Statistical analysis was done by ANOVA with Tukey's test. (* : P-value<0.01 and ** : P-value<0.05 in figure 19B and * : P-value<0.0001 in figure 19D)

3.5 HS-5 Cells Express Both Fibulin-1C and Fibulin-1D Isoforms, and TGF-β Treatment Led to a Suppression of Both Isoforms.

Fibulin-1C and fibulin-1D are the two major isoforms that have been reported in many organs, tissues and cell cultures as well as the signals from MS/MS data [171, 172, 195]. In addition, the opposing effects between the tumor supportive fibulin-1C and tumor suppressive fibulin-1D have been suggested in many experiments [168, 224-227]. Therefore, the basal expression of fibulin-1C and fibulin-1D in HS-5 cells was investigated by qRT-PCR. The results showed that HS-5 cells expressed both fibulin-1C and 1D. Moreover, it was shown that the level of a tumor suppressive isoform, fibulin-1D was approximately 5 fold higher by than fibulin-1C in HS-5 cells (Figure 20A). This differential expression showed the correlation between tumor suppressive effects of fibulin-1D and PCa death inducing activity from HS-5 CM. Results from previous experiment showed a reduction of fibulin-1 in HS-5 cells pretreated with TGF-β1 (Figure 19), so the effects of TGF-β1 treatment on the expression of fibulin-1C and 1D were examined. The results showed that TGF-β1 suppressed the expression of both fibulin-1C and 1D corresponding to a reduction in PCa cell death induction in HS-5/TGF-β1 CM. This suggested that TGF-β1 suppressed gene expression for FBLN1 gene overall rather than altering splicing toward any particular isoform.

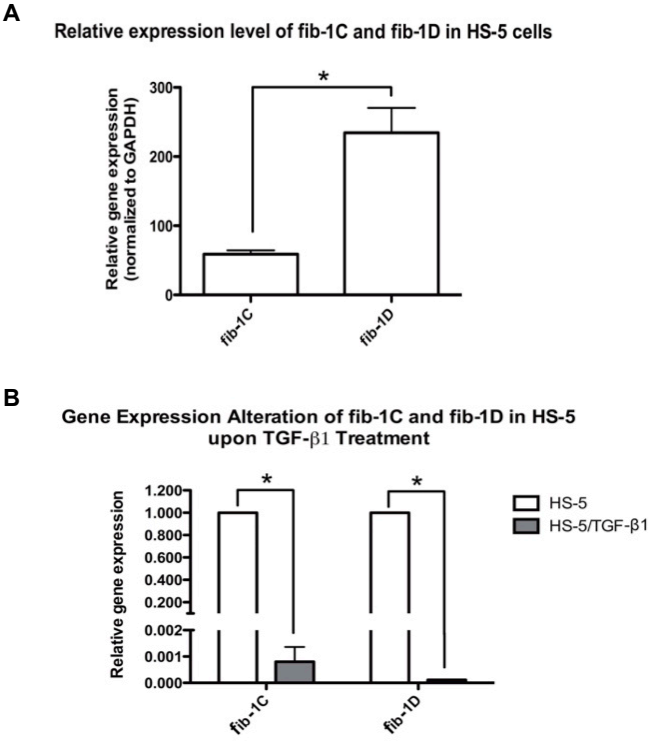

Figure 20: A) Levels of fibulin-1C and 1D expression in HS-5 cells were tested by qRT-PCR. The results showed significantly higher expression of fibulin-1D than fibulin-1C in HS-5 cells. The results were shown in relative gene expression normalized to GAPDH. B) Results from qRT-PCR showed that TGF-β1 treatment led to a reduction of both fibulin-1C and 1D as compared to control HS-5 cells. This indicated the effects of TGF-β1 to suppress fibulin-1 gene expression. All experiments were done in 3 biological replicates. Statistical analysis was done by ANOVA with Tukey's test. (* : P-value<0.0001)

3.6 Fibulin-1 Expression Correlated with PCa Death Inducing Activity from CM

To further test for a probability of fibulin-1 as a HS-5 DF, which could induce PCa cells death, CM from cell lines expressing different level of fibulin-1 was collected. In this experiment, the expression level of fibulin-1 in HS-5 cells, HS-27a (another bone marrow stromal cells) and HEK293 (human embryonic kidney) cells was compared in both whole cell lysates (Figure 21A and B) and in their CMs (Figure 21C and D). The results showed that HS-5 cells expressed significantly higher levels of fibulin-1 in cell lysates compared to the other two cell types. Fibulin-1 was moderately expressed in HS-27a and expressed at very low levels in HEK293 cells. CMs collected from these cell lines showed the same trend with the highest fibulin-1 level in HS-5 CM followed by HS-27a CM and HEK293 CM respectively. When these CMs were introduced to PCa cells, HS-5 CM significantly induced PCa cell death compared to SF DMEM control, HS-27a CM and HEK293 CM. Corresponding to fibulin-1 expression, HS-27a CM showed higher death inducing activity on PCa cells than SF DMEM and HEK293 CM (Figure 21E) but considerably less than HS-5 cell and CM. Taken together, the higher expression levels of fibulin-1 in HS-5 CM correlated with greater PCa death inducing activity compared to other cell lines with lower fibulin-1 expression. This indicated the potential of fibulin-1 to function as HS-5 DF inducing PCa cell death.

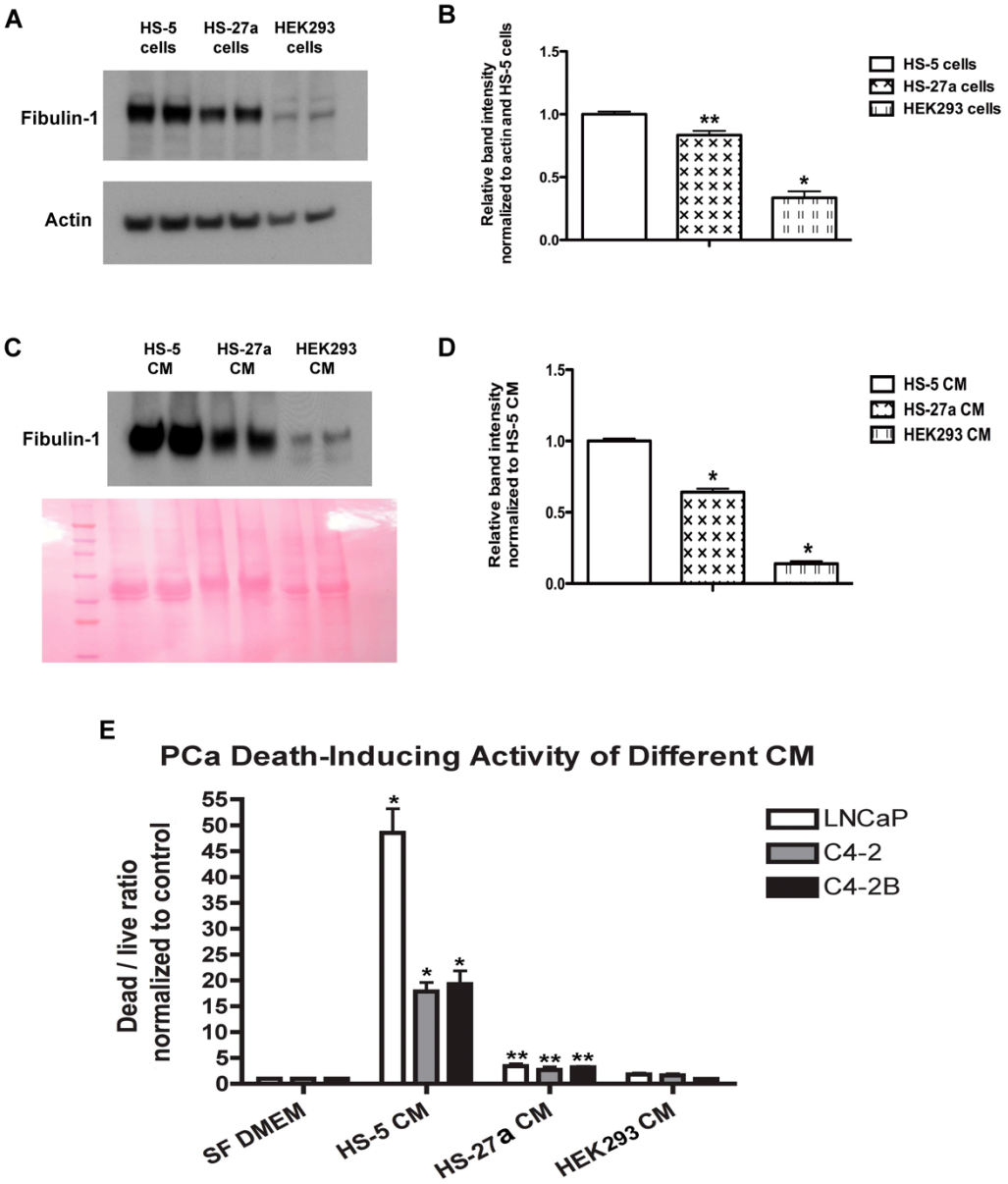
A
HS-5 cells
HS-27a cells
HEK293 cells
Fibulin-1
Actin
B
Relative band intensity normalized to actin and HS-5 cells
1.5
1.0
0.5
0.0
**
*
HS-5 cells
HS-27a cells
HEK293 cells
C
HS-5 CM
HS-27a CM
HEK293 CM
Fibulin-1
D
Relative band intensity normalized to HS-5 CM
1.5
1.0
0.5
0.0
*
*
HS-5 CM
HS-27a CM
HEK293 CM
E
PCa Death-Inducing Activity of Different CM
Dead / live ratio normalized to control
55
50
45
40
35
30
25
20
15
10
5
0
*
*
*
**
**
**
LNCaP
C4-2
C4-2B
SF DMEM
HS-5 CM
HS-27a CM
HEK293 CM

Figure 21 A) Fibulin-1 expression in HS-5, HS-27a and HEK293 cells was analyzed by western blot. The expression was significantly higher in HS-5 cells than in the other two cells. HS-27a showed moderate expression of fibulin-1; while HEK293 cells express fiblulin-1 weakly. B) Quantified data from western blot in experiments showed statistically significant difference of fibulin-1 expression in HS-5 cells as compared to HS-27a and HEK293 cells. C) Fibulin-1 levels in CM collected from HS-5 cells, HS-27a cells and HEK293 cells were tested by western blot. The same quantity of protein was loaded on the gel as shown by a Ponceau S stained blot. The results were consistent with cellular levels showing significant higher expression in HS-5 CM as compared to HS-27a CM and HEK293 CM. D) Quantified data from western blot in experiments showed statistically significant difference of fibulin-1 secretion in HS-5 CM as compared to HS-27a and HEK293 CMs. E) PCa cells were treated by CMs collected from different cell lines for 48 hours before being subjected to live/dead assays. PCa cell death induction was notably higher in HS-5 CM than HS-27a CM and HEK293 CM. Quantified data from live/dead assays were taken from at least 5 fields for each treatment. Experiments were done in 3 biological replicates from both PCa cells and the cells from which CMs were collected. Statistical analysis was done by ANOVA with Tukey's test. (* : P-value<0.0001, ** : P-value<0.05)

3.7 Partial Removal of Fibulin-1 from HS-5 CM Led to Lower Induction of PCa Death Induction from HS-5 CM

To determine the direct involvement of fibulin-1 in HS-5 CM and its PCa death induction, fibulin-1 was partially removed from HS-5 CM by immunoprecipitation (IP). Starting from the same pull of HS-5 CM, the results showed that HS-5 CM that underwent IP with fibulin-1 specific antibody showed significantly lower fibulin-1 level in CM compared to HS-5 CM that underwent only the preclearing step with protein A agarose or the one underwent IP with an isotype specific IgG antibody control (Figure 22A). The IP samples from each condition also showed the successful IP of fibulin-1 from HS-5 CM (Figure 22B). While HS-5 CM from other groups showed similar PCa death inducing activity, CM from fibulin-1 IP showed significantly lower PCa death induction. The decrease in PCa cell death in HS-5 CM after fibulin-1 IP could be observed in all PCa cell lines used: LNCaP, C4-2 and C4-2B (Figure 22C-E). Similar trends for the HS-5 DF response could be seen in this experiment. LNCaP showed the most response to HS-5 DF with the average of 92.13 fold of dead/live ratio normalized to control followed by C4-2 and C4-2B, which had 51.12 and 18.91 fold respectively. After IP with fibulin-1 specific antibody (HS-5 CM IP with Fib-1 atb), PCa death induction was decreased in all PCa cells tested. LNCaP, C4-2 and C4-2B showed 28.31%, 44.98% and 47.88% reduction in dead/live ratio respectively. These results suggested that fibulin-1 in HS-5 CM contributed to PCa cell death induction by the CM; therefore, partial removal of fibulin-1 out of HS-5 CM led to a substantial reduction in PCa cell death.

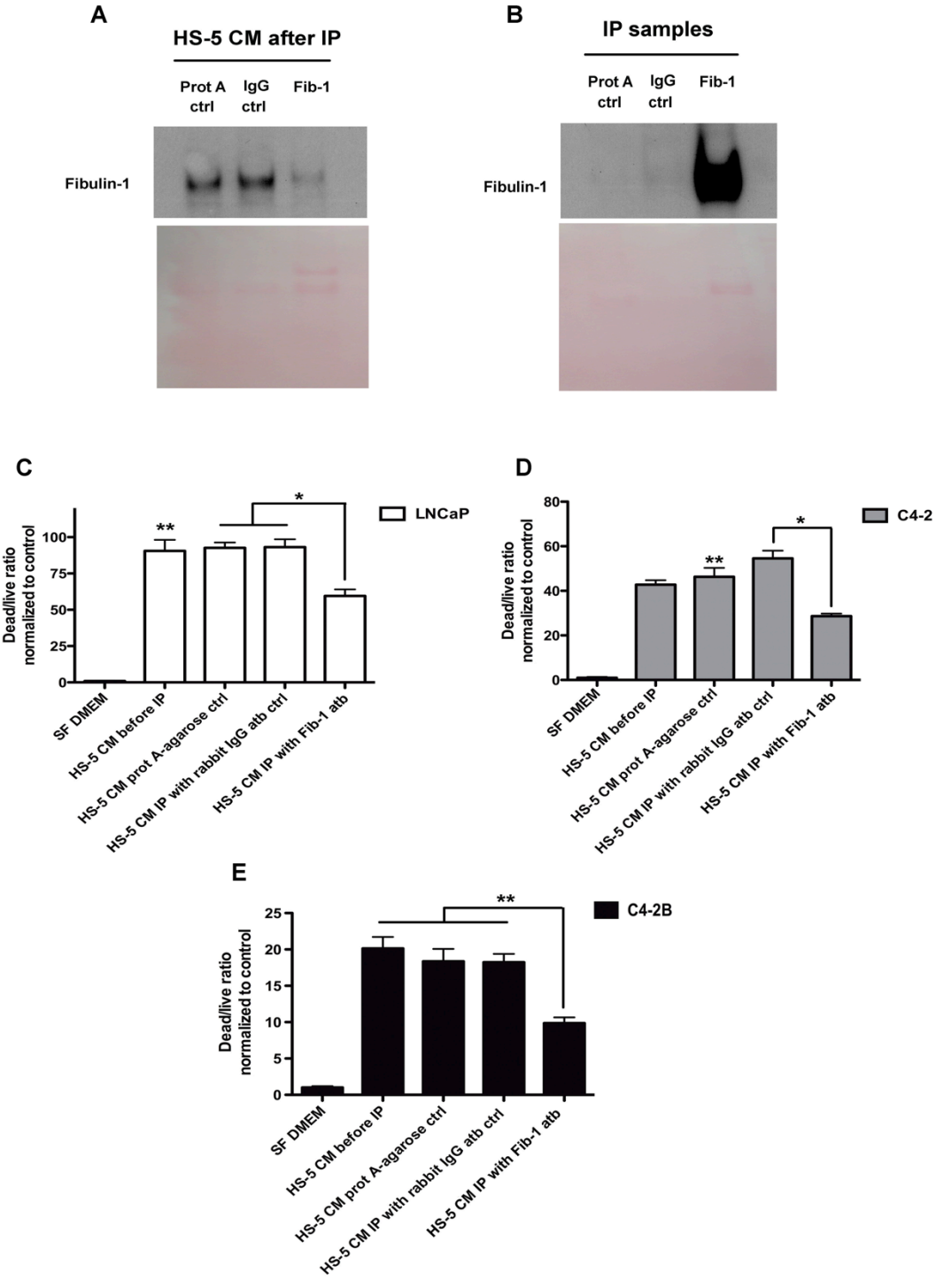
A
HS-5 CM after IP
Prot A ctrl
IgG ctrl
Fib-1
Fibulin-1
B
IP samples
Prot A ctrl
IgG ctrl
Fib-1
Fibulin-1
C
LNCaP
Dead/live ratio normalized to control
SF DMEM
HS-5 CM before IP
HS-5 CM prot A-agarose ctrl
HS-5 CM IP with rabbit IgG atb ctrl
HS-5 CM IP with Fib-1 atb
D
C4-2
Dead/live ratio normalized to control
SF DMEM
HS-5 CM before IP
HS-5 CM prot A-agarose ctrl
HS-5 CM IP with rabbit IgG atb ctrl
HS-5 CM IP with Fib-1 atb
E
C4-2B
Dead/live ratio normalized to control
SF DMEM
HS-5 CM before IP
HS-5 CM prot A-agarose ctrl
HS-5 CM IP with rabbit IgG atb ctrl
HS-5 CM IP with Fib-1 atb

Figure 22: Fibulin-1 was removed partially from HS-5 CM by IP. A) HS-5 CMs after underwent a pre-clearing process, IP with IgG isotype control antibody or IP with fibulin-1 antibody. Eluates were run on SDS-PAGE and probed with fibulin-1 antibody in western blot. The level of fibulin-1 in HS-5 CM after IP with fibulin-1 antibody was significantly reduced as compared to other groups. This indicated the partial removal of fibulin-1 from this HS-5 CM. B) IP samples from each condition showed a successful IP of fibulin-1 from HS-5 CM. C-E) HS-5 CM containing lower fibulin-1 level after IP showed significantly lower PCa cell death induction compared to CM from other groups. The CMs came from 5 biological replicates of HS-5 CM and IPs. Results on PCa cells came from at least 2 biological replicates of each cell line. Quantified data from live/dead assay were taken from at least 5 fields for each treatment. Statistical analysis was done by ANOVA with Tukey's test. (* : P-value<0.0001, ** : P-value<0.01 compared to HS-5 CM IP with Fib-1 antibody)

3.8 Knocking Down Fibulin-1 in HS-5 Cells (HS-5^{CRISPR_fib1}) Led to a Drastic Reduction of PCa Cell Death Induction from HS-5^{CRISPR_fib1} CM

As all data indicated strong associations between fibulin-1 levels and PCa cell death inducing activity from HS-5 CM, this experiment was set up to test for the ability of HS-5 CM to retain its PCa cell death induction after fibulin-1 gene was knocked down in HS-5 cells. Using CRISPR/Cas9 system, HS-5 cells were engineered to knockdown fibulin 1 targeting exon 11. Following screening of more than 120 clones, three clones were chosen for further analysis based on extremely low fibulin 1 expression levels (Appendix C). They were HS-5^{CRISPR_fib1_11A}, HS-5^{CRISPR_fib1_11B} and HS-5^{CRISPR_fib1_11C} . Low level fibulin 1 expression was confirmed in both whole cell lysate and in CM (Figure 23A and B) as compared to HS-5^{CRISPR_GFP} control cells and CM.

When the CM from HS-5^{CRISPR_fib1_11} cells was introduced to PCa cells, PCa cell death was reduced significantly compared to the CM from HS-5 cells transfected with the control plasmid (HS-5^{CRISPR_GFP}) (Figure 23C-E). The results are consistent in all PCa cell lines used including LNCaP, C4-2 and C4-2B showing 66.30%, 62.86% and 71.07% reduction in dead/live ratio as compared to PCa cells treated with HS-5^{CRISPR_GFP} CM, respectively. This indicated the association of fibulin-1 expression in HS-5 cells and HS-5 CM with HS-5 DF responsible for the induction of PCa death by HS-5 CM. Accordingly, HS-5 derived fibulin-1 shows strong potential to function as the HS-5 DF inducing PCa cell death.

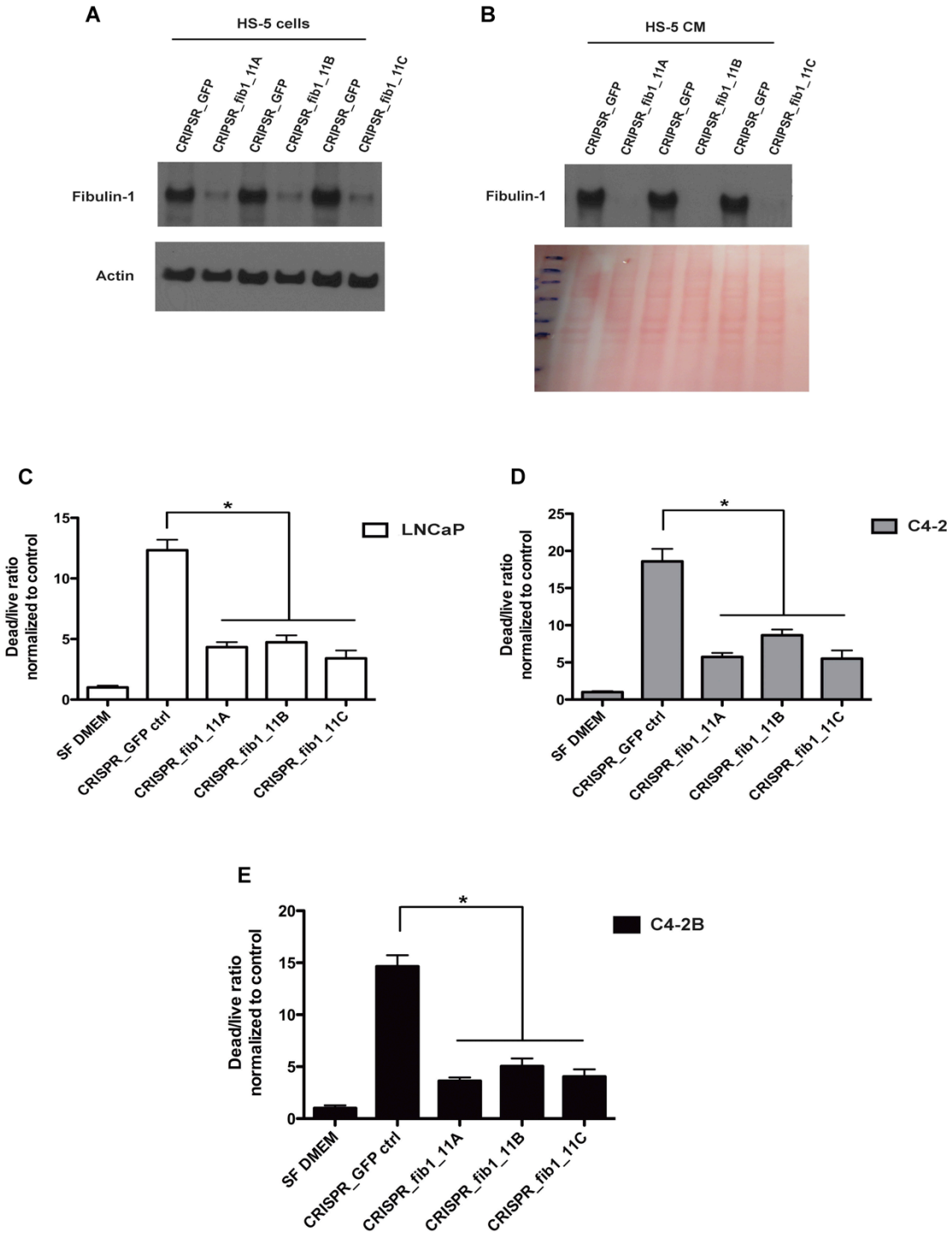
A
HS-5 cells
CRIPSR_GFP
CRIPSR_fib1_11A
CRIPSR_GFP
CRIPSR_fib1_11B
CRIPSR_GFP
CRIPSR_fib1_11C
Fibulin-1
Actin
B
HS-5 CM
CRIPSR_GFP
CRIPSR_fib1_11A
CRIPSR_GFP
CRIPSR_fib1_11B
CRIPSR_GFP
CRIPSR_fib1_11C
Fibulin-1
C
Dead/live ratio normalized to control
LNCaP
SF DMEM
CRISPR_GFP ctrl
CRISPR_fib1_11A
CRISPR_fib1_11B
CRISPR_fib1_11C
D
Dead/live ratio normalized to control
C4-2
SF DMEM
CRISPR_GFP ctrl
CRISPR_fib1_11A
CRISPR_fib1_11B
CRISPR_fib1_11C
E
Dead/live ratio normalized to control
C4-2B
SF DMEM
CRISPR_GFP ctrl
CRISPR_fib1_11A
CRISPR_fib1_11B
CRISPR_fib1_11C

Figure 23: Knocking down fibulin-1 in HS-5 cells led to lower PCa death induction from HS-5 CM. HS-5 CM from fibulin-1 knock down cells (HS-5^{CRISPR_fib1} CM) showed significantly lower PCa death induction compared to CM from control plasmid transfected cells (HS-5^{CRIPR_GFP} CM). Three clones of HS-5 cells transfected with CRIPSR plasmid targeted on exon 11 of fibulin-1 gene were selected, namely HS-$5^{CRISPR\_fib1\_11A}$, HS-$5^{CRISPR\_fib1\_11B}$ and HS-5^{CRISPR_fib1C}. A-B) The clones showed significantly lower expression of fibulin-1 in both whole cell lysates and in the CMs. C-E) CMs collected from HS-5^{CRIPR_fib1} showed makedly lower PCa cell death induction in LNCaP, C4-2 and C4-2B compared to HS-5^{CRIPR_GFP} CM. Results on PCa cells came from 2 biological replicates of each cell line. Quantified data came from live/dead assays taken from at least 5 fields for each treatment. Statistical analysis was done by ANOVA with Tukey's test. (*P-value<0.0001)

Chapter 4

DISSCUSSION

With early detection and proper treatment, localized PCa can be managed leading to an increase of a 5-year survival rate of almost 100%. The survival rate drops dramatically to around 30% in patients with advance metastatic PCa. [12, 13]. Among PCa metastatic sites, bone is a primary metastatic site for PCa leading to multiple bone-related symptoms including bone pain, bone fracture and spinal cord compression [14]. Therefore, bone metastases not only lead to lower survival rates, but also to a reduced quality of life. Moreover, the mechanisms behind PCa bone metastasis and PCa colonization of bone remain elusive. In contrary to the notorious Paget's seed and soil theory [25], the negative interactions between PCa cells and bone microenvironment have been reported in many studies [29-33]. In studies from Sikes' lab, human bone marrow stromal cell lines established by Roecklein and Torok-Storb [158] and PCa cell lines from LNCaP progression model [231, 232] were used as the representatives for bone microenvironment and PCa cells. It has been shown that HS-5 CM contained cytokines that support the proliferation of committed hematopoietic progenitor cells, which reside in the sinusoidal area of bone [158-160]. This suggested that this cell population could be one of the first cell types in the bone microenvironment that PCa cells encounter during PCa bone colonization. In contrast, another BMS cell line, HS-27a was shown to support cobblestone area formation for hematopoietic stem cells indicating the location of HS-27a niche to be located more toward the endosteal area in bone [160]. Previous studies showed that one specific

bone marrow stromal cell line, HS-5, secreted soluble factor(s) in its CM (HS-5 DF) that induce PCa apoptosis and neuroendocrine differentiation; while HS-27a CM does not showed such effects [32, 33, 87]. Corresponding to previous studies [29-33], this phenomenon indicated that the initial interactions between PCa cells and bone morrow microenvironment could be negative or hostile. Apoptotic induction from HS-5 cells could be a selective pressure for the PCa cells that arrive at bone. Subsequently, to escape from this pressure, the surviving cells undergo NED, which has been shown to correlate with an aggressive form of PCa when found locally [238-240]. This hypothesis was supported by other studies showing that PCa metastasis progressed from genetically heterogeneous DPCs to genetically homogeneous PCa tumors at the metastatic sites [164-166]. My results, as well as results from previous studies, showed that PCa cells from LNCaP progression model responded to HS-5 DF to different degrees. Most of the time, the results showed highest PCa death induction in a non-metastatic and androgen sensitive LNCaP cells. In contrast, PCa death induction in a metastatic and androgen independent, C4-2 cells were significantly lower, and the least response could be seen in a bone adapted C4-2B cells [31, 32]. This inverse relationship between HS-5 mediated PCa death induction and the progression status of PCa cell lines also supports the hypothesis of PCa selection during bone colonization.

To identify possible candidate(s) for HS-5 DF, biochemical characteristics of the HS-5 DF that induced PCa cell death were determined. I has shown that HS-5 DF is a trypsin sensitive, and the induction of PCa death after being exposed to trypsin induction. This data indicated a protein property with at least one trypsin recognition site on HS-5 DF. Heat sensitivity tests also confirmed the protein characteristics of HS-5 DF. The results showed that PCa cell death inducing activity from HS-DF kept

decreasing as the temperatures were increasing. Even though it has been shown that prolong heat treatments could lead to the degradation of low molecular weight carbohydrates (monosaccharides an disaccharides) [241], the sizes of these molecules (<500 Da) were far smaller then the tentative size of HS-5 DF that was discovered in later experiments. Moreover, other heat-induced effects in carbohydrate including gelatinization and browning processes [241] were not found in HS-5 CM after being exposed to high temperature. Other studies showed that heat treatment on plant-derived and animal-derived lipids had no effect on lipid content; in contrast, the activity of lipase enzyme was reduced significantly with heat treatment [242, 243]. Accordingly, the data from my experiment continued to support the idea that HS-5 DF was proteinaceous. Recognized as HS-5 derived protein(s), other protein characteristics were tested in the following experiments. The ability of HS-5 DF to retain its PCa death induction in varied pH has been tested for future experiments. The results showed that HS-5 DF could retain functionality across pH 4-10, suggesting the possibilities to use many proteomics techniques to identify HS-5 DF without loosing its functional structure. In addition, the requirement of disulfide binding in its structure was tested. The results showed that HS-5 DF was sensitive to DTT treatment thereby indicating the requirement of disulfide bonding for HS-5 DF to function properly. The results were consistent between a metastatic PCa line, C4-2 and a bone adaptive PCa line, C4-2B showing a significant reduction of HS-5 DF's activity after DTT treatment. However, the results showed no difference between HS-5 DF inducing PCa death in an androgen sensitive, LNCaP cells from HS-5 CM before and after DTT treatment. This suggested the differential responses of HS-5 DF death induction between an androgen sensitive PCa cell line and androgen independent PCa cell lines.

One possible explanation was due to the difference in reducing protective enzyme, sulfyhydryl oxidase Q6 (Qscn6) that can re-introduce disulfide bonds into protein structures. It has been shown that Qscn6 was expressed higher expressed in non-metastatic PCa, but the expression of these enzymes was significantly lower as the PCa progressed to a more aggressive stage [244]. In addition, the tentative size for HS-5 DF was determined using centrifugal filters for size selection experiments. The results showed the activity of HS-5 DF retained in the fractions containing proteins, which are bigger than 30 kDa, but smaller than 100 kDa. This indicated that the tentative size for HS-5 DF would be between 30 kDa - 100 kDa. Interestingly, an increase in HS-5 DF's activity in fractions with smaller proteins was seen in both 30 kDa and 100 kDa size selections after DTT treatment. This suggested possible roles of disulfide bonding in oligomerization and/or multi-protein interaction of HS-5 DF proteinaceous. Lastly, the ability of HS-5 DF to conserve its functional structure after protein concentration was tested. Sample concentration method was determined for further proteomic studies as well as for the enrichment of samples for the purification and subsequent functionality tests. Several protein concentration methods including two subsequent size selections through 100 and 30 kDa filters as well as protein precipitation by Methanol-chloroform [245] were tested. Both methods failed to preserve HS-5 DF activity to induce PCa cell death after the concentration processes (data was not shown). However, the data from this study showed that PCa death inducing activity of HS-5 DF was not reduced after protein concentration using speed vacuum concentration. This could be a result from an extended period (1 hour) of high-speed centrifugation (550 x g), which led to the denaturation of the protein samples in two subsequent size selections as compared to the milder freeze drying

concentration at 207 x g for the shorter time (10 minutes). On the other hand, methanol/chloroform precipitation was widely used in protein structure studies [245]. However, exposing the protein samples to high volume of organic solvents could affect the functionality of the proteins. Similar to tissue fixation, methanol could lead to the dehydration of proteins to fix the protein structures, but at the same time, this fixation could lead to protein denaturation. Therefore, this method could be used to study protein structure, but the denaturation could lead to the lost of protein functions in situ. Interestingly, not only was the activity of HS-5 DF preserved in speed vacuum concentration, but an increase in HS-5 DF's activity was also observed after the concentration. This data further supported the possibility that HS-5 DF could co-exist and interact with other factors including labile molecule (s), which could not survive the concentration process. However, these experiments showed that protein concentration by speed vacuum concentrator could be used to prepare HS-5 CM samples to study/purify HS-5 DF in future experiments.

The correlations between high TGF-β1 in patient sera and the incidence of PCa bone metastasis were shown in many studies [235, 236]. The effects of TGF-β1 on HS-5 DF were investigated. Consistent with the previous study [32, 33, 246], my results showed that PCa death induction from HS-5 CM was suppressed by TGF-β1. TGF-β1 was highly expressed in PCa [247] and released by a vicious cycle where PCa cells stimulated bone turnover to provide a favorable environment for PCa bone colonization [52]. HS-5 DF suppression by TGF-β1 suggested that high levels of TGF-β1 also could play a role in the survival of PCa by reducing HS-5 DF during PCa bone colonization. To identify possible HS-5 DF candidates, HS-5/TGF-β CM was used as a sample that contain lower level of HS-5 DF correlating with its decreased

ability to induce PCa death. Results from high resolution SDS-PAGE showed that TGF-β1 treatment on HS-5 cells led to protein pattern alterations in HS-5/TGF-β1 CM as compared to control HS-5 CM where many protein bands were up- and downregulated due to TGF-β1 treatment. To further verify possible HS-5 DF candidates, protein bands that showed differential expression upon TGF-β1 treatment were picked as samples for MS/MS analysis. The data from MS/MS analysis showed the upregulation of many proteins including TIMP-1, type 1 collagen, moesin and ECM protein-1. On the other hand, some proteins also showed a downregulation with TGF-β1 including MMP-1, MMP-3, Prommp-1 and fibulin-1. Among the HS-5 DF candidates, fibulin-1 was shown to be the strongest candidate for HS-5 DF for many reasons. Firstly, cancer suppression effects from fibulin-1 were noted in many types of cancer including fibrosarcomas, renal cancer, nasopharyngeal carcinoma, gastric cancer and liver cancer [169, 216, 218, 219]. These studies showed the abilities of fibulin-1 to suppress growth of cancer both in vitro and in vivo as well as the capabilities to inhibit cancer migration. In addition, downregulation of FBLN1 gene via promoter methylation was shown in several types of cancer including gastric cancer, renal cancer and liver cancer. For PCa, the downregulation of both fibulin-1C and fibulin-1D in PCa cells and in cancerous tissue as compared to benign tissue was reported [223]. The downregulation of FBLN1 gene and lower level of fibulin-1 protein in many types of cancer, including PCa, supported its tumor suppression potential in PCa. Secondly, the size for fibulin-1 is 90 kDa in a native form and 77 kDa in reducing-denatured SDS-PAGE; therefore, the size of fibulin-1 corresponded to the tentative size of HS-5 DF. In addition, fibulin-1 was shown to be a protein with many disulfide bonds in its structure, which also corresponded to the sensitivity of a

reducing agent, DTT. Last but not least, anti-cancer activities of fibulin-1 were revealed in many studies; while, the opposite effect was noted in ovarian and breast cancer, which showed an increase in fibulin-1 as compared to benign samples [224-227]. Corresponding to these results, a specificity test for HS-5 DF was performed in a previous study from Sikes' lab. These results showed that HS-5 DF in HS-5 CM induced PCa cell death specifically, but had no effect on breast cancer or fibroblast cell survival (Appendix E) [33]. Accordingly, fibulin-1 showed the strongest potential above other candidates; therefore, it was selected for further investigation.

To verify fibulin-1 as HS-DF that induced PCa cell death, the basal level of fibulin-1 in HS-5 BMS and PCa cells was compared. My data showed that HS-5 cells expressed dramatically higher level of fibulin-1 than PCa cells from LNCaP progression model including LNCaP, C4-2 and C4-2B (Figure 18). These results were consistent to previous research from other groups showing significant reduction in PCa cell lines as compared to normal prostate epithelium and in PCa tissue samples as compared to non-cancerous samples [223]. Thereby, fibulin-1 showed a potential to be a tumor suppressor in PCa. Even though low level of fibulin-1 could be seen in BPH-1 cells as well, the possibility that HS-5 DF might also interact with other factor(s) in PCa death induction was shown from my previous experiments. This interaction could also contribute to the different responses in PCa cells and BPH-1 to HS-5 CM (Appendix E). TGF-β1 has been thought to be a stimulator for PCA aggressiveness and serum levels in patient's correlate with bone metastasis. Furthermore, data from my experiments indicated that TGF-β1 decreased levels of fibulin-1 in HS-5 cells and HS-5 CM. These data implied that the HS-5 DF should be TGF-β1 responsive. Indeed, the results showed that fibulin-1 levels were significantly lower in HS-5/TGF-β1 cells

and HS-5/TGF-β1 CM than control HS-5 cells and CM. (Figure 19) A reduction in fibulin-1 level in both cellular level and in CM corresponded to a decrease in HS-5 DF's activity; therefore, these results indicated the possibility of fibulin-1 to function as HS-5 DF. It also provides a mechanism to explain PCa colonization of bone in the presence of high serum TGF-β. Essentially, TGF-β1 decreases the expression of fibulin 1 in the bone creating a less hostile environment that is more suitable for PCa colonization and growth.

Since the opposing effects of tumor supressive fibulin-1D and tumor promoting fibulin-1C were reported in other studies [224-227], expression levels of both isoforms were studied in HS-5 cells. The data showed that HS-5 expressed significantly higher (5X) tumor supressive fibulin-1D than tumor promoting fibulin-1C. These data corespond well to the induction of PCa cell death from HS-5 CM. In addition, the effects of TGF-β1 on fibulin-1C and fibulin-1D expression were also investigated. After 96 hours of TGF-β1 of treatment, expression levels of fibulin-1C and fibulin-1D in HS-5/TGF-β1 cells were determined in comparison to the control HS-5 cells. The data showed that the expression of both fibulin-1C and fibulin-1D were suppressed significantly upon TGF-β1 treatment correlating with HS-5 DF's activity. This suggested an inhibitory effect of TGF-β1 on FBLN1 gene expression rather than to favor RNA splicing toward any specific isoform. PCa death induction from CM collected cell lines expressing different levels of fibulin-1 was tested to determine the correlation between fibulin-1 and PCa death induction from HS-5 CM compared to others CMs. In this experiment, fibulin-1 in HS-5, HS-27a and HEK293 cells and CMs were determined by western blot analysis. The results showed that HS-5 expressed highest level of fibulin-1 in both cellular level and in HS-5 CM as

compared to the other two. HS-27a expressed moderate level of fibulin-1 followed by HEK293, which weakly expressed fibulin-1 in both whole cell lysates and in their CMs. As these CMs were introduced to PCa cells, the cells responded to PCa death induction from CMs correlating to fibulin-1 level in CMs (Figure 21). Taken together, these data show a correlation between fibulin-1 level in CMs and the induction of PCa death and strongly support the potential of fibulin-1 to function as HS-5 DF.

To test the direct involvement of fibulin-1 in HS-5 derived PCa death induction, fibulin-1 was partially removed from HS-5 CM by IP. The results showed that IP successfully removed most fibulin-1 out of CMs as can be seen from HS-5 CMs and IP samples after IP with fibulin-1 specific antibody (Figure 22). HS-5 CMs after protein A preclearing, IP with IgG control antibody and IP with fibulin-1 antibody were introduced to PCa cells to determine their ability to induce PCa death. The results showed that HS-5 CM containing less fibulin-1 from HS-5 CM after IP with fibulin-1 antibody had significantly lower PCa cell death induction. Accordingly, the results showed that fibulin-1 in HS-5 CM contributed to PCa death induction. To further verify fibulin-1 as HS-5 DF, FBLN-1 gene was knocked down from HS-5 cells by using CRISPR-Cas9 system. CRISPR plasmids carrying gRNA targeted on exon 11 of FBLN1 gene (CRISPR_fib1_11) were used. The results showed that CRISPR_fib1_11 plasmid successfully knocked down FBLN1 leading to a decrease in fibulin-1 level in both whole cell lysate (HS-$5^{CRISPR\_fib1\_11}$) and in HS-$5^{CRISPR\_fib1\_11}$ CMs (Figure 23). After HS-$5^{CRISPR\_fib1\_11}$ CMs were introduced to PCa cells for 48 hours, HS-$5^{CRISPR\_fib1\_11}$ CMs showed notably lower induction of PCa cell death as compared to CM from HS-5 transfected with CRISPR_GFP control (HS-5^{CRISPR_GFP} CM). These results demonstrated that fibulin-1 secreted from HS-5 cells directly

participates in the induction of PCa cell death by HS-5 CM. Accordingly, results from my study indicated that fibulin-1 correlates with PCa death inducing activity of HS-5 CM, and could function as HS-5 DF inducing PCa cell death in all PCa cells from LNCaP progression model.

Chapter 5

FUTURE DIRECTIONS AND SIGNIFICANCE

5.1 Future Directions

Previous results from Sikes' lab demonstrated a negative interaction between HS-5 CM and PCa cells in the LNCaP progression model [31-33]. These results indicated the ability of HS-5 cells to secrete an apoptotic inducer for PCa cells leading to significant cell apoptosis and death upon HS-5 CM treatment. As a crucial step in understanding this mechanism as well as the initial interaction between BMS cells and PCa, the goal for my project was to identify the HS-5 DF contributing to PCa cell death. My results showed a correlation between fibulin-1 expression and ability of CM to induce PCa cell death. Moreover, removing fibulin-1 from CM and knocking down FBLN1 in HS-5 cells led to a significant decrease in PCa cell death induction. Therefore, all data indicated that fibulin-1 could function as the HS-5 DF that induced PCa cell death. However, unique functions of the two prominent fibulin-1 isoforms were noted in many studies [224-227]. Therefore, one of the future directions for this project would be to study the effects of each isoform on PCa cell death. Since HS-5 cells expressed significantly higher level of tumor suppressive fibulin-1D than fibulin-1C, I hypothesize that fibulin-1D could be the only functional fibulin-1 mediating PCa cell death. To test this hypothesis, each specific isoform of fibulin-1 could be knocked down from HS-5 cells by using shRNA targeting on fibulin-1C and fibulin-1D separately. After transfection, the level of fibulin-1C and 1D could be determined by qRT-PCR and western blot analysis using fibulin-1C and fibulin-1D specific

antibodies as compared to HS-5 cells transfected with scramble control (HS-$5^{sh\_scramble}$). The clones, which showed a successful knockdown including HS-5^{sh_fib1C} and HS-5^{sh_fib1D} cells would be selected for future experiments. HS-5^{sh_fib1C} CM, HS-5^{sh_fib1D} CM and HS-$5^{sh\_scramble}$ CM would be used to treat PCa cells to determine their relative PCa cell death inducing activity. I would expect to see significant lower PCa cell death induction from HS-5^{sh_fib1D} CM as compared to other groups indicating the PCa death inducing activity results from fibulin-1D. In addition, to test for the isoform specificity for PCa death induction, overexpression of fibulin-1C and fibulin-1D could be done in HEK293 cells, which has been shown to have a very low basal expression of fibulin-1. Similar to the previous experiment, an overexpression of fibulin-1C and fibulin-1D could be tested by qRT-PCR and western blot analysis. HEK293 CM containing high level of fibulin-1C (HEK$^{fib\text{-}1C}$ CM) and fibulin-1D (HEK$^{fib\text{-}1D}$ CM) could be used as crude samples to test for PCa death induction from each isoform. Further, this approach would allow one to determine if there are additional proteins in HS-5 CM that are not in HEK293 cell CM. On the other hand, these fibulin-1C and fibulin-1D rich CM could also be used as samples for fibulin-1C and fibulin-1D purification. The purified proteins could be tested on PCa cells to demonstrate PCa cell death induction from each isoform. HS-5 CM might be used in combination with the crude CMs or purified proteins to test for BMS specific co-factor; however, I would expect to see significant higher PCa cell death induction in PCa cells treated with crude HEK$^{fib\text{-}1D}$ CM or purified fibulin-1D with or without HS-5 CM.

Since the mechanisms behind fibulin-1 mediated PCa cell death induction has not been elucidated, identification of an associated protein(s) would be a crucial step to investigate a possible mechanism for PCa death induction. In my study, I

successfully immune-precipitated fibulin-1 from HS-5 CM leading to significant reduction of PCa death inducing activity. Moreover, the possibility of multi-proteins interaction of HS-5 DF was shown from previous experiments (Figure 13 & 14). Accordingly, fibulin-1 IP samples could be used as samples to identify possible interacting proteins that co-IP with fibulin-1. Fibulin-1 IP samples would be used for MS/MS analysis to acquire the protein IDs of fibulin-1 interacting proteins. This result would be an important clue for the mechanism behind fibulin-1 mediated PCa cell death induction. Genetic modification of the gene(s) coding for this interacting protein(s) could be done by either CRISPR-Cas system, Transcription activator-like effector nucleases (TALENs) or short hairpin RNA (shRNA) to study the effect of this candidate on fibulin-1 mediated PCa cell death.

As a potential therapy and/or a novel maker for PCa bone metastasis, animal and human studies will be needed. Since HS-5 CM and HS-5 derived fibulin-1 showed a potential to suppress PCa by induing PCa cell death, these samples could be used for animal experiments. Firstly, PCa death induction by HS-5 CM would be confirmed in SCID mice. A highly metastatic C4-2 PCa cell line would be injected subcutaneously on each mouse. After the tumors are formed, mice would be injected with either SF-DMEM control or HS-5 CM for a period of time. Then, the size of tumors would be measured in comparison between two groups. Before sacrifice, PCa bone metastasis would be determined by computerized tomography (CT) scan. The tumors from each site would be used for TUNEL assay to determine cell apoptosis in tumor from each treatment. I would expect that the tumor size from HS-5 CM treatment group would be smaller and undergo more apoptosis than SF-DMEM control group according to PCa death induction of HS-5 CM. I also expect to see less bone metastasis in mice treated

with HS-5 CM. Similar experiments could be carried out using purified fibulin-1, purified fibulin-1C or fibulin-1D and vehicle control treatment to study effects of fibulin-1 and its specific isoform on PCa growth and bone metastasis. If fibulin-1 showed a potential to be a novel therapeutic agents in animal studies as expected, further experiments could be done for a targeted treatment for PCa cells. In this case, fusion proteins between fibulin-1 or fibulin-1C and 1D specific C-terminal fragments would be fused with antibody against PCa specific surface antigen. I expect that this targeted treatment would lead to a higher inhibitory effect on PCa with lower side effects on other cell types. Once the results have been confirmed in animal models, human trials could be designed by using antibody tagged fibulin-1 for advance stage and bone metastatic PCa patients in the future.

HS-5 cells were hypothesized to reside among the sinusoid area and showed potential for initial negative interactions between PCa cells and BMS. HS-5 DF, fibulin-1, could function as an environmental pressure against the newly arriving PCa cells. Therefore, I hypothesize that the level of fibulin-1 might correlate and can be used as a good indicator for PCa bone metastasis. To test this hypothesis, C4-2 PCa cells would be injected to SCID mice; then, serum level of fibulin-1 would be measured in a timely manner from localized tumor until the bone metastases were found by CT-scan. If fibulin-1 showed a potential as an effective marker for PCa bone metastasis, the level of fibulin-1 should correlate with PCa bone metastatic events. Furthermore, with the potential initial interactions between HS-5 derived fibulin-1 and PCa cells during PCa bone colonization, fibulin-1 could be used as a potential novel marker to early detect PCa bone metastasis in patients' serum. In this study, serum level of fibulin-1 would be determined in patients' serum with different stages of PCa.

I expect to see a correlation between fibulin-1 level in patients' serum with PCa bone metastasis. Therefore, fibulin-1 level is expected to be higher in patients with bone metastatic PCa as compared to patients with earlier stages of PCa or PCa metastasis to other sites.

On the other hand, the regulatory mechanism that TGF-β1 led to a suppression of HS-5 DF is still unknown. Previous study from Sikes' lab showed that an inhibition of TGF-β signaling by using a dominant-negative mutant of TGF-β receptor type II (DN-TβRII) in HS-5 cells led to a prevention of HS-5 DF inhibition by TGF-β1 [33]. To confirm this investigation, in vivo experiments using TGF-β receptor 2 (TGFBR2) knockout mice specifically in bone stromal could be used if available in the future. I would expect that fibulin-1 levels would be higher in serum of TGFBR2 knockout mice than SCID control mice leading to lower bone metastases in TGFBR2 knockout mice as compared to the control group. HS-5 CM treatment would also have higher effects on tumor inhibition in TGFBR2 knockout mice than SCID control mice if TGF-β not only suppress FBLN1 expression, but also lead to the expression of fibulin-1 antogonist(s). Results from this experiment, would confirm the mechanism for HS-5 DF inhibition by TGF-β1 via TGFBR2. Other signaling molecules in TGF-β signaling, such as different types of TGFBR1 could be tested similarly by using gene modification tools, such as TALENs, CRISPR or shRNA to knock down the gene of interest in HS-5 cells for an in vitro study. TGF-β1 treatment would be given to the knocked down HS-5 cells and the control HS-5 cells. Then CM from each group would be introduced to PCa cells to compare PCa cell death induction from HS-5 CM and the effect of TGF-β1 on HS-5 DF from each group. I would expect the to see no reversal of the death effect from TGF-β1 treatment on HS-5 DF from the knocked out

HS-5 cells if the proteins of interest participate in HS-5 DF suppression by TGF-β1. The investigation could be confirmed by using animal models with specific knock out as mentioned.

5.2 Significance

As a critical metastatic site for PCa, the mechanism behind PCa bone metastasis and the initial interactions between PCa cells and bone environment are still elusive. Interestingly, previous data from Sikes' lab suggests a negative interaction between soluble factor(s) from HS-5 BMS cells and PCa. We have shown that CM from HS-5 cells contains an unidentified soluble factor(s) that induces PCa death and NED. This suggested an environmental pressure by which they try to eliminate PCa and force subpopulations of PCa to die or differentiate to survive. As HS-5 CM showed specific PCa cell death inducing activity, identification of the HS-5 DF that induces PCa cell death is needed.

In this study, I was able to identify fibulin-1 as one of HS-5 DF that induced PCa cell death. This study not only confirmed previous investigations about negative interactions between PCa cells and factor(s) in bone microenvironment, but this also is the first report on the novel role of fibulin-1 in PCa bone metastasis. My results showed the correlations between fibulin-1 level and PCa cell death as well as verifed that HS-5 derived fibulin-1 contributed to PCa cell death from HS-5 CM. Even though more researches is still needed, this study has provided better understanding to the initial interaction between PCa and the bone microenvironment and may lead to better diagnosis and therapy for PCa patients with bone metastases. As a HS-5 DF, fibulin-1 could be a new candidate for novel therapy for those who are suffering with PCa bone metastasis In addition; the presence of this factor might also be used as a novel

biomarker for early detection of patients at risk to develop PCa bone metastasis in the future.

REFERENCES

[1] Prins GS. What is the prostate and what are its functions? Handbook of Andrology 2014; 11-11 - 11-14.

[2] Siegel RL, Miller KD and Jemal A. Cancer statistics, 2015. CA: a cancer journal for clinicians 2015; 65: 5-29.

[3] Bubendorf L, Schopfer A, Wagner U, Sauter G, Moch H, Willi N, Gasser TC and Mihatsch MJ. Metastatic patterns of prostate cancer: an autopsy study of 1,589 patients. Human pathology 2000; 31: 578-583.

[4] International Agency for Research on Cancer (Wolrd Health Organization). Global Cancer Facts and Figures. Atlanta: American Cancer Society, 2015.

[5] World Cancer Research Fund International. Cancer Worldwide data. World Cancer Research Fund International, 2015.

[6] American Cancer Society. Cancer Facts and Figure 2015. Atlanta: American Cancer Society, 2015.

[7] National Cancer Institute. Treatment Choices for Men with Early-Stage Prostate Cancer. U.S. Department of Health and Human Services. National Institutes of Health, 2015.

[8] American Cancer Society. Prostate Cancer Overview. Atlanta: American Cancer Society, 2015.

[9] Heidenreich A, Bastian PJ, Bellmunt J, Bolla M, Joniau S, van der Kwast T, Mason M, Matveev V, Wiegel T, Zattoni F and Mottet N. EAU guidelines on prostate cancer. part 1: screening, diagnosis, and local treatment with curative intent-update 2013. European urology 2014; 65: 124-137.

[10] Heidenreich A, Bastian PJ, Bellmunt J, Bolla M, Joniau S, van der Kwast T, Mason M, Matveev V, Wiegel T, Zattoni F and Mottet N. EAU guidelines on prostate cancer. Part II: Treatment of advanced, relapsing, and castration-resistant prostate cancer. European urology 2014; 65: 467-479.

[11] Saad F and Miller K. Treatment options in castration-resistant prostate cancer: current therapies and emerging docetaxel-based regimens. Urologic oncology 2014; 32: 70-79.

[12] Walsh PC. Dr. Patrick Walsh's Guide to Surviving Prostate Cancer. New York: Warner Books, 2001.

[13] Mishra A, Shiozawa Y, Pienta KJ and Taichman RS. Homing of cancer cells to the bone. Cancer microenvironment : official journal of the International Cancer Microenvironment Society 2011; 4: 221-235.

[14] Gater A, Abetz-Webb L, Battersby C, Parasuraman B, McIntosh S, Nathan F and Piault EC. Pain in castration-resistant prostate cancer with bone metastases: a qualitative study. Health and quality of life outcomes 2011; 9: 88.
[15] Hering F, Rodrigues PR and Lipay M. Clodronate for treatment of bone metastases in hormone refractory prostate cancer. International braz j urol : official journal of the Brazilian Society of Urology 2003; 29: 228-233.
[16] Omlin A, Pezaro C, Mukherji D, Mulick Cassidy A, Sandhu S, Bianchini D, Olmos D, Ferraldeschi R, Maier G, Thompson E, Parker C, Attard G and de Bono J. Improved survival in a cohort of trial participants with metastatic castration-resistant prostate cancer demonstrates the need for updated prognostic nomograms. European urology 2013; 64: 300-306.
[17] Bahl A, Masson S, Birtle A, Chowdhury S and de Bono J. Second-line treatment options in metastatic castration-resistant prostate cancer: a comparison of key trials with recently approved agents. Cancer treatment reviews 2014; 40: 170-177.
[18] Heidenreich A BP, Bellmunt J, Bolla M, Joniau S, Mason MD, Matveev V, Mottet N, van der Kwast TH, Wiegel T, Zattoni F. Guidelines on Prostate Cancer. 2012.
[19] Gruber R. Reader's digest of the pathophysiology of bone metastases. Wiener medizinische Wochenschrift 2012; 162: 370-373.
[20] Israeli RS. Managing bone loss and bone metastases in prostate cancer patients: a focus on bisphosphonate therapy. Reviews in urology 2008; 10: 99-110.
[21] Collins R, Fenwick E, Trowman R, Perard R, Norman G, Light K, Birtle A, Palmer S and Riemsma R. A systematic review and economic model of the clinical effectiveness and cost-effectiveness of docetaxel in combination with prednisone or prednisolone for the treatment of hormone-refractory metastatic prostate cancer. Health technology assessment 2007; 11: iii-iv, xv-xviii, 1-179.
[22] Cheville JC, Tindall D, Boelter C, Jenkins R, Lohse CM, Pankratz VS, Sebo TJ, Davis B and Blute ML. Metastatic prostate carcinoma to bone: clinical and pathologic features associated with cancer-specific survival. Cancer 2002; 95: 1028-1036.
[23] Keller ET. The Biology of Skeletal Metastases. Kluwer Academic Publisher, 2004.
[24] Suzman DL, Boikos SA and Carducci MA. Bone-targeting agents in prostate cancer. Cancer metastasis reviews 2014; 33: 619-628.
[25] Paget S. The distribution of secondary growths in cancer of the breast. 1889. Cancer metastasis reviews 1989; 8: 98-101.
[26] Buijs JT and van der Pluijm G. Osteotropic cancers: from primary tumor to bone. Cancer letters 2009; 273: 177-193.

[27] Lee RJ and Smith MR. Cabozantinib and prostate cancer: inhibiting seed and disrupting soil? Clinical cancer research : an official journal of the American Association for Cancer Research 2014; 20: 525-527.
[28] Yang W and Levine AC. Androgens and prostate cancer bone metastases: effects on both the seed and the soil. Endocrinology and metabolism clinics of North America 2011; 40: 643-653, x.
[29] Knerr K, Ackermann K, Neidhart T and Pyerin W. Bone metastasis: Osteoblasts affect growth and adhesion regulons in prostate tumor cells and provoke osteomimicry. International journal of cancer. Journal international du cancer 2004; 111: 152-159.
[30] O'Connor JC, Farach-Carson MC, Schneider CJ and Carson DD. Coculture with prostate cancer cells alters endoglin expression and attenuates transforming growth factor-beta signaling in reactive bone marrow stromal cells. Molecular cancer research : MCR 2007; 5: 585-603.
[31] Zhang C, Soori M, Miles FL, Sikes RA, Carson DD, Chung LW and Farach-Carson MC. Paracrine factors produced by bone marrow stromal cells induce apoptosis and neuroendocrine differentiation in prostate cancer cells. The Prostate 2011; 71: 157-167.
[32] Miles FL. TGF-BETA SIGNALING INDUCES CYTOSTATIC AND ANTI-METASTATIC RESPONSES IN CASTRATE-RESISTANT PROSTATE CANCER CELLS AND MODULATES PARACRINE CYTOTOXIC EFFECTS OF BONE MARROW STROMAL CELLS. Biological Sciences 2011; Doctor of Philosophy in Biological Sciences:
[33] Kurtoglu S. MODULATION OF PARACRINE INTERACTIONS BETWEEN PROSTATE CANCER CELLS AND BONE MARROW STROMAL CELLS BY TRANSFORMING GROWTH FACTOR-BETA SIGNALING DURING COLONIZATION OF BONE. Biological Sciences 2014; Doctor of Philosophy in Biological Sciences:
[34] Jin JK, Dayyani F and Gallick GE. Steps in prostate cancer progression that lead to bone metastasis. International journal of cancer. Journal international du cancer 2011; 128: 2545-2561.
[35] Gravdal K, Halvorsen OJ, Haukaas SA and Akslen LA. A switch from E-cadherin to N-cadherin expression indicates epithelial to mesenchymal transition and is of strong and independent importance for the progress of prostate cancer. Clinical cancer research : an official journal of the American Association for Cancer Research 2007; 13: 7003-7011.
[36] Umbas R, Schalken JA, Aalders TW, Carter BS, Karthaus HF, Schaafsma HE, Debruyne FM and Isaacs WB. Expression of the cellular adhesion molecule E-cadherin is reduced or absent in high-grade prostate cancer. Cancer research 1992; 52: 5104-5109.
[37] Umbas R, Isaacs WB, Bringuier PP, Schaafsma HE, Karthaus HF, Oosterhof GO, Debruyne FM and Schalken JA. Decreased E-cadherin expression is

associated with poor prognosis in patients with prostate cancer. Cancer research 1994; 54: 3929-3933.
[38] Tran NL, Nagle RB, Cress AE and Heimark RL. N-Cadherin expression in human prostate carcinoma cell lines. An epithelial-mesenchymal transformation mediating adhesion withStromal cells. The American journal of pathology 1999; 155: 787-798.
[39] Jaggi M, Johansson SL, Baker JJ, Smith LM, Galich A and Balaji KC. Aberrant expression of E-cadherin and beta-catenin in human prostate cancer. Urologic oncology 2005; 23: 402-406.
[40] Saha B, Arase A, Imam SS, Tsao-Wei D, Naritoku WY, Groshen S, Jones LW and Imam SA. Overexpression of E-cadherin and beta-catenin proteins in metastatic prostate cancer cells in bone. The Prostate 2008; 68: 78-84.
[41] Schmelz M, Cress AE, Scott KM, Burger F, Cui H, Sallam K, McDaniel KM, Dalkin BL and Nagle RB. Different phenotypes in human prostate cancer: alpha6 or alpha3 integrin in cell-extracellular adhesion sites. Neoplasia 2002; 4: 243-254.
[42] Mol AJ, Geldof AA, Meijer GA, van der Poel HG and van Moorselaar RJ. New experimental markers for early detection of high-risk prostate cancer: role of cell-cell adhesion and cell migration. Journal of cancer research and clinical oncology 2007; 133: 687-695.
[43] Morgia G, Falsaperla M, Malaponte G, Madonia M, Indelicato M, Travali S and Mazzarino MC. Matrix metalloproteinases as diagnostic (MMP-13) and prognostic (MMP-2, MMP-9) markers of prostate cancer. Urological research 2005; 33: 44-50.
[44] Wood M, Fudge K, Mohler JL, Frost AR, Garcia F, Wang M and Stearns ME. In situ hybridization studies of metalloproteinases 2 and 9 and TIMP-1 and TIMP-2 expression in human prostate cancer. Clinical & experimental metastasis 1997; 15: 246-258.
[45] Lichtinghagen R, Musholt PB, Lein M, Romer A, Rudolph B, Kristiansen G, Hauptmann S, Schnorr D, Loening SA and Jung K. Different mRNA and protein expression of matrix metalloproteinases 2 and 9 and tissue inhibitor of metalloproteinases 1 in benign and malignant prostate tissue. European urology 2002; 42: 398-406.
[46] Trudel D, Fradet Y, Meyer F, Harel F and Tetu B. Significance of MMP-2 expression in prostate cancer: an immunohistochemical study. Cancer research 2003; 63: 8511-8515.
[47] Festuccia C, Dolo V, Guerra F, Violini S, Muzi P, Pavan A and Bologna M. Plasminogen activator system modulates invasive capacity and proliferation in prostatic tumor cells. Clinical & experimental metastasis 1998; 16: 513-528.
[48] Kumano M, Miyake H, Muramaki M, Furukawa J, Takenaka A and Fujisawa M. Expression of urokinase-type plasminogen activator system in prostate cancer: correlation with clinicopathological outcomes in patients undergoing radical prostatectomy. Urologic oncology 2009; 27: 180-186.

[49] Koeneman KS, Yeung F and Chung LW. Osteomimetic properties of prostate cancer cells: a hypothesis supporting the predilection of prostate cancer metastasis and growth in the bone environment. The Prostate 1999; 39: 246-261.
[50] Watt KW, Lee PJ, M'Timkulu T, Chan WP and Loor R. Human prostate-specific antigen: structural and functional similarity with serine proteases. Proceedings of the National Academy of Sciences of the United States of America 1986; 83: 3166-3170.
[51] Webber MM, Waghray A and Bello D. Prostate-specific antigen, a serine protease, facilitates human prostate cancer cell invasion. Clinical cancer research : an official journal of the American Association for Cancer Research 1995; 1: 1089-1094.
[52] Cook LM, Shay G, Araujo A and Lynch CC. Integrating new discoveries into the "vicious cycle" paradigm of prostate to bone metastases. Cancer metastasis reviews 2014; 33: 511-525.
[53] Pedersen EA, Shiozawa Y, Pienta KJ and Taichman RS. The prostate cancer bone marrow niche: more than just 'fertile soil'. Asian journal of andrology 2012; 14: 423-427.
[54] Shiozawa Y, Pedersen EA, Havens AM, Jung Y, Mishra A, Joseph J, Kim JK, Patel LR, Ying C, Ziegler AM, Pienta MJ, Song J, Wang J, Loberg RD, Krebsbach PH, Pienta KJ and Taichman RS. Human prostate cancer metastases target the hematopoietic stem cell niche to establish footholds in mouse bone marrow. The Journal of clinical investigation 2011; 121: 1298-1312.
[55] Aiuti A, Tavian M, Cipponi A, Ficara F, Zappone E, Hoxie J, Peault B and Bordignon C. Expression of CXCR4, the receptor for stromal cell-derived factor-1 on fetal and adult human lympho-hematopoietic progenitors. European journal of immunology 1999; 29: 1823-1831.
[56] Nagasawa T, Tachibana K and Kishimoto T. A novel CXC chemokine PBSF/SDF-1 and its receptor CXCR4: their functions in development, hematopoiesis and HIV infection. Seminars in immunology 1998; 10: 179-185.
[57] Ponomaryov T, Peled A, Petit I, Taichman RS, Habler L, Sandbank J, Arenzana-Seisdedos F, Magerus A, Caruz A, Fujii N, Nagler A, Lahav M, Szyper-Kravitz M, Zipori D and Lapidot T. Induction of the chemokine stromal-derived factor-1 following DNA damage improves human stem cell function. The Journal of clinical investigation 2000; 106: 1331-1339.
[58] Wang J, Shiozawa Y, Wang Y, Jung Y, Pienta KJ, Mehra R, Loberg R and Taichman RS. The role of CXCR7/RDC1 as a chemokine receptor for CXCL12/SDF-1 in prostate cancer. The Journal of biological chemistry 2008; 283: 4283-4294.
[59] Sun YX, Fang M, Wang J, Cooper CR, Pienta KJ and Taichman RS. Expression and activation of alpha v beta 3 integrins by SDF-1/CXC12

increases the aggressiveness of prostate cancer cells. The Prostate 2007; 67: 61-73.
[60] Sun YX, Schneider A, Jung Y, Wang J, Dai J, Cook K, Osman NI, Koh-Paige AJ, Shim H, Pienta KJ, Keller ET, McCauley LK and Taichman RS. Skeletal localization and neutralization of the SDF-1(CXCL12)/CXCR4 axis blocks prostate cancer metastasis and growth in osseous sites in vivo. Journal of bone and mineral research : the official journal of the American Society for Bone and Mineral Research 2005; 20: 318-329.
[61] Sun YX, Wang J, Shelburne CE, Lopatin DE, Chinnaiyan AM, Rubin MA, Pienta KJ and Taichman RS. Expression of CXCR4 and CXCL12 (SDF-1) in human prostate cancers (PCa) in vivo. Journal of cellular biochemistry 2003; 89: 462-473.
[62] Lehr JE and Pienta KJ. Preferential adhesion of prostate cancer cells to a human bone marrow endothelial cell line. Journal of the National Cancer Institute 1998; 90: 118-123.
[63] Cooper CR, McLean L, Walsh M, Taylor J, Hayasaka S, Bhatia J and Pienta KJ. Preferential adhesion of prostate cancer cells to bone is mediated by binding to bone marrow endothelial cells as compared to extracellular matrix components in vitro. Clinical cancer research : an official journal of the American Association for Cancer Research 2000; 6: 4839-4847.
[64] Honn KV and Tang DG. Adhesion molecules and tumor cell interaction with endothelium and subendothelial matrix. Cancer metastasis reviews 1992; 11: 353-375.
[65] Cooper CR, Chay CH, Gendernalik JD, Lee HL, Bhatia J, Taichman RS, McCauley LK, Keller ET and Pienta KJ. Stromal factors involved in prostate carcinoma metastasis to bone. Cancer 2003; 97: 739-747.
[66] Scott LJ, Clarke NW, George NJ, Shanks JH, Testa NG and Lang SH. Interactions of human prostatic epithelial cells with bone marrow endothelium: binding and invasion. British journal of cancer 2001; 84: 1417-1423.
[67] Mazo IB and von Andrian UH. Adhesion and homing of blood-borne cells in bone marrow microvessels. Journal of leukocyte biology 1999; 66: 25-32.
[68] Martensson S, Bigler SA, Brown M, Lange PH, Brawer MK and Hakomori S. Sialyl-Lewis(x) and related carbohydrate antigens in the prostate. Human pathology 1995; 26: 735-739.
[69] Romanov VI and Goligorsky MS. RGD-recognizing integrins mediate interactions of human prostate carcinoma cells with endothelial cells in vitro. The Prostate 1999; 39: 108-118.
[70] Grothey A and McCrea PD. Re: Preferential adhesion of prostate cancer cells to a human bone marrow endothelial cell line. Journal of the National Cancer Institute 1998; 90: 547.
[71] Nesbitt S, Nesbit A, Helfrich M and Horton M. Biochemical characterization of human osteoclast integrins. Osteoclasts express alpha v beta 3, alpha 2 beta

1, and alpha v beta 1 integrins. The Journal of biological chemistry 1993; 268: 16737-16745.
[72] Zheng DQ, Woodard AS, Fornaro M, Tallini G and Languino LR. Prostatic carcinoma cell migration via alpha(v)beta3 integrin is modulated by a focal adhesion kinase pathway. Cancer research 1999; 59: 1655-1664.
[73] Cooper CR, Chay CH and Pienta KJ. The role of alpha(v)beta(3) in prostate cancer progression. Neoplasia 2002; 4: 191-194.
[74] Zheng DQ, Woodard AS, Tallini G and Languino LR. Substrate specificity of alpha(v)beta(3) integrin-mediated cell migration and phosphatidylinositol 3-kinase/AKT pathway activation. The Journal of biological chemistry 2000; 275: 24565-24574.
[75] Hall CL, Dubyk CW, Riesenberger TA, Shein D, Keller ET and van Golen KL. Type I collagen receptor (alpha2beta1) signaling promotes prostate cancer invasion through RhoC GTPase. Neoplasia 2008; 10: 797-803.
[76] Rabinovitz I, Nagle RB and Cress AE. Integrin alpha 6 expression in human prostate carcinoma cells is associated with a migratory and invasive phenotype in vitro and in vivo. Clinical & experimental metastasis 1995; 13: 481-491.
[77] Chu K, Cheng CJ, Ye X, Lee YC, Zurita AJ, Chen DT, Yu-Lee LY, Zhang S, Yeh ET, Hu MC, Logothetis CJ and Lin SH. Cadherin-11 promotes the metastasis of prostate cancer cells to bone. Molecular cancer research : MCR 2008; 6: 1259-1267.
[78] Havens AM, Jung Y, Sun YX, Wang J, Shah RB, Buhring HJ, Pienta KJ and Taichman RS. The role of sialomucin CD164 (MGC-24v or endolyn) in prostate cancer metastasis. BMC cancer 2006; 6: 195.
[79] Jung Y, Wang J, Song J, Shiozawa Y, Havens A, Wang Z, Sun YX, Emerson SG, Krebsbach PH and Taichman RS. Annexin II expressed by osteoblasts and endothelial cells regulates stem cell adhesion, homing, and engraftment following transplantation. Blood 2007; 110: 82-90.
[80] Shiozawa Y, Havens AM, Jung Y, Ziegler AM, Pedersen EA, Wang J, Lu G, Roodman GD, Loberg RD, Pienta KJ and Taichman RS. Annexin II/annexin II receptor axis regulates adhesion, migration, homing, and growth of prostate cancer. Journal of cellular biochemistry 2008; 105: 370-380.
[81] Shiozawa Y, Pedersen EA, Patel LR, Ziegler AM, Havens AM, Jung Y, Wang J, Zalucha S, Loberg RD, Pienta KJ and Taichman RS. GAS6/AXL axis regulates prostate cancer invasion, proliferation, and survival in the bone marrow niche. Neoplasia 2010; 12: 116-127.
[82] Ibrahim T, Flamini E, Mercatali L, Sacanna E, Serra P and Amadori D. Pathogenesis of osteoblastic bone metastases from prostate cancer. Cancer 2010; 116: 1406-1418.
[83] Hauschka PV, Mavrakos AE, Iafrati MD, Doleman SE and Klagsbrun M. Growth factors in bone matrix. Isolation of multiple types by affinity chromatography on heparin-Sepharose. The Journal of biological chemistry 1986; 261: 12665-12674.

[84] Boyle WJ, Simonet WS and Lacey DL. Osteoclast differentiation and activation. Nature 2003; 423: 337-342.
[85] Mundy GR. Mechanisms of bone metastasis. Cancer 1997; 80: 1546-1556.
[86] Huang L, Cheng YY, Chow LT, Zheng MH and Kumta SM. Tumour cells produce receptor activator of NF-kappaB ligand (RANKL) in skeletal metastases. Journal of clinical pathology 2002; 55: 877-878.
[87] Zhang J, Dai J, Yao Z, Lu Y, Dougall W and Keller ET. Soluble receptor activator of nuclear factor kappaB Fc diminishes prostate cancer progression in bone. Cancer research 2003; 63: 7883-7890.
[88] Penno H, Nilsson O, Brandstrom H, Winqvist O and Ljunggren O. Expression of RANK-ligand in prostate cancer cell lines. Scandinavian journal of clinical and laboratory investigation 2009; 69: 151-155.
[89] Chu GC and Chung LW. RANK-mediated signaling network and cancer metastasis. Cancer metastasis reviews 2014; 33: 497-509.
[90] Lynch CC, Hikosaka A, Acuff HB, Martin MD, Kawai N, Singh RK, Vargo-Gogola TC, Begtrup JL, Peterson TE, Fingleton B, Shirai T, Matrisian LM and Futakuchi M. MMP-7 promotes prostate cancer-induced osteolysis via the solubilization of RANKL. Cancer cell 2005; 7: 485-496.
[91] Smith MR, Saad F, Coleman R, Shore N, Fizazi K, Tombal B, Miller K, Sieber P, Karsh L, Damiao R, Tammela TL, Egerdie B, Van Poppel H, Chin J, Morote J, Gomez-Veiga F, Borkowski T, Ye Z, Kupic A, Dansey R and Goessl C. Denosumab and bone-metastasis-free survival in men with castration-resistant prostate cancer: results of a phase 3, randomised, placebo-controlled trial. Lancet 2012; 379: 39-46.
[92] Sturge J, Caley MP and Waxman J. Bone metastasis in prostate cancer: emerging therapeutic strategies. Nature reviews. Clinical oncology 2011; 8: 357-368.
[93] Danielpour D. Functions and regulation of transforming growth factor-beta (TGF-beta) in the prostate. European journal of cancer 2005; 41: 846-857.
[94] Bello-DeOcampo D and Tindall DJ. TGF-betal/Smad signaling in prostate cancer. Current drug targets 2003; 4: 197-207.
[95] Dallas SL, Zhao S, Cramer SD, Chen Z, Peehl DM and Bonewald LF. Preferential production of latent transforming growth factor beta-2 by primary prostatic epithelial cells and its activation by prostate-specific antigen. Journal of cellular physiology 2005; 202: 361-370.
[96] Josson S, Matsuoka Y, Chung LW, Zhau HE and Wang R. Tumor-stroma co-evolution in prostate cancer progression and metastasis. Seminars in cell & developmental biology 2010; 21: 26-32.
[97] Buijs JT, Rentsch CA, van der Horst G, van Overveld PG, Wetterwald A, Schwaninger R, Henriquez NV, Ten Dijke P, Borovecki F, Markwalder R, Thalmann GN, Papapoulos SE, Pelger RC, Vukicevic S, Cecchini MG, Lowik CW and van der Pluijm G. BMP7, a putative regulator of epithelial

homeostasis in the human prostate, is a potent inhibitor of prostate cancer bone metastasis in vivo. The American journal of pathology 2007; 171: 1047-1057.
[98] Liao J, Li X, Koh AJ, Berry JE, Thudi N, Rosol TJ, Pienta KJ and McCauley LK. Tumor expressed PTHrP facilitates prostate cancer-induced osteoblastic lesions. International journal of cancer. Journal international du cancer 2008; 123: 2267-2278.
[99] Keller ET, Zhang J, Cooper CR, Smith PC, McCauley LK, Pienta KJ and Taichman RS. Prostate carcinoma skeletal metastases: cross-talk between tumor and bone. Cancer metastasis reviews 2001; 20: 333-349.
[100] Vela I, Gregory L, Gardiner EM, Clements JA and Nicol DL. Bone and prostate cancer cell interactions in metastatic prostate cancer. BJU international 2007; 99: 735-742.
[101] Dougherty KM, Blomme EA, Koh AJ, Henderson JE, Pienta KJ, Rosol TJ and McCauley LK. Parathyroid hormone-related protein as a growth regulator of prostate carcinoma. Cancer research 1999; 59: 6015-6022.
[102] Blomme EA, Dougherty KM, Pienta KJ, Capen CC, Rosol TJ and McCauley LK. Skeletal metastasis of prostate adenocarcinoma in rats: morphometric analysis and role of parathyroid hormone-related protein. The Prostate 1999; 39: 187-197.
[103] Rabbani SA, Gladu J, Harakidas P, Jamison B and Goltzman D. Over-production of parathyroid hormone-related peptide results in increased osteolytic skeletal metastasis by prostate cancer cells in vivo. International journal of cancer. Journal international du cancer 1999; 80: 257-264.
[104] Cramer SD, Chen Z and Peehl DM. Prostate specific antigen cleaves parathyroid hormone-related protein in the PTH-like domain: inactivation of PTHrP-stimulated cAMP accumulation in mouse osteoblasts. The Journal of urology 1996; 156: 526-531.
[105] Iwamura M, Hellman J, Cockett AT, Lilja H and Gershagen S. Alteration of the hormonal bioactivity of parathyroid hormone-related protein (PTHrP) as a result of limited proteolysis by prostate-specific antigen. Urology 1996; 48: 317-325.
[106] Behrens J, von Kries JP, Kuhl M, Bruhn L, Wedlich D, Grosschedl R and Birchmeier W. Functional interaction of beta-catenin with the transcription factor LEF-1. Nature 1996; 382: 638-642.
[107] Hall CL, Kang S, MacDougald OA and Keller ET. Role of Wnts in prostate cancer bone metastases. Journal of cellular biochemistry 2006; 97: 661-672.
[108] Hall CL, Daignault SD, Shah RB, Pienta KJ and Keller ET. Dickkopf-1 expression increases early in prostate cancer development and decreases during progression from primary tumor to metastasis. The Prostate 2008; 68: 1396-1404.
[109] Hall CL, Bafico A, Dai J, Aaronson SA and Keller ET. Prostate cancer cells promote osteoblastic bone metastases through Wnts. Cancer research 2005; 65: 7554-7560.

[110] Chiao JW, Moonga BS, Yang YM, Kancherla R, Mittelman A, Wu-Wong JR and Ahmed T. Endothelin-1 from prostate cancer cells is enhanced by bone contact which blocks osteoclastic bone resorption. British journal of cancer 2000; 83: 360-365.
[111] Clines GA, Mohammad KS, Bao Y, Stephens OW, Suva LJ, Shaughnessy JD, Jr., Fox JW, Chirgwin JM and Guise TA. Dickkopf homolog 1 mediates endothelin-1-stimulated new bone formation. Molecular endocrinology 2007; 21: 486-498.
[112] Nelson JB, Hedican SP, George DJ, Reddi AH, Piantadosi S, Eisenberger MA and Simons JW. Identification of endothelin-1 in the pathophysiology of metastatic adenocarcinoma of the prostate. Nature medicine 1995; 1: 944-949.
[113] Nelson JB. Endothelin inhibition: novel therapy for prostate cancer. The Journal of urology 2003; 170: S65-67; discussion S67-68.
[114] Kopetz ES, Nelson JB and Carducci MA. Endothelin-1 as a target for therapeutic intervention in prostate cancer. Investigational new drugs 2002; 20: 173-182.
[115] Nelson JB, Nguyen SH, Wu-Wong JR, Opgenorth TJ, Dixon DB, Chung LW and Inoue N. New bone formation in an osteoblastic tumor model is increased by endothelin-1 overexpression and decreased by endothelin A receptor blockade. Urology 1999; 53: 1063-1069.
[116] Le Brun G, Aubin P, Soliman H, Ropiquet F, Villette JM, Berthon P, Creminon C, Cussenot O and Fiet J. Upregulation of endothelin 1 and its precursor by IL-1beta, TNF-alpha, and TGF-beta in the PC3 human prostate cancer cell line. Cytokine 1999; 11: 157-162.
[117] Russo A, Bronte G, Rizzo S, Fanale D, Di Gaudio F, Gebbia N and Bazan V. Anti-endothelin drugs in solid tumors. Expert opinion on emerging drugs 2010; 15: 27-40.
[118] Abe E, Yamamoto M, Taguchi Y, Lecka-Czernik B, O'Brien CA, Economides AN, Stahl N, Jilka RL and Manolagas SC. Essential requirement of BMPs-2/4 for both osteoblast and osteoclast formation in murine bone marrow cultures from adult mice: antagonism by noggin. Journal of bone and mineral research : the official journal of the American Society for Bone and Mineral Research 2000; 15: 663-673.
[119] Gori F, Thomas T, Hicok KC, Spelsberg TC and Riggs BL. Differentiation of human marrow stromal precursor cells: bone morphogenetic protein-2 increases OSF2/CBFA1, enhances osteoblast commitment, and inhibits late adipocyte maturation. Journal of bone and mineral research : the official journal of the American Society for Bone and Mineral Research 1999; 14: 1522-1535.
[120] Lai TH, Fong YC, Fu WM, Yang RS and Tang CH. Osteoblasts-derived BMP-2 enhances the motility of prostate cancer cells via activation of integrins. The Prostate 2008; 68: 1341-1353.

[121] Masuda H, Fukabori Y, Nakano K, Takezawa Y, T CS and Yamanaka H. Increased expression of bone morphogenetic protein-7 in bone metastatic prostate cancer. The Prostate 2003; 54: 268-274.
[122] Thomas R, Anderson WA, Raman V and Reddi AH. Androgen-dependent gene expression of bone morphogenetic protein 7 in mouse prostate. The Prostate 1998; 37: 236-245.
[123] Autzen P, Robson CN, Bjartell A, Malcolm AJ, Johnson MI, Neal DE and Hamdy FC. Bone morphogenetic protein 6 in skeletal metastases from prostate cancer and other common human malignancies. British journal of cancer 1998; 78: 1219-1223.
[124] Thomas BG and Hamdy FC. Bone morphogenetic protein-6: potential mediator of osteoblastic metastases in prostate cancer. Prostate cancer and prostatic diseases 2000; 3: 283-285.
[125] Dai J, Keller J, Zhang J, Lu Y, Yao Z and Keller ET. Bone morphogenetic protein-6 promotes osteoblastic prostate cancer bone metastases through a dual mechanism. Cancer research 2005; 65: 8274-8285.
[126] Feeley BT, Gamradt SC, Hsu WK, Liu N, Krenek L, Robbins P, Huard J and Lieberman JR. Influence of BMPs on the formation of osteoblastic lesions in metastatic prostate cancer. Journal of bone and mineral research : the official journal of the American Society for Bone and Mineral Research 2005; 20: 2189-2199.
[127] Koch H, Jadlowiec JA and Campbell PG. Insulin-like growth factor-I induces early osteoblast gene expression in human mesenchymal stem cells. Stem cells and development 2005; 14: 621-631.
[128] Rubin J, Chung LW, Fan X, Zhu L, Murphy TC, Nanes MS and Rosen CJ. Prostate carcinoma cells that have resided in bone have an upregulated IGF-I axis. The Prostate 2004; 58: 41-49.
[129] Ritchie CK, Andrews LR, Thomas KG, Tindall DJ and Fitzpatrick LA. The effects of growth factors associated with osteoblasts on prostate carcinoma proliferation and chemotaxis: implications for the development of metastatic disease. Endocrinology 1997; 138: 1145-1150.
[130] Ryan CJ, Haqq CM, Simko J, Nonaka DF, Chan JM, Weinberg V, Small EJ and Goldfine ID. Expression of insulin-like growth factor-1 receptor in local and metastatic prostate cancer. Urologic oncology 2007; 25: 134-140.
[131] Gleave ME and Miyake H. Castration-induced upregulation of insulin-like growth factor binding protein-5 potentiates IGF-1 and accelerates androgen-independent progression in prostate cancer. Prostate cancer and prostatic diseases 2000; 3: S16.
[132] Cohen P, Peehl DM and Rosenfeld RG. The IGF axis in the prostate. Hormone and metabolic research = Hormon- und Stoffwechselforschung = Hormones et metabolisme 1994; 26: 81-84.
[133] Harman SM, Metter EJ, Blackman MR, Landis PK and Carter HB. Serum levels of insulin-like growth factor I (IGF-I), IGF-II, IGF-binding protein-3,

and prostate-specific antigen as predictors of clinical prostate cancer. The Journal of clinical endocrinology and metabolism 2000; 85: 4258-4265.
[134] Rubin J, Fan X, Rahnert J, Sen B, Hsieh CL, Murphy TC, Nanes MS, Horton LG, Beamer WG and Rosen CJ. IGF-I secretion by prostate carcinoma cells does not alter tumor-bone cell interactions in vitro or in vivo. The Prostate 2006; 66: 789-800.
[135] Ueha S, Shand FH and Matsushima K. Myeloid cell population dynamics in healthy and tumor-bearing mice. International immunopharmacology 2011; 11: 783-788.
[136] Lechner MG, Liebertz DJ and Epstein AL. Characterization of cytokine-induced myeloid-derived suppressor cells from normal human peripheral blood mononuclear cells. Journal of immunology 2010; 185: 2273-2284.
[137] Yang L, Edwards CM and Mundy GR. Gr-1+CD11b+ myeloid-derived suppressor cells: formidable partners in tumor metastasis. Journal of bone and mineral research : the official journal of the American Society for Bone and Mineral Research 2010; 25: 1701-1706.
[138] Yang L, DeBusk LM, Fukuda K, Fingleton B, Green-Jarvis B, Shyr Y, Matrisian LM, Carbone DP and Lin PC. Expansion of myeloid immune suppressor Gr+CD11b+ cells in tumor-bearing host directly promotes tumor angiogenesis. Cancer cell 2004; 6: 409-421.
[139] Sawant A, Deshane J, Jules J, Lee CM, Harris BA, Feng X and Ponnazhagan S. Myeloid-derived suppressor cells function as novel osteoclast progenitors enhancing bone loss in breast cancer. Cancer research 2013; 73: 672-682.
[140] Danilin S, Merkel AR, Johnson JR, Johnson RW, Edwards JR and Sterling JA. Myeloid-derived suppressor cells expand during breast cancer progression and promote tumor-induced bone destruction. Oncoimmunology 2012; 1: 1484-1494.
[141] Pang Y, Gara SK, Achyut BR, Li Z, Yan HH, Day CP, Weiss JM, Trinchieri G, Morris JC and Yang L. TGF-beta signaling in myeloid cells is required for tumor metastasis. Cancer discovery 2013; 3: 936-951.
[142] Joyce JA and Pollard JW. Microenvironmental regulation of metastasis. Nature reviews. Cancer 2009; 9: 239-252.
[143] Glofcheskie BD and Surgeoner GA. Muscovy ducks as an adjunct for the control of the house fly (Diptera: Muscidae). Journal of economic entomology 1990; 83: 788-791.
[144] Dirkx AE, Oude Egbrink MG, Wagstaff J and Griffioen AW. Monocyte/macrophage infiltration in tumors: modulators of angiogenesis. Journal of leukocyte biology 2006; 80: 1183-1196.
[145] Mizutani K, Sud S, McGregor NA, Martinovski G, Rice BT, Craig MJ, Varsos ZS, Roca H and Pienta KJ. The chemokine CCL2 increases prostate tumor growth and bone metastasis through macrophage and osteoclast recruitment. Neoplasia 2009; 11: 1235-1242.

[146] Herroon MK, Rajagurubandara E, Rudy DL, Chalasani A, Hardaway AL and Podgorski I. Macrophage cathepsin K promotes prostate tumor progression in bone. Oncogene 2013; 32: 1580-1593.
[147] Di Lorenzo G, Buonerba C and Kantoff PW. Immunotherapy for the treatment of prostate cancer. Nature reviews. Clinical oncology 2011; 8: 551-561.
[148] Djaafar S, Pierroz DD, Chicheportiche R, Zheng XX, Ferrari SL and Ferrari-Lacraz S. Inhibition of T cell-dependent and RANKL-dependent osteoclastogenic processes associated with high levels of bone mass in interleukin-15 receptor-deficient mice. Arthritis and rheumatism 2010; 62: 3300-3310.
[149] Sawant A, Hensel JA, Chanda D, Harris BA, Siegal GP, Maheshwari A and Ponnazhagan S. Depletion of plasmacytoid dendritic cells inhibits tumor growth and prevents bone metastasis of breast cancer cells. Journal of immunology 2012; 189: 4258-4265.
[150] Nakashima T and Takayanagi H. Osteoimmunology: crosstalk between the immune and bone systems. Journal of clinical immunology 2009; 29: 555-567.
[151] Kiesel JR, Buchwald ZS and Aurora R. Cross-presentation by osteoclasts induces FoxP3 in CD8+ T cells. Journal of immunology 2009; 182: 5477-5487.
[152] Zhao E, Wang L, Dai J, Kryczek I, Wei S, Vatan L, Altuwaijri S, Sparwasser T, Wang G, Keller ET and Zou W. Regulatory T cells in the bone marrow microenvironment in patients with prostate cancer. Oncoimmunology 2012; 1: 152-161.
[153] Li X, Koh AJ, Wang Z, Soki FN, Park SI, Pienta KJ and McCauley LK. Inhibitory effects of megakaryocytic cells in prostate cancer skeletal metastasis. Journal of bone and mineral research : the official journal of the American Society for Bone and Mineral Research 2011; 26: 125-134.
[154] Deutsch VR and Tomer A. Advances in megakaryocytopoiesis and thrombopoiesis: from bench to bedside. British journal of haematology 2013; 161: 778-793.
[155] Morse MA and Lyerly HK. Clinical applications of dendritic cell vaccines. Current opinion in molecular therapeutics 2000; 2: 20-28.
[156] Small EJ, Fratesi P, Reese DM, Strang G, Laus R, Peshwa MV and Valone FH. Immunotherapy of hormone-refractory prostate cancer with antigen-loaded dendritic cells. Journal of clinical oncology : official journal of the American Society of Clinical Oncology 2000; 18: 3894-3903.
[157] Baxevanis CN, Papamichail M and Perez SA. Prostate cancer vaccines: the long road to clinical application. Cancer immunology, immunotherapy : CII 2015; 64: 401-408.
[158] Roecklein BA and Torok-Storb B. Functionally distinct human marrow stromal cell lines immortalized by transduction with the human papilloma virus E6/E7 genes. Blood 1995; 85: 997-1005.

[159] Graf L, Iwata M and Torok-Storb B. Gene expression profiling of the functionally distinct human bone marrow stromal cell lines HS-5 and HS-27a. Blood 2002; 100: 1509-1511.
[160] Torok-Storb B, Iwata M, Graf L, Gianotti J, Horton H and Byrne MC. Dissecting the marrow microenvironment. Annals of the New York Academy of Sciences 1999; 872: 164-170.
[161] Sung SY, Hsieh CL, Law A, Zhau HE, Pathak S, Multani AS, Lim S, Coleman IM, Wu LC, Figg WD, Dahut WL, Nelson P, Lee JK, Amin MB, Lyles R, Johnstone PA, Marshall FF and Chung LW. Coevolution of prostate cancer and bone stroma in three-dimensional coculture: implications for cancer growth and metastasis. Cancer research 2008; 68: 9996-10003.
[162] Windus LC, Glover TT and Avery VM. Bone-stromal cells up-regulate tumourigenic markers in a tumour-stromal 3D model of prostate cancer. Molecular cancer 2013; 12: 112.
[163] Rhee HW, Zhau HE, Pathak S, Multani AS, Pennanen S, Visakorpi T and Chung LW. Permanent phenotypic and genotypic changes of prostate cancer cells cultured in a three-dimensional rotating-wall vessel. In vitro cellular & developmental biology. Animal 2001; 37: 127-140.
[164] Klein CA, Blankenstein TJ, Schmidt-Kittler O, Petronio M, Polzer B, Stoecklein NH and Riethmuller G. Genetic heterogeneity of single disseminated tumour cells in minimal residual cancer. Lancet 2002; 360: 683-689.
[165] Arya M, Bott SR, Shergill IS, Ahmed HU, Williamson M and Patel HR. The metastatic cascade in prostate cancer. Surgical oncology 2006; 15: 117-128.
[166] Pienta KJ, McGregor N, Axelrod R and Axelrod DE. Ecological therapy for cancer: defining tumors using an ecosystem paradigm suggests new opportunities for novel cancer treatments. Translational oncology 2008; 1: 158-164.
[167] Kobayashi A, Okuda H, Xing F, Pandey PR, Watabe M, Hirota S, Pai SK, Liu W, Fukuda K, Chambers C, Wilber A and Watabe K. Bone morphogenetic protein 7 in dormancy and metastasis of prostate cancer stem-like cells in bone. The Journal of experimental medicine 2011; 208: 2641-2655.
[168] Gallagher WM, Currid CA and Whelan LC. Fibulins and cancer: friend or foe? Trends in molecular medicine 2005; 11: 336-340.
[169] Obaya AJ, Rua S, Moncada-Pazos A and Cal S. The dual role of fibulins in tumorigenesis. Cancer letters 2012; 325: 132-138.
[170] Argraves WS, Greene LM, Cooley MA and Gallagher WM. Fibulins: physiological and disease perspectives. EMBO reports 2003; 4: 1127-1131.
[171] de Vega S, Iwamoto T and Yamada Y. Fibulins: multiple roles in matrix structures and tissue functions. Cellular and molecular life sciences : CMLS 2009; 66: 1890-1902.

[172] Timpl R, Sasaki T, Kostka G and Chu ML. Fibulins: a versatile family of extracellular matrix proteins. Nature reviews. Molecular cell biology 2003; 4: 479-489.
[173] Argraves WS, Dickerson K, Burgess WH and Ruoslahti E. Fibulin, a novel protein that interacts with the fibronectin receptor beta subunit cytoplasmic domain. Cell 1989; 58: 623-629.
[174] Pan TC, Kluge M, Zhang RZ, Mayer U, Timpl R and Chu ML. Sequence of extracellular mouse protein BM-90/fibulin and its calcium-dependent binding to other basement-membrane ligands. European journal of biochemistry / FEBS 1993; 215: 733-740.
[175] Lecka-Czernik B, Lumpkin CK, Jr. and Goldstein S. An overexpressed gene transcript in senescent and quiescent human fibroblasts encoding a novel protein in the epidermal growth factor-like repeat family stimulates DNA synthesis. Molecular and cellular biology 1995; 15: 120-128.
[176] Giltay R, Timpl R and Kostka G. Sequence, recombinant expression and tissue localization of two novel extracellular matrix proteins, fibulin-3 and fibulin-4. Matrix biology : journal of the International Society for Matrix Biology 1999; 18: 469-480.
[177] Kowal RC, Richardson JA, Miano JM and Olson EN. EVEC, a novel epidermal growth factor-like repeat-containing protein upregulated in embryonic and diseased adult vasculature. Circulation research 1999; 84: 1166-1176.
[178] Nakamura T, Ruiz-Lozano P, Lindner V, Yabe D, Taniwaki M, Furukawa Y, Kobuke K, Tashiro K, Lu Z, Andon NL, Schaub R, Matsumori A, Sasayama S, Chien KR and Honjo T. DANCE, a novel secreted RGD protein expressed in developing, atherosclerotic, and balloon-injured arteries. The Journal of biological chemistry 1999; 274: 22476-22483.
[179] Vogel BE and Hedgecock EM. Hemicentin, a conserved extracellular member of the immunoglobulin superfamily, organizes epithelial and other cell attachments into oriented line-shaped junctions. Development 2001; 128: 883-894.
[180] de Vega S, Iwamoto T, Nakamura T, Hozumi K, McKnight DA, Fisher LW, Fukumoto S and Yamada Y. TM14 is a new member of the fibulin family (fibulin-7) that interacts with extracellular matrix molecules and is active for cell binding. The Journal of biological chemistry 2007; 282: 30878-30888.
[181] Gu YC, Nilsson K, Eng H and Ekblom M. Association of extracellular matrix proteins fibulin-1 and fibulin-2 with fibronectin in bone marrow stroma. British journal of haematology 2000; 109: 305-313.
[182] Sasaki T, Wiedemann H, Matzner M, Chu ML and Timpl R. Expression of fibulin-2 by fibroblasts and deposition with fibronectin into a fibrillar matrix. Journal of cell science 1996; 109 (Pt 12): 2895-2904.
[183] Miosge N, Sasaki T, Chu ML, Herken R and Timpl R. Ultrastructural localization of microfibrillar fibulin-1 and fibulin-2 during heart development

indicates a switch in molecular associations. Cellular and molecular life sciences : CMLS 1998; 54: 606-613.
[184] Zhang HY, Timpl R, Sasaki T, Chu ML and Ekblom P. Fibulin-1 and fibulin-2 expression during organogenesis in the developing mouse embryo. Developmental dynamics : an official publication of the American Association of Anatomists 1996; 205: 348-364.
[185] Zhang HY, Chu ML, Pan TC, Sasaki T, Timpl R and Ekblom P. Extracellular matrix protein fibulin-2 is expressed in the embryonic endocardial cushion tissue and is a prominent component of valves in adult heart. Developmental biology 1995; 167: 18-26.
[186] Miosge N, Gotz W, Sasaki T, Chu ML, Timpl R and Herken R. The extracellular matrix proteins fibulin-1 and fibulin-2 in the early human embryo. The Histochemical journal 1996; 28: 109-116.
[187] Ehlermann J, Weber S, Pfisterer P and Schorle H. Cloning, expression and characterization of the murine Efemp1, a gene mutated in Doyne-Honeycomb retinal dystrophy. Gene expression patterns : GEP 2003; 3: 441-447.
[188] McLaughlin PJ, Bakall B, Choi J, Liu Z, Sasaki T, Davis EC, Marmorstein AD and Marmorstein LY. Lack of fibulin-3 causes early aging and herniation, but not macular degeneration in mice. Human molecular genetics 2007; 16: 3059-3070.
[189] Xiang Y, Sekine T, Nakamura H, Imajoh-Ohmi S, Fukuda H, Yudoh K, Masuko-Hongo K, Nishioka K and Kato T. Fibulin-4 is a target of autoimmunity predominantly in patients with osteoarthritis. Journal of immunology 2006; 176: 3196-3204.
[190] Nakamura T, Lozano PR, Ikeda Y, Iwanaga Y, Hinek A, Minamisawa S, Cheng CF, Kobuke K, Dalton N, Takada Y, Tashiro K, Ross Jr J, Honjo T and Chien KR. Fibulin-5/DANCE is essential for elastogenesis in vivo. Nature 2002; 415: 171-175.
[191] Hirai M, Ohbayashi T, Horiguchi M, Okawa K, Hagiwara A, Chien KR, Kita T and Nakamura T. Fibulin-5/DANCE has an elastogenic organizer activity that is abrogated by proteolytic cleavage in vivo. The Journal of cell biology 2007; 176: 1061-1071.
[192] Schultz DW, Klein ML, Humpert AJ, Luzier CW, Persun V, Schain M, Mahan A, Runckel C, Cassera M, Vittal V, Doyle TM, Martin TM, Weleber RG, Francis PJ and Acott TS. Analysis of the ARMD1 locus: evidence that a mutation in HEMICENTIN-1 is associated with age-related macular degeneration in a large family. Human molecular genetics 2003; 12: 3315-3323.
[193] Schultz DW, Weleber RG, Lawrence G, Barral S, Majewski J, Acott TS and Klein ML. HEMICENTIN-1 (FIBULIN-6) and the 1q31 AMD locus in the context of complex disease: review and perspective. Ophthalmic genetics 2005; 26: 101-105.

[194] Chowdhury A, Herzog C, Hasselbach L, Khouzani HL, Zhang J, Hammerschmidt M, Rudat C, Kispert A, Gaestel M, Menon MB, Tudorache I, Hilfiker-Kleiner D, Muhlfeld C, Schmitto JD, Muller M and Theilmeier G. Expression of fibulin-6 in failing hearts and its role for cardiac fibroblast migration. Cardiovascular research 2014; 103: 509-520.
[195] Argraves WS, Tran H, Burgess WH and Dickerson K. Fibulin is an extracellular matrix and plasma glycoprotein with repeated domain structure. The Journal of cell biology 1990; 111: 3155-3164.
[196] Roark EF, Keene DR, Haudenschild CC, Godyna S, Little CD and Argraves WS. The association of human fibulin-1 with elastic fibers: an immunohistological, ultrastructural, and RNA study. The journal of histochemistry and cytochemistry : official journal of the Histochemistry Society 1995; 43: 401-411.
[197] Godyna S, Mann DM and Argraves WS. A quantitative analysis of the incorporation of fibulin-1 into extracellular matrix indicates that fibronectin assembly is required. Matrix biology : journal of the International Society for Matrix Biology 1995; 14: 467-477.
[198] Pan TC, Kostka G, Zhang RZ, Timpl R and Chu ML. Complete exon-intron organization of the mouse fibulin-1 gene and its comparison with the human fibulin-1 gene. FEBS letters 1999; 444: 38-42.
[199] Balbona K, Tran H, Godyna S, Ingham KC, Strickland DK and Argraves WS. Fibulin binds to itself and to the carboxyl-terminal heparin-binding region of fibronectin. The Journal of biological chemistry 1992; 267: 20120-20125.
[200] Miner JH and Yurchenco PD. Laminin functions in tissue morphogenesis. Annual review of cell and developmental biology 2004; 20: 255-284.
[201] Aspberg A, Adam S, Kostka G, Timpl R and Heinegard D. Fibulin-1 is a ligand for the C-type lectin domains of aggrecan and versican. The Journal of biological chemistry 1999; 274: 20444-20449.
[202] Lee NV, Rodriguez-Manzaneque JC, Thai SN, Twal WO, Luque A, Lyons KM, Argraves WS and Iruela-Arispe ML. Fibulin-1 acts as a cofactor for the matrix metalloprotease ADAMTS-1. The Journal of biological chemistry 2005; 280: 34796-34804.
[203] Ng KM, Catalano MG, Pinos T, Selva DM, Avvakumov GV, Munell F and Hammond GL. Evidence that fibulin family members contribute to the steroid-dependent extravascular sequestration of sex hormone-binding globulin. The Journal of biological chemistry 2006; 281: 15853-15861.
[204] Kluge M, Mann K, Dziadek M and Timpl R. Characterization of a novel calcium-binding 90-kDa glycoprotein (BM-90) shared by basement membranes and serum. European journal of biochemistry / FEBS 1990; 193: 651-659.
[205] Pan TC, Sasaki T, Zhang RZ, Fassler R, Timpl R and Chu ML. Structure and expression of fibulin-2, a novel extracellular matrix protein with multiple EGF-

like repeats and consensus motifs for calcium binding. The Journal of cell biology 1993; 123: 1269-1277.
[206] Godyna S, Diaz-Ricart M and Argraves WS. Fibulin-1 mediates platelet adhesion via a bridge of fibrinogen. Blood 1996; 88: 2569-2577.
[207] Tran H, Tanaka A, Litvinovich SV, Medved LV, Haudenschild CC and Argraves WS. The interaction of fibulin-1 with fibrinogen. A potential role in hemostasis and thrombosis. The Journal of biological chemistry 1995; 270: 19458-19464.
[208] Kostka G, Giltay R, Bloch W, Addicks K, Timpl R, Fassler R and Chu ML. Perinatal lethality and endothelial cell abnormalities in several vessel compartments of fibulin-1-deficient mice. Molecular and cellular biology 2001; 21: 7025-7034.
[209] Cooley MA, Kern CB, Fresco VM, Wessels A, Thompson RP, McQuinn TC, Twal WO, Mjaatvedt CH, Drake CJ and Argraves WS. Fibulin-1 is required for morphogenesis of neural crest-derived structures. Developmental biology 2008; 319: 336-345.
[210] Muriel JM, Dong C, Hutter H and Vogel BE. Fibulin-1C and Fibulin-1D splice variants have distinct functions and assemble in a hemicentin-dependent manner. Development 2005; 132: 4223-4234.
[211] Weigell-Weber M, Sarra GM, Kotzot D, Sandkuijl L, Messmer E and Hergersberg M. Genomewide homozygosity mapping and molecular analysis of a candidate gene located on 22q13 (fibulin-1) in a previously undescribed vitreoretinal dystrophy. Archives of ophthalmology 2003; 121: 1184-1188.
[212] Kennan A, Aherne A, Palfi A, Humphries M, McKee A, Stitt A, Simpson DA, Demtroder K, Orntoft T, Ayuso C, Kenna PF, Farrar GJ and Humphries P. Identification of an IMPDH1 mutation in autosomal dominant retinitis pigmentosa (RP10) revealed following comparative microarray analysis of transcripts derived from retinas of wild-type and Rho(-/-) mice. Human molecular genetics 2002; 11: 547-557.
[213] Debeer P, Schoenmakers EF, Twal WO, Argraves WS, De Smet L, Fryns JP and Van De Ven WJ. The fibulin-1 gene (FBLN1) is disrupted in a t(12;22) associated with a complex type of synpolydactyly. Journal of medical genetics 2002; 39: 98-104.
[214] Michaelides M, Jenkins SA, Brantley MA, Jr., Andrews RM, Waseem N, Luong V, Gregory-Evans K, Bhattacharya SS, Fitzke FW and Webster AR. Maculopathy due to the R345W substitution in fibulin-3: distinct clinical features, disease variability, and extent of retinal dysfunction. Investigative ophthalmology & visual science 2006; 47: 3085-3097.
[215] Twal WO, Czirok A, Hegedus B, Knaak C, Chintalapudi MR, Okagawa H, Sugi Y and Argraves WS. Fibulin-1 suppression of fibronectin-regulated cell adhesion and motility. Journal of cell science 2001; 114: 4587-4598.
[216] Qing J, Maher VM, Tran H, Argraves WS, Dunstan RW and McCormick JJ. Suppression of anchorage-independent growth and matrigel invasion and

delayed tumor formation by elevated expression of fibulin-1D in human fibrosarcoma-derived cell lines. Oncogene 1997; 15: 2159-2168.
[217] Hayashido Y, Lucas A, Rougeot C, Godyna S, Argraves WS and Rochefort H. Estradiol and fibulin-1 inhibit motility of human ovarian- and breast-cancer cells induced by fibronectin. International journal of cancer. Journal international du cancer 1998; 75: 654-658.
[218] Xiao W, Wang J, Li H, Guan W, Xia D, Yu G, Xiao H, Lang B, Ma X, Liu J, Zhang X, Ye Z and Xu H. Fibulin-1 is down-regulated through promoter hypermethylation and suppresses renal cell carcinoma progression. The Journal of urology 2013; 190: 291-301.
[219] Xie L, Palmsten K, MacDonald B, Kieran MW, Potenta S, Vong S and Kalluri R. Basement membrane derived fibulin-1 and fibulin-5 function as angiogenesis inhibitors and suppress tumor growth. Experimental biology and medicine 2008; 233: 155-162.
[220] Du M, Fan X, Hong E and Chen JJ. Interaction of oncogenic papillomavirus E6 proteins with fibulin-1. Biochemical and biophysical research communications 2002; 296: 962-969.
[221] Cheng YY, Jin H, Liu X, Siu JM, Wong YP, Ng EK, Yu J, Leung WK, Sung JJ and Chan FK. Fibulin 1 is downregulated through promoter hypermethylation in gastric cancer. British journal of cancer 2008; 99: 2083-2087.
[222] Kanda M, Nomoto S, Okamura Y, Hayashi M, Hishida M, Fujii T, Nishikawa Y, Sugimoto H, Takeda S and Nakao A. Promoter hypermethylation of fibulin 1 gene is associated with tumor progression in hepatocellular carcinoma. Molecular carcinogenesis 2011; 50: 571-579.
[223] Wlazlinski A, Engers R, Hoffmann MJ, Hader C, Jung V, Muller M and Schulz WA. Downregulation of several fibulin genes in prostate cancer. The Prostate 2007; 67: 1770-1780.
[224] Moll F, Katsaros D, Lazennec G, Hellio N, Roger P, Giacalone PL, Chalbos D, Maudelonde T, Rochefort H and Pujol P. Estrogen induction and overexpression of fibulin-1C mRNA in ovarian cancer cells. Oncogene 2002; 21: 1097-1107.
[225] Greene LM, Twal WO, Duffy MJ, McDermott EW, Hill AD, O'Higgins NJ, McCann AH, Dervan PA, Argraves WS and Gallagher WM. Elevated expression and altered processing of fibulin-1 protein in human breast cancer. British journal of cancer 2003; 88: 871-878.
[226] Forti S, Scanlan MJ, Invernizzi A, Castiglioni F, Pupa S, Agresti R, Fontanelli R, Morelli D, Old LJ, Pupa SM and Menard S. Identification of breast cancer-restricted antigens by antibody screening of SKBR3 cDNA library using a preselected patient's serum. Breast cancer research and treatment 2002; 73: 245-256.
[227] Roger P, Pujol P, Lucas A, Baldet P and Rochefort H. Increased immunostaining of fibulin-1, an estrogen-regulated protein in the stroma of

human ovarian epithelial tumors. The American journal of pathology 1998; 153: 1579-1588.
[228] Bardin A, Moll F, Margueron R, Delfour C, Chu ML, Maudelonde T, Cavailles V and Pujol P. Transcriptional and posttranscriptional regulation of fibulin-1 by estrogens leads to differential induction of messenger ribonucleic acid variants in ovarian and breast cancer cells. Endocrinology 2005; 146: 760-768.
[229] Finehout EJ and Lee KH. Comparison of automated in-gel digest methods for femtomole level samples. Electrophoresis 2003; 24: 3508-3516.
[230] Ran FA, Hsu PD, Wright J, Agarwala V, Scott DA and Zhang F. Genome engineering using the CRISPR-Cas9 system. Nature protocols 2013; 8: 2281-2308.
[231] Horoszewicz JS, Leong SS, Chu TM, Wajsman ZL, Friedman M, Papsidero L, Kim U, Chai LS, Kakati S, Arya SK and Sandberg AA. The LNCaP cell line--a new model for studies on human prostatic carcinoma. Progress in clinical and biological research 1980; 37: 115-132.
[232] Horoszewicz JS, Leong SS, Kawinski E, Karr JP, Rosenthal H, Chu TM, Mirand EA and Murphy GP. LNCaP model of human prostatic carcinoma. Cancer research 1983; 43: 1809-1818.
[233] Thalmann GN, Anezinis PE, Chang SM, Zhau HE, Kim EE, Hopwood VL, Pathak S, von Eschenbach AC and Chung LW. Androgen-independent cancer progression and bone metastasis in the LNCaP model of human prostate cancer. Cancer research 1994; 54: 2577-2581.
[234] Thalmann GN, Sikes RA, Wu TT, Degeorges A, Chang SM, Ozen M, Pathak S and Chung LW. LNCaP progression model of human prostate cancer: androgen-independence and osseous metastasis. The Prostate 2000; 44: 91-103 Jul 101;144(102).
[235] Kakehi Y, Oka H, Mitsumori K, Itoh N, Ogawa O and Yoshida O. Elevation of serum transforming growth factor-beta1 Level in patients with metastatic prostate cancer. Urologic oncology 1996; 2: 131-135.
[236] Adler HL, McCurdy MA, Kattan MW, Timme TL, Scardino PT and Thompson TC. Elevated levels of circulating interleukin-6 and transforming growth factor-beta1 in patients with metastatic prostatic carcinoma. The Journal of urology 1999; 161: 182-187.
[237] Chen L, Ge Q, Black JL, Deng L, Burgess JK and Oliver BG. Differential regulation of extracellular matrix and soluble fibulin-1 levels by TGF-beta(1) in airway smooth muscle cells. PloS one 2013; 8: e65544.
[238] Grigore AD, Ben-Jacob E and Farach-Carson MC. Prostate cancer and neuroendocrine differentiation: more neuronal, less endocrine? Frontiers in oncology 2015; 5: 37.
[239] Parimi V, Goyal R, Poropatich K and Yang XJ. Neuroendocrine differentiation of prostate cancer: a review. American journal of clinical and experimental urology 2014; 2: 273-285.

[240] Alshalalfa M, Crisan A, Vergara IA, Ghadessi M, Buerki C, Erho N, Yousefi K, Sierocinski T, Haddad Z, Black PC, Karnes RJ, Jenkins RB and Davicioni E. Clinical and genomic analysis of metastatic prostate cancer progression with a background of postoperative biochemical recurrence. BJU international 2014;
[241] Food and Agriculture Organization of the United Nations. Effects of Food Processing on Dietary Carbohydrates. 2015;
[242] Pekka Lehtinen KK, Ilkka LehtomaÈki, Simo Laakso. Effect of Heat Treatment on Lipid Stability in Processed Oats. Journal of Careal Science 2003; 37: 215-221.
[243] Zdzisław Domiszewski GB, Dominika Plust. EFFECTS OF DIFFERENT HEAT TREATMENTS ON LIPID QUALITY OF STRIPED CATFISH(PANGASIUS HYPOPHTHALMUS). Acta Scientiarum Polonorum 2011; 10: 359-373.
[244] Ouyang X, DeWeese TL, Nelson WG and Abate-Shen C. Loss-of-function of Nkx3.1 promotes increased oxidative damage in prostate carcinogenesis. Cancer research 2005; 65: 6773-6779.
[245] Fic E, Kedracka-Krok S, Jankowska U, Pirog A and Dziedzicka-Wasylewska M. Comparison of protein precipitation methods for various rat brain structures prior to proteomic analysis. Electrophoresis 2010; 31: 3573-3579.
[246] Miles FL. TGF-BETA SIGNALING INDUCES CYTOSTATIC AND ANTI-METASTATIC RESPONSES IN CASTRATE-RESISTANT PROSTATE CANCER CELLS AND MODULATES PARACRINE CYTOTOXIC EFFECTS OF BONE MARROW STROMAL CELLS. Biological Sciences 2011; Doctor of Philosophy in Biological Sciences
[247] Wikstrom P, Bergh A and Damber JE. Transforming growth factor-beta1 and prostate cancer. Scandinavian journal of urology and nephrology 2000; 34: 85-94.

Appendix A

SDS-PAGE GEL FOR MS/MS ANALYSIS

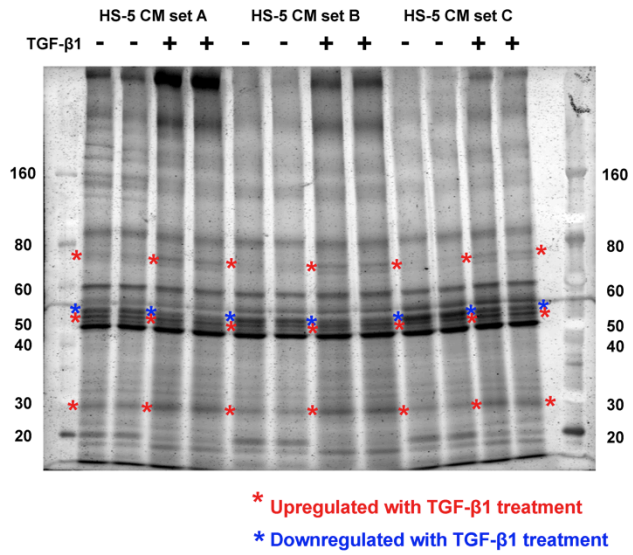

Figure 24: HS-5 CM and HS-5/TGF-β1 CM samples from Figure 16 were used for SDS-PAGE. 5%-11% gradient gel was used followed by Sypro Ruby staining. The gel was prepared and run using the same conditions as for Figure 17. The bands labeled in red and blue showed proteins, which were upregulated and downregulated with TGF-β1 treatment respectively. These indicated bands were used as samples for MS/MS analysis to identify possible HS-5 DF candidates.

Appendix B

GEL ELECTROPHORESIS FOR RNA QUALITY CHECK PRIOR TO qRT_PCR

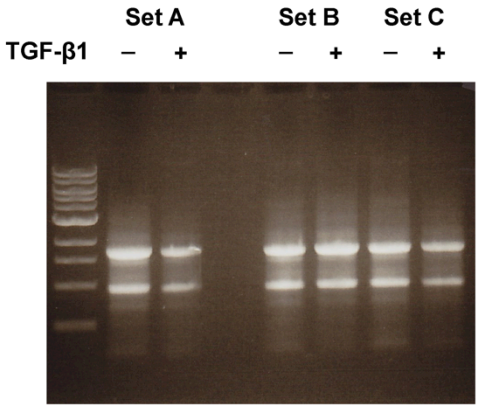

Figure 25: Five µg of RNA from HS-5 cells, with and without TGF-β1 treatment were separated in 0.8% w/v agarose in 0.5X Tris-acetate (TAE) buffer with 0.5 µg/mL ethidium bromide. The results showed intact 28S (top bands) and 18S (bottom bands) rRNA. According to these results, all RNA samples were intact and qualified for qRT-PCR for all 3 biological replicates.

Appendix C

CLONAL SCREENING FOR HS-5^{CRISPR_fib1}

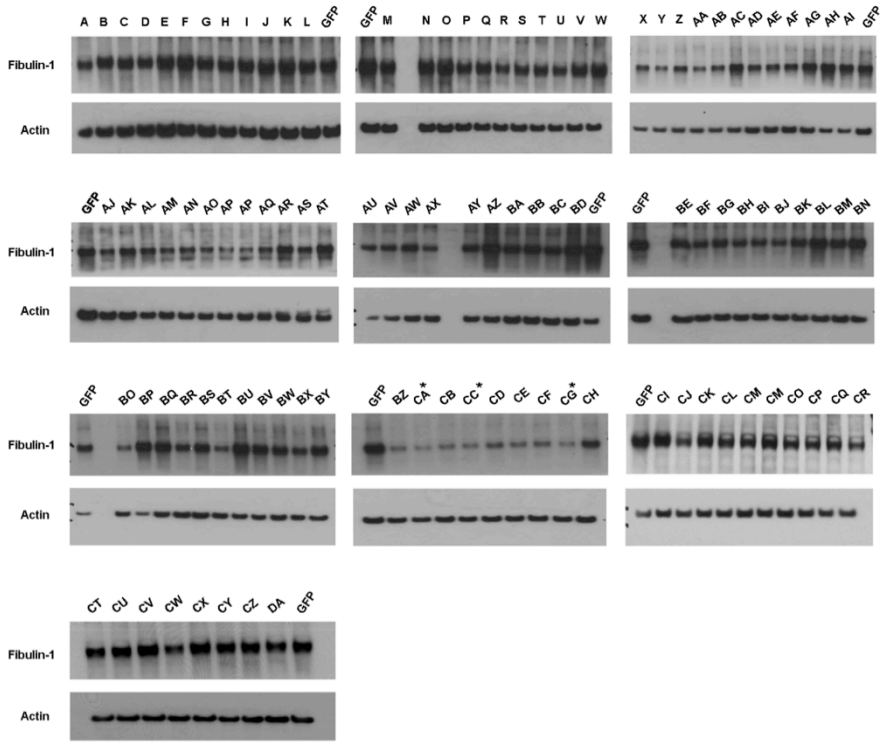

Figure 26: Fibulin-1 western blots for clone screening for HS-5^{CRISPR_fib1}. Levels of fibulin-1 were compared to the level in HS-5 cells transfected with a control plasmid (HS-5^{CRISPR_GFP}). The clones were labeled as GFP for HS-5^{CRISPR_GFP} and the letters from A to DA represented clone IDs for HS-5^{CRISPR_fib1}. Clones that showed significantly lower expression of fibuin-1 (*) were selected and renamed as HS-5^{CRISPR_fib1_11A}, HS-5^{CRISPR_fib1_11B} and HS-5^{CRISPR_fib1_11C} for future experiments.

Appendix D

PREVIOUS RESULTS SHOWED PCa APOPTOTIC INDUCTION AND NED BY HS-5 CM

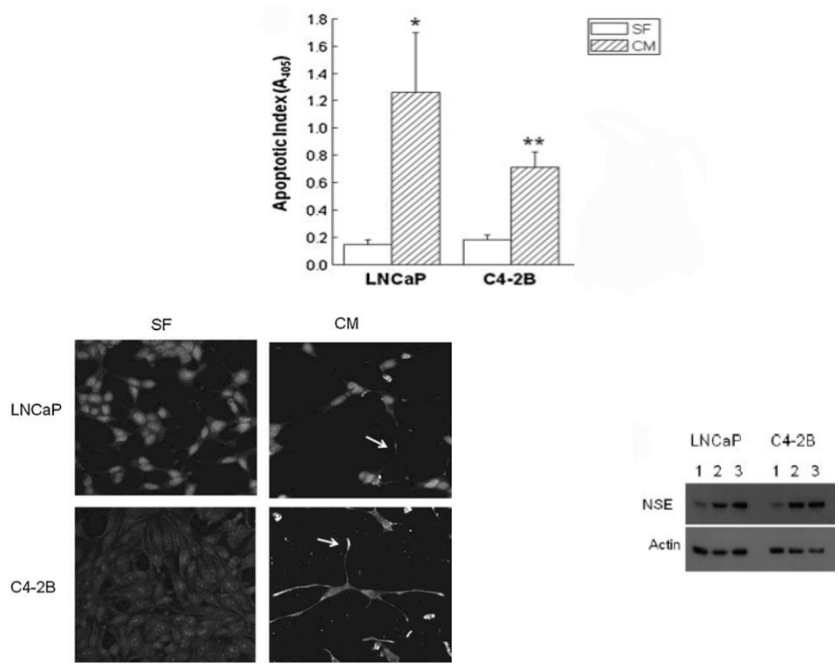

Figure 27: Previous research from Sikes' lab showed PCa apoptosis induction from HS-5 CM on LNCaP and C4-2B. Both LNCaP and C4-2B underwent more apoptosis with HS-5 CM treatment. While part of cell populations underwent apoptosis, another part underwent NED, which showed long processes extending from cell bodies and higher level of neuronal-specific enolase (NSE): 1= cells treated with SF DMEM, 2= cells treated with HS-5 CM, 3= cells treated with HS-5 + HS-27a CM. (used with permission [31])

Appendix E

HS-5 CM SHOWED AN APOPTOTIC INDUCTION SPECIFICITY TO PCa CELLS FROM LNCaP PROGRESSION MODEL

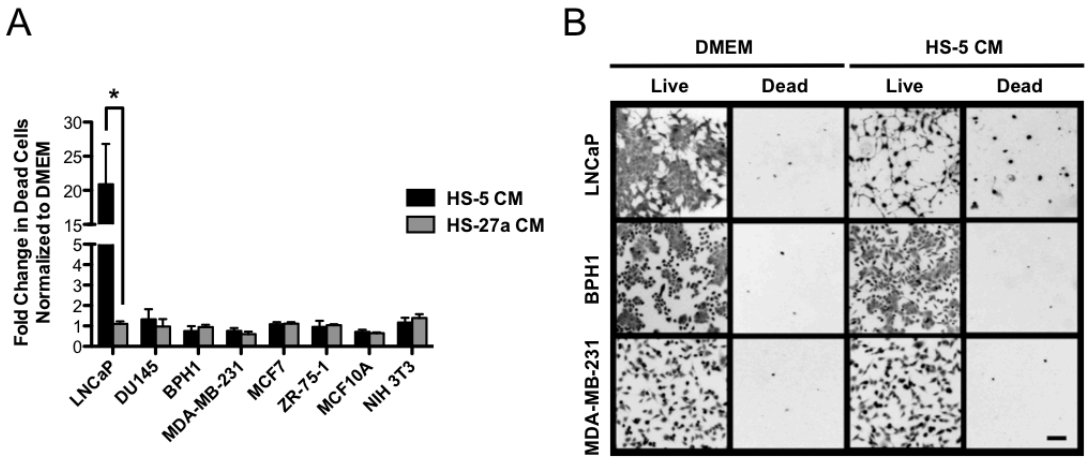

Figure 28: Results from previous experiments showed that HS-5 CM, but not HS-27a CM, induced PCa cell death specifically. A) HS-5 CM induced apoptosis in LNCaP, but have no effect on DU145 (AR negative PCa cells), BPH1 (benign prostatic hyperplasia), MDA-MB-231 (osteolytic breast cancer cells), MCF7 (breast cancer cells), ZR-75-1 (osteoblastic breast cancer cells), MCF10A (benign transformed breast cells) and NIH3T3 (fibroblasts). B) Representative pictures from live/dead assay in LNCaP, BPH1 and MDA-MB-231 treated with SF DMEM control versus HS-5 CM treatment. LNCaP showed significantly higher dead/live ratio after HS-5 CM. (used with permission [33])

Appendix F

BUFFER RECIPES

Experiments in molecular biology require many buffers, which could be slightly varied. Here, I recorded some important buffer recipes used in this dissertation.

F.1 Phosphate Buffer Saline (PBS): 10X, 1L

- 80 g NaCl
- 2 g KCl
- 11.5 g Na_2HPO_4

Adjust to 1 L with distilled water; Final pH: 7.4

Autoclave it needed.

F.2 PBST

PBST was made from 1X PBS with 0.1% of Tween-20

F.3 Tris Buffer Saline (TBS): 20X

- 24 g Tris base (FW: 121.1 g)
- 88 g NaCl

Adjust to 500 mL with distilled water; Final pH: 7.6 (with 12N HCl)

F.4 TBST

TBST was made from 1X TBS with 0.1% of Tween-20

F.5 Radio Immunoassay Precipitation Buffer (RIPA): 1X

- 150 mM NaCl
- 1% NP-40 or Titron X-100
- 0.5% Sodium deoxycholate ($C_{24}H_{39}O_4Na$)
- 0.1% SDS
- 50 mM Tris-HCl pH 8.0

F.6 Tris Acetate Buffer (TAE): 50X, 1L

- 100 mL of 0.5M EDTA
- 292 g Tris base
- 57.1 mL Glacial acetic acid

Adjust to 1 L with distilled water; Do not add water to acid

F.7 LB Broth

- 10 g Tryptone
- 5 g Yeast extract
- 10 g NaCl

Adjust to 1 L with distilled water; Final pH: 7.0

Autoclave before use

F.8 LB Agar

LB agar could be made by adding 15% agar into LB broth before autoclave or prepared from premixed LB powder according to the instruction provided.

F.9 SOC Medium

- 2% Tryptone
- 0.5% Yeast extract

- 10 mM HCl
- 2.5 mM KCl
- 10 mM $MgCl_2$
- 10 mM $MgSO_4$
- 20 mM Glucose

Appendix G

PERMISSION to USE MATERIALS FOR DISSERTATION

Some published and non-published materials were used in this dissertation as parts of the introduction, discussion and appendixes. The permission documents are attached here:

NATURE PUBLISHING GROUP LICENSE
TERMS AND CONDITIONS

Feb 27, 2015

This is a License Agreement between KORNKAMON NOPMONGKOL ("You") and Nature Publishing Group ("Nature Publishing Group") provided by Copyright Clearance Center ("CCC"). The license consists of your order details, the terms and conditions provided by Nature Publishing Group, and the payment terms and conditions.

All payments must be made in full to CCC. For payment instructions, please see information listed at the bottom of this form.

License Number	3577140873056
License date	Feb 27, 2015
Licensed content publisher	Nature Publishing Group
Licensed content publication	Nature Reviews Molecular Cell Biology
Licensed content title	Fibulins: a versatile family of extracellular matrix proteins
Licensed content author	Rupert Timpl, Takako Sasaki, Gunter Kostka and Mon-Li Chu
Licensed content date	Jun 1, 2003
Volume number	4
Issue number	6
Type of Use	reuse in a dissertation / thesis
Requestor type	academic/educational
Format	print and electronic
Portion	figures/tables/illustrations
Number of figures/tables /illustrations	2
High-res required	no
Figures	parts of figure 1 and 3
Author of this NPG article	no
Your reference number	151
Title of your thesis / dissertation	Identification of BMS derived factor leading to PCa cell death
Expected completion date	Jun 2015
Estimated size (number of pages)	150
Total	0.00 USD
Terms and Conditions	

ELSEVIER LICENSE
TERMS AND CONDITIONS

Feb 28, 2015

This is a License Agreement between KORNKAMON NOPMONGKOL ("You") and Elsevier ("Elsevier") provided by Copyright Clearance Center ("CCC"). The license consists of your order details, the terms and conditions provided by Elsevier, and the payment terms and conditions.

All payments must be made in full to CCC. For payment instructions, please see information listed at the bottom of this form.

Supplier	Elsevier Limited The Boulevard,Langford Lane Kidlington,Oxford,OX5 1GB,UK
Registered Company Number	1982084
Customer name	KORNKAMON NOPMONGKOL
Customer address	120 Wolf Hall. Newark, DE 19716
License number	3577870402535
License date	Feb 28, 2015
Licensed content publisher	Elsevier
Licensed content publication	Trends in Molecular Medicine
Licensed content title	Fibulins and cancer: friend or foe?
Licensed content author	William M. Gallagher,Caroline A. Currid,Linda C. Whelan
Licensed content date	July 2005
Licensed content volume number	11
Licensed content issue number	7
Number of pages	5
Start Page	336
End Page	340
Type of Use	reuse in a thesis/dissertation
Intended publisher of new work	other
Portion	figures/tables/illustrations

NATURE PUBLISHING GROUP LICENSE
TERMS AND CONDITIONS

Mar 03, 2015

This is a License Agreement between KORNKAMON NOPMONGKOL ("You") and Nature Publishing Group ("Nature Publishing Group") provided by Copyright Clearance Center ("CCC"). The license consists of your order details, the terms and conditions provided by Nature Publishing Group, and the payment terms and conditions.

All payments must be made in full to CCC. For payment instructions, please see information listed at the bottom of this form.

License Number	3581490675912
License date	Mar 03, 2015
Licensed content publisher	Nature Publishing Group
Licensed content publication	Nature Protocols
Licensed content title	Genome engineering using the CRISPR-Cas9 system
Licensed content author	F Ann Ran, Patrick D Hsu, Jason Wright, Vineeta Agarwala, David A Scott, Feng Zhang
Licensed content date	Oct 24, 2013
Volume number	8
Issue number	11
Type of Use	reuse in a dissertation / thesis
Requestor type	academic/educational
Format	print and electronic
Portion	figures/tables/illustrations
Number of figures/tables /illustrations	3
High-res required	no
Figures	figure 1, 2, 4
Author of this NPG article	no
Your reference number	205
Title of your thesis / dissertation	Identification of BMS derived factor leading to PCa cell death
Expected completion date	Jun 2015
Estimated size (number of pages)	150
Total	0.00 USD

JOHN WILEY AND SONS LICENSE
TERMS AND CONDITIONS

Apr 02, 2015

This Agreement between KORNKAMON NOPMONGKOL ("You") and John Wiley and Sons ("John Wiley and Sons") consists of your license details and the terms and conditions provided by John Wiley and Sons and Copyright Clearance Center.

License Number	3600821383182
License date	Apr 02, 2015
Licensed Content Publisher	John Wiley and Sons
Licensed Content Publication	Prostate
Licensed Content Title	Paracrine factors produced by bone marrow stromal cells induce apoptosis and neuroendocrine differentiation in prostate cancer cells
Licensed Content Author	Chu Zhang,Mehrnoosh Soori,Fayth L. Miles,Robert A. Sikes,Daniel D. Carson,Leland W.K. Chung,Mary C. Farach-Carson
Licensed Content Date	Jul 21, 2010
Pages	11
Type of use	Dissertation/Thesis
Requestor type	University/Academic
Format	Print and electronic
Portion	Figure/table
Number of figures/tables	2
Original Wiley figure/table number(s)	figure 3 & 7
Will you be translating?	No
Title of your thesis / dissertation	Identification of BMS derived factor leading to PCa cell death
Expected completion date	Jun 2015
Expected size (number of pages)	150
Requestor Location	KORNKAMON NOPMONGKOL 120 Wolf Hall. Department of Biological Sciences University of Delaware Newark, DE 19716 United States Attn: KORNKAMON NOPMONGKOL
Billing Type	Invoice

Google apps @UDel.edu

Kornkamon Nopmongkol <korn@udel.edu>

Asking for a permission to use data in your dissertation?

2 messages

Kornkamon Nopmongkol <korn@udel.edu> Thu, Apr 2, 2015 at 10:09 AM
To: Senem Kurtoglu <senem@udel.edu>
Cc: Kornkamon Nopmongkol <korn@udel.edu>

Dear Dr. Kurtoglu,

My name is Kornkamon nopmongkol. I am a Ph.D. candidate from University of Delaware. I would like to ask for your permission to use your figure 4 in my appendix for my dissertation. Could you please consider this?

Regards,

Kornkamon Nopmongkol

Senem Kurtoglu <senem@udel.edu> Thu, Apr 2, 2015 at 1:28 PM
To: Kornkamon Nopmongkol <korn@udel.edu>

[Quoted text hidden]
Dear Jume,

You have my permission to use my data in your dissertation as long as you cite my name/dissertation in the text.

Best of luck!

Regards,

Senem

--
Senem Kurtoglu, Ph.D., MBA
Department of Biological Sciences
University of Delaware
Newark, DE 19716
302-831-6977